JOURNAL OF APPLIED PHYSICS

JOURNAL OF APPLIED

PHYSICS

FEBRUARY, 1940 Vol. 11, No. 2

In This Issue

Page

Columbus Meeting 87

Electrical Conductivity of Metals JOHN BARDEEN 88

Stresses in Freely Falling Chimneys and Columns FRANCIS P. BUNDY 112

Resumés of Recent Research 124

Contributed Original Research

Investigation into the Gettering Powers of Various Metals for the Gases Hydrogen, Oxygen, Nitrogen, Carbon Dioxide and Air LOUIS F. EHRKE AND CHARLES M. SLACK 129

Infra-Red Transmission of Thin Films of Various Organic Materials A. J. WELLS 137

Studies in Lubrication. VI. Electrolytic Models of Full Journal Bearings F. MORGAN, M. MUSKAT AND D. W. REED 141

Behavior of Willemite Under Electron Bombardment E. R. PIORE AND G. A. MORTON 153

Letters to the Editor

Concerning "Physics of Flames and Explosions of Gases" W. T. DAVID 157

Answer to Communication by W. T. David BERNARD LEWIS AND GUENTHER VON ELBE 158

In Every Issue

Here and There 126

Recent Booklets vi

Contributors to This Issue 128

Innovations in Instruments iv

Index to Advertisers viii

BOARD OF EDITORS

ELMER HUTCHISSON, *Editor*

Associate Editors

F. BITTER
W. E. FORSYTHE
L. A. JONES
B. E. WARREN
J. B. WHITEHEAD

Publication of the American Institute of Physics

ADMINISTRATIVE STAFF

HENRY A. BARTON, *Director*

MADELINE M. MITCHELL, *Publications Manager*

GOVERNING BOARD

JOHN T. TATE, *Chairman*
KARL T. COMPTON
E. C. CRITTENDEN
WHEELER P. DAVEY
FLOYD A. FIRESTONE
HARVEY FLETCHER
ARTHUR C. HARDY
PAUL E. KLOPSTEG
MELVIN MOONEY
FREDERIC PALMER, JR.
R. L. PEEK, JR.
GEORGE B. PEGRAM
W. B. RAYTON
F. K. RICHTMYER*
WALLACE WATERFALL

* Deceased.

THE JOURNAL OF APPLIED PHYSICS, published monthly at Prince and Lemon Sts., Lancaster, Pa., is devoted to physics in its role as the science basic to other natural sciences and to the arts and industries. Previous to 1937 this publication was known as PHYSICS. It aims to be of service not only in physical laboratories, but also in the laboratories of industrial, chemical, geological, geophysical, meteorological, radio, and similar concerns. THE JOURNAL OF APPLIED PHYSICS publishes editorials, news of physicists and reviews, as well as technical papers of applied physics.

SUBSCRIPTION PRICE

	U. S., POSS. AND CANADA	FOREIGN
To members of scientific societies	$5.00	$5.70
To all others	7.00	7.70

Manuscripts should be submitted to Elmer Hutchisson, Editor, University of Pittsburgh, Pittsburgh, Pennsylvania.

Changes of address and proofs should be addressed to the Publications Manager.

Subscriptions and orders for back numbers should be addressed to Prince and Lemon Streets, Lancaster, Pa. or to the American Institute of Physics, 175 Fifth Avenue, New York, N. Y.

Advertising rates supplied on request. Orders, advertising copy and cuts should be sent to the American Institute of Physics.

Entered as second class matter at the Post Office at Lancaster, Pennsylvania, under the Act of March 3, 1897. Accepted for mailing at the special rate of postage provided for in the Act of February 28, 1925, authorized May 2, 1932.

Copyright 1940, by the American Institute of Physics.

Journal of Applied

Physics

Volume 11 February, 1940 Number 2

The Columbus Meeting

THE trend of the times was evident at the Columbus meeting of the A.A.A.S. by the presence in the general program of such lectures as "The Public Relations of Science," "Who is Responsible for Peace," and "Science, War and Reconstruction." The last-named lecture was given by Dr. Julian S. Huxley and was the first lecture in America under the exchange plan of the British and the American Associations for the Advancement of Science. Dr. Huxley formulated on as scientific a basis as possible a scheme for the reconstruction of a league or union of the European nations which would give a good probability of perpetual peace. Undoubtedly many such proposals will be made in the future, and it is encouraging to see the scientist taking an active part in such discussions.

In many ways the American Physical Society meeting was an exceptionally interesting one. Professor I. I. Rabi's paper on the radiofrequency spectra of atoms and molecules was a model of clarity and deservedly won the A.A.A.S. thousand-dollar prize for a noteworthy paper. In Professor Rabi's ingenious method a beam of atoms passes from a heated furnace through two nonhomogeneous magnetic fields with gradients oppositely directed into a narrow slit connected with some recording device. If during the transit, the magnetic moment of the atom is changed by an electromagnetic field, the atoms are deflected in such a way that they no longer pass through the recording slit, thus providing a very sensitive indicator of the effect of the magnetic field. In this way atomic energy levels and magnetic moments may be measured which are quite beyond ordinary spectroscopic methods.

Papers on applied physics were not entirely lacking in the program. There were papers on circuit networks, changes in metals by hammering, order in alloys, high power light sources, lubrication, improved camera lenses, etc. However, considering the large amount of industrial and other applied physics research now being carried on, the showing was rather meager. It is to be hoped that in the near future the applied physicists will really surprise the membership and show their strength in the form of a sizable group of contributed papers.

Even at one of the Physical Society meetings one was reminded of our good fortune to be living in a free country by Dr. Herbert E. Ives, who at the end of his stimulating paper on the existence of an ether quoted the famous remark of Patrick Henry: "If this be treason, make the most of it."

For March

Glass as an Electrical Insulator, by C. J. PHILLIPS

Ferromagnetic Domains and the Magnetization Curve, by WILLIAM F. BROWN, JR.

Also contributed research papers on:

The Formation and Maintenance of Electron and Ion Beams,

Remarks on the Study of Structural Viscosity in Liquids,

Diffusion of Hydrogen from Water Through Steel.

Electrical Conductivity of Metals

JOHN BARDEEN

Department of Physics, University of Minnesota, Minneapolis, Minnesota

I. Introduction

THE classical theories of the electrical conductivity of metals as developed mainly by Drude and Lorentz, while successful in some respects, most notably in regard to the Weidemann-Franz law, encountered serious difficulties. These difficulties have been almost completely removed by modern quantum theory as applied to the problem by Sommerfeld, Houston, Bloch, Mott, and others. Before discussing the modern theories, it will be instructive to give a review of some of the salient experimental facts which an adequate theory of conductivity must explain, and also to give a brief discussion of the older theories, as they contain many elements of truth. In fact, the basic concepts are largely unchanged, even though the formal theory is quite different in appearance.

The fundamental idea of the theories of Drude and Lorentz, and of all later theories, is that the current is carried by electrons which have become detached from the atoms which make up the metal and may move about more or less freely. The most direct experimental proof of this fact was not obtained until some years after the theory was first proposed. Experiments of Tolman and various collaborators indicate that the current is carried by particles of negative charge and with a mass close to that of an electron. The earliest is that of Tolman and Stewart.[1] A coil of wire rotating at high speeds is connected to a sensitive ballistic galvanometer. When the coil is suddenly stopped from rotating, an impulse of current is sent through the galvanometer. The kinetic energy which the electrons acquired when the coil was rotating is dissipated by the resistance. From the velocity of the coil and the total charge carried by the impulse of current, together with a knowledge of the resistance and dimensions of the coil, one can find the ratio of the charge to the mass of the particles that carry the current. Tolman and Stewart find for this ratio, e/m, the following values:

for Cu	1.60×10^{7} e.m.u.
for Ag	1.485×10^{7} e.m.u.
for Al	1.54×10^{7} e.m.u.

These values are rather close to the value for perfectly free electrons,[2] 1.77×10^{7} e.m.u. Later experiments made with the use of oscillating cylinders gave similar results. These experiments indicate that the current is carried by electrons which move through the crystal lattice.

II. Summary of Experimental Facts

A. Conductors and Insulators

Perhaps the most important thing an adequate theory of conductivity must explain is the remarkable difference in conductivity between metals and insulators. The resistivity of metals if of the order of 10^{-5} ohm cm, of insulators, the order of 10^{12} ohm cm. There is no satisfactory explanation on any classical basis.

B. Temperature Dependence

At high temperatures, the resistance of a pure metal is roughly proportional to the absolute temperature. It decreases rapidly as the temperature is lowered, and at very low temperatures is proportional to T^{5}. On the other hand, the resistance of insulators increases as the temperature is decreased. This is a characteristic property which distinguishes metals and nonmetals.

Gruneisen[3] has shown that the resistance of most metals can be given by a universal function of the temperature:

$$R=R_0 f(T/\Theta). \tag{1}$$

Here Θ is a characteristic temperature for the particular metal, which is generally rather close to the Debye characteristic temperature for specific heats. Experimental points for a number of metals are shown in Fig. 1.

There is thus indicated a close connection between the conductivity of pure metals and the thermal motion of the atoms which is responsible for the specific heat. W. Wein has suggested that the conductivity is proportional to the mean square amplitude of the motion of the ions. The resistance would then be proportional to the absolute temperature, T, at high temperatures, and to T^4 at very low temperatures. The theoretical curve shown in Fig. 1, which was used by Gruneisen, is based on an approximate theoretical expression due to Bloch, which will be discussed more at length later on. According to this expression the resistance should be proportional to T^5 instead of T^4 at low temperatures, and is in better agreement with experiment. Both theory and experiment indicate that one of the most important factors in the resistance of a pure metal is the mean square amplitude of motion of the atoms of the crystal.

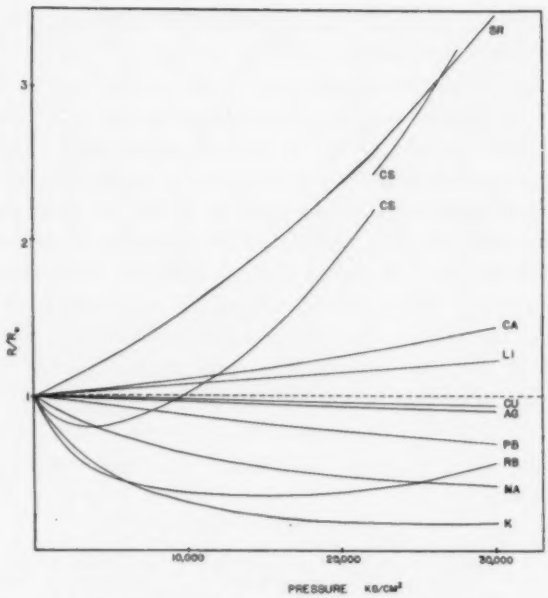

FIG. 2. Pressure variation of resistance of various metals. Data from Bridgman (reference 4).

C. Dependence on Pressure

The resistance of most metals decreases with increasing pressure. Fig. 2, shows the resistance as a function of pressure for a number of the softer metals in the pressure range extending to about 30,000 atmospheres. These curves have been obtained recently by Bridgman.[4] The resistances of a few of the metals (Li, Sr, Ca) increase with increasing pressure; some (Rb, Cs, Ba) show a reversal, decreasing at low pressures to a minimum and then increasing as the pressure is further increased. Most of the anomalous metals are shown in the figure; the normal behavior is a gradual decrease with pressure. Gruneisen has explained this normal decrease as due to the decrease in the thermal motion of the atoms as the pressure is increased and the atoms are bound with greater forces to their positions of equilibrium.

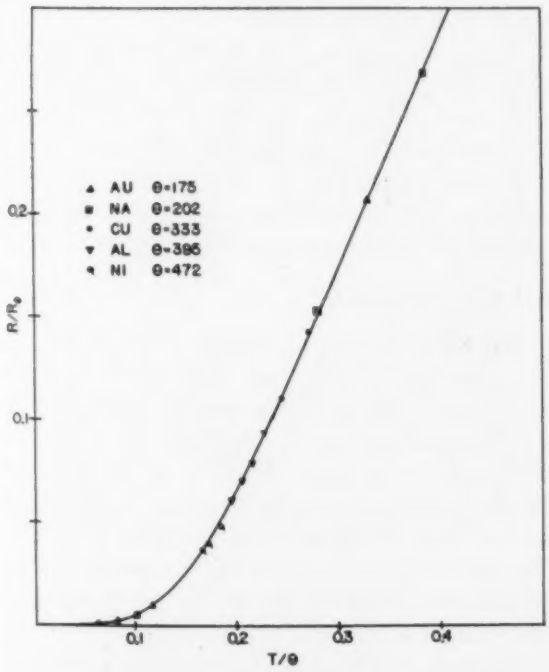

FIG. 1. Temperature variation of resistance of various metals. The curve is a plot of the Bloch-Gruneisen function (Eq. (28)). Data from values quoted by Meissner (cf. Bibliography).

D. Matthiessen's Rule

Any actual metal contains a certain amount of impurities and as the temperature is decreased to the absolute zero, the resistance does not go to zero, but approaches a constant value which depends on the amount of impurity. The purer the metal, the smaller is the residual resistance. Matthiessen has pointed out that the resistance is the sum of two terms,

$$R = R_0 + R_T, \tag{2}$$

a constant term (independent of temperature), which is proportional to the amount of impurity, and a temperature dependent term, characteristic of the pure metal, which goes to zero as the temperature approaches the absolute zero. This is known as Matthiessen's rule, and is in approximate agreement with experiment for the increase in resistance of a metal due to a small concentration of a second metal in solid solution. Electrons may be scattered by impurity atoms in the lattice, giving rise to an added resistance. For small concentrations, the resistances caused by impurities and by thermal motion are additive.

In finding the resistance of a pure metal, a correction is generally made for the residual resistance.

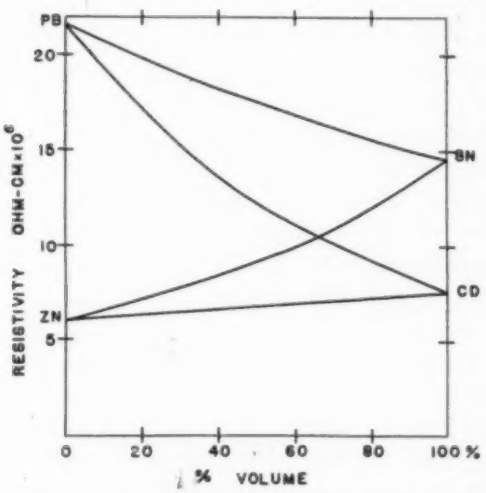

FIG. 3. Resistivity of heterogeneous mixtures. Data from values quoted by Meissner.

E. RESISTANCE OF ALLOYS

If an alloy is made up of a mixture of microcrystals of individual pure metals, the resistance is roughly the average resistance of the components. Fig. 3 illustrates the curves for the resistances of the Pb-Sn, Pb-Cd, Zn-Cd, and Zn-Sn series as a function of concentration. These metals are mutually insoluble in one another.

If, on the other hand, there is a solid solution, the resistance is much greater than that of either of the components. Results for the Ag-Au alloys, which form a solid solution for all concentrations, are given in Fig. 4. The resistance is a maximum at about 50 percent concentration. In this alloy there is no superlattice; the Ag and Au atoms are distributed at random over the lattice points. Let us now see what happens when an ordered structure is formed. Fig. 5 illustrates the Cu-Au system, which has been studied extensively by a large number of workers. The quenched alloy, in which there is no superlattice, has a resistance curve of the same general shape as that of the Ag-Au system. If the alloy is annealed, a superlattice is formed in the neighborhood of 25 percent Cu, 75 percent Au, and of 50 percent Cu, 50 percent Au. The Cu and Au atoms then take up more or less regular ordered positions in the lattice. It is seen that the resistance drops markedly and approaches that of a pure metal. We will consider this system in more detail later on; we now merely want to emphasize the fact that an ordering of the atoms decreases the resistance.

The facts enumerated above indicate that resistance is due to irregularities in the lattice, and that these may be caused by either (1) thermal motion of the atoms; (2) impurities, or, in alloys, from a random solid solution. A further cause is the disorder existing in a liquid or amorphous solid.

These are but a few of the facts which a complete theory of conductivity must explain. The theory should give the absolute values of the conductivities of the different pure metals and their dependence on temperature and pressure. Why does copper have a low resistance and iron a comparatively high resistance?

III. Early Theories

The early theories of Drude and Lorentz[5] did not attempt to give an explanation of these facts in any detail; they merely attempted to give the mechanism of conductivity. It will be instructive to consider the elementary theory of Drude as it is very simple and its fundamental notions are preserved in the later theories. The essential idea is that the current is carried by electrons which may move about more or less freely, but are subject to collisions with the crystal lattice. The mean time between collisions will be called 2τ (τ is the time of relaxation). We suppose that on the average the momentum of the electron is destroyed at each collision. In

spite of the large interaction between electrons, we suppose, for simplicity, that the electrons move freely between collisions so that the equation of motion is

$$m dv_x/dt = -eF,$$

in which $-e$ and m are the charge and mass of the electron, and F is the field strength, which is assumed to act in the x direction. The mean drift velocity in the direction of the field is therefore

$$v_d = \tfrac{1}{2} \cdot (-eF/m) \cdot 2\tau = -eF\tau/m. \quad (4)$$

If there are N electrons per unit volume, the current will be $J = -Nev_d$, and the conductivity

$$\sigma = J/F = Ne^2\tau/m. \quad (5)$$

Drude made the admittedly simplified assumption that all electrons move with the same mean velocity, U, and that this velocity could be obtained from the equipartition law:

$$\tfrac{1}{2}mU^2 = \tfrac{3}{2}\kappa T, \quad (6)$$

where κ is Boltzmann's constant. The mean free path l is defined by:

$$l = 2\tau U. \quad (7)$$

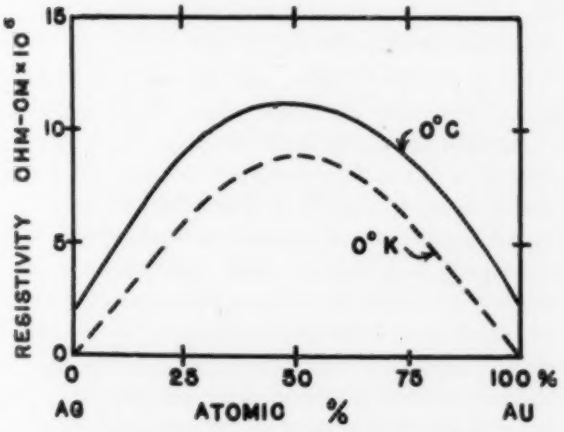

FIG. 4. Resistivity of Ag-Au alloys. Curve for 0°K extrapolated from results of Clay, quoted by Meissner.

In terms of the mean free path,

$$\sigma = Ne^2 l/2mU. \quad (8)$$

This formula gives about the right order of magnitude for the conductivity at room temperature if N is of the order of magnitude of the number of atoms per unit volume and l of the interatomic distance. However, in order to account for the temperature variation, it is necessary to assume that l increases very rapidly as the temperature is decreased. This peculiar variation was difficult to explain. Furthermore, one would expect that as the pressure is increased and the mean distance between atoms is decreased, l will decrease, and consequently the conductivity will decrease. As we have seen, this is contrary to the normal behavior.

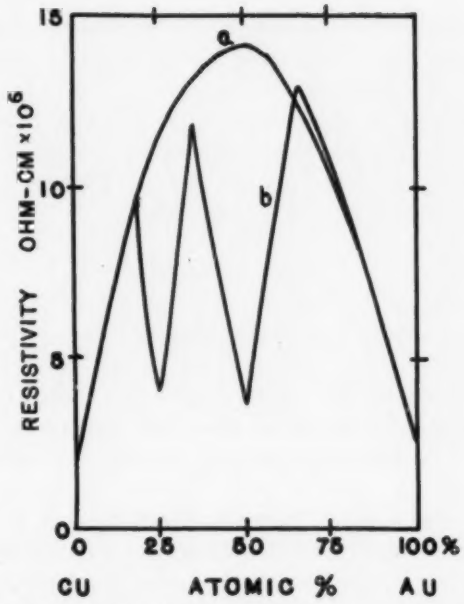

FIG. 5. Resistivity of Cu-Au alloys. (*a*) Quenched from 650°C. (*b*) Annealed at 200°C.*

Perhaps the most serious difficulty was in connection with the specific heat. Classically the electrons should contribute $3R/2$ times the number of free electrons per atom to the molar heat capacity. However, most of the heat capacity of metals is accounted for by the thermal motion of the atoms. Any contribution from the electrons must be very much less than R. As is probably well known to most readers, this difficulty was removed by Sommerfeld by the application of Fermi-Dirac statistics to the electrons.

More refined calculations by Lorentz, based on the same physical assumptions, merely served to emphasize the difficulties inherent in the Drude theory.

* Data from Johansson and Linde, Ann. d. Physik **25**, 1 (1936).

The great success of the theory was its explanation of the Wiedemann-Franz law which states that the ratio of the thermal to the electrical conductivity is proportional to the absolute temperature. On the same assumptions that were used in the theory of the electrical Drude found for the thermal conductivity:

$$K = \tfrac{1}{2} N \kappa U l, \tag{9}$$

so that

$$K/\sigma = 3(\kappa^2/e^2)T. \tag{10}$$

The constant of proportionality, which involves only the fundamental physical constants, is in approximate agreement with the experimental values.

In the classical theories there was no way to calculate the absolute value of the conductivity of a metal, nor to explain the differences in the conductivities of different metals.

IV. The Hall Effect

One of the most important phenomena in the historical development of the subject is the Hall effect. An electric current flows in a plate normal to which there is a magnetic field.

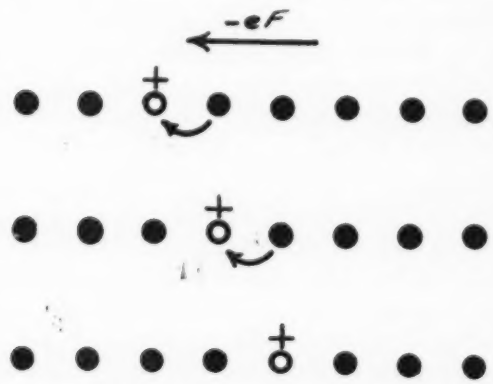

FIG. 6. Illustrating transfer of charge by associated electrons, according to Hall.

A potential difference is then set up across the plate in a direction transverse to the direction of the current. A very rough explanation is that the paths of the electrons are bent by the magnetic field. In order that there be no component of current in the transverse direction, a potential gradient must be set up. The sign of the gradient depends on the sign of the charge which carries the current. For most metals, the sign is such as would be expected for electrons (negative charge), but some metals show an anomalous sign (Zn, Cd). This fact gave rise to the dual conduction theories, which were developed mainly by Hall.[6] He assumed that the current is carried not only by "free" electrons but also by "associated" electrons. An atom in the metal may become ionized by giving rise to a "free" electron. The ion is then left positively charged. A bound electron from a neighboring atom may be transferred to this ion. In this way the position of the positively charged ion may move through the metal (cf. Fig. 6). A current arising from such a transfer of charge would give rise to an anomalous Hall coefficient. We will see later on that the modern theory gives some justification for this point of view.

V. The Sommerfeld-Bloch Theory

The remainder of the article will be devoted mainly to modern theories of electrical conductivity and their applications to various problems. Only a very brief discussion of the basic concepts of the general quantum theory of metals, which we shall need for the discussion of conductivity, will be given here. For further details, the reader is referred to the excellent series of articles by Seitz and Johnson[7] which have appeared in this Journal, or to one of the recent books on the subject (cf. Bibliography).

According to the modern picture, the valence electrons (i.e., the electrons outside of closed shells) become detached from the atoms which make up the metal and are free to move throughout the crystal lattice. These are the conduction electrons, which not only give the metallic bond, but also play the major role in the various electric and magnetic properties. Our discussion will be confined to these electrons; the ion cores will usually be replaced by an effective potential field in which the conduction electrons move.

This picture is not greatly different from that of Drude and Lorentz. What is responsible for recent progress is the application of quantum rather than classical mechanics to the problem. The two principles of quantum theory most important for the new development are (1) the wave property of electrons, and (2) the Pauli exclusion principle.

A. Electron Waves

Associated with each electron is a wave which is propagated in the direction of motion of the electron. For free electrons (i.e., electrons subject to no forces) the wave-length, λ, is given by the de Broglie relation:

$$\lambda = h/mv, \tag{11}$$

where h is Planck's constant, m is the mass of the electron, and v is the velocity. This relation has been verified experimentally by Davisson and Germer, Thomson, and others. If the electrons, instead of being free, are considered to be moving in the periodic potential field of the crystal lattice, the relation between wave-length and velocity is no longer given by (11) but by a somewhat more complicated equation which will be given later (Eq. (17)). Instead of using the wave-length or velocity to define the state of an electron, it is more convenient to use the wave vector, $\mathbf{k}$, whose direction is the direction of propagation, and which has a magnitude $2\pi/\lambda$. The energy of the electron, $E(k)$, will be a function of the vector $\mathbf{k}$. For free electrons

$$E = \tfrac{1}{2}mv^2 = h^2k^2/8\pi^2m. \tag{12}$$

The latter equality is a consequence of (11) as may easily be verified. Again, the general expression for the energy of an electron moving in a periodic field is more complicated.

The Pauli exclusion principle, as applied to the present situation, states that at most only two electrons can be in the same state, or, in other words, have the same wave-length and direction of propagation. The factor two arises from the two possible values of the electron spin. In an infinite crystal, the possible wave-lengths are continuously distributed, but in any finite crystal, they are limited to a discrete set of values. As long as the wave-length is small compared with the dimensions of the crystal, the number of states between two wave-lengths λ and $\lambda+\Delta\lambda$ is proportional to the volume of the crystal and is independent of its shape. Thus the number of electrons per unit volume which can have wave-lengths in the interval λ, $\lambda+\Delta\lambda$, is independent of the size or shape of the crystal, as of course it must be, if the properties of the crystal are independent of size and shape.

B. Specific Heat of Electrons

One consequence of the exclusion principle is that even at the absolute zero of temperature the energies of the different conduction electrons are spread over a wide band which may be several electron volts in width. Fig. 7 shows the average number of electrons in the different states at $T=0°K$, and also at some higher temperature. At $T=0°K$, all states with energies below a certain maximum, E_{max}, are occupied;

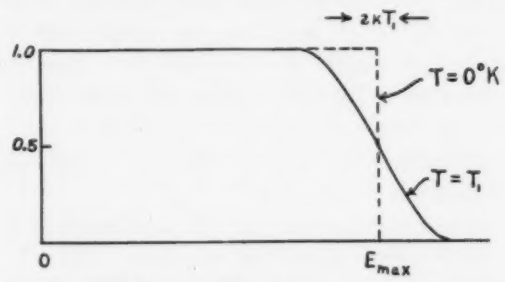

Fig. 7. The Fermi distribution function, giving the probability that an electronic state is occupied at a given temperature.

those above, unoccupied. At higher temperatures, a few electrons in states near the top of the filled band become excited to states of higher energies, and a distribution somewhat like that shown in Fig. 7 results. The fraction of electrons which are excited is of the order $\kappa T/E_{max}$, and the average energy of excitation of those electrons which are excited to higher states is of the order κT. Thus the average thermal energy per electron is of order $(\kappa T)^2/E_{max}$, and if there is about one free electron per atom, the specific heat is of order $(\kappa T/E_{max})R$ where R is the gas constant. Since at room temperature, $\kappa T/E_{max}$ is less than 0.01 for most metals, the heat capacity of the electrons is negligible compared with that of the thermal vibrations of the lattice ($\sim 3R$). It is only at very low (liquid He) temperatures that the electronic specific heat can be observed. As Sommerfeld first demonstrated, an application of the Pauli exclusion principle and Fermi-Dirac statistics gives an explanation of the specific heat difficulty which was inherent in the theories of Drude and Lorentz.

C. Sommerfeld Theory of Conductivity

In the theory of Sommerfeld, as in the theory of Drude, it is assumed that each electron moves

freely between collisions, and so is accelerated by the field. The field acting on a given electron due to the ions and due to the remaining electrons is neglected. Drude's formula (8) for the conductivity will therefore apply. The main difference is that the mean free path

$$l=2\tau U \tag{13}$$

will be much larger, since U, the mean velocity of an electron, will be much larger than that obtained from the equipartition theorem (kinetic energy $=\frac{3}{2}\kappa T$). If one assumes about one free electron per atom, it turns out that the mean free path at room temperature is of the order of 100 interatomic distances instead of, as in the Drude theory, the order of the distance between neighboring atoms.

The long mean free path is a consequence of the wave property of the electrons. While it is difficult to see how a particle could move very far through a crystal lattice without being scattered, it is not difficult to see that a wave can be propagated without serious attenuation. The situation is similar to the propagation of a light wave, or perhaps better, an x-ray, through a crystal: the wavelets scattered from each atom interfere constructively so as to continuously build up the wave front. An estimate of the mean free path on this basis was first given by Houston.

D. The Bloch Theory

The concept of electrons moving in an electrostatic field having the period of the crystal lattice was introduced by Bloch. Just as for the case of perfectly free electrons, it is possible to assign to each electron wave a definite wavelength and direction of propagation. Instead of being plane, the waves are modulated by a function having the period of the lattice. The wave function is of the form

$$\psi_k(x, y, z) = U_k(x, y, z)\exp\left[i(k_x x+k_y y+k_z z)\right]. \tag{14}$$

The vector $\mathbf{k}$, with components (k_x, k_y, k_z) is the propagation vector defined above. The second factor, $\exp\left[i(k_x x+k_y y+k_z z)\right]$ is the wave function of a plane wave; it is multiplied by a factor $U_k(x, y, z)$ which is periodic with the period of the lattice. The energy, $E(\mathbf{k})$ of an electron in the state $\mathbf{k}$ depends on the particular field in which the electron moves.

E. Velocity of the Electrons

To obtain the velocity of an electron in the state k, one may use the expression for the group velocity of any waves. For the case of waves moving in one dimension, this expression is:

$$v=d\nu/d(1/\lambda). \tag{15}$$

In our case, the frequency ν is given by E/h, and since $k=2\pi/\lambda$,

$$v=(2\pi/h)(dE/dk). \tag{16}$$

In the general case of three-dimensional motion, the expression for, say, the x component of the velocity is

$$v_x=(2\pi/h)(\partial E/\partial k_x). \tag{17}$$

The current contributed by the electron is

$$j_k=-ev_x=-(2\pi e/h)(\partial E/\partial k_x). \tag{18}$$

The total current can be obtained by summing the contribution from each electron over all occupied states. If more electrons are traveling in one direction than the opposite, there will be a net component of current in this direction. Since the states we have been considering are stationary states, this current will not diminish in time. Thus a perfect periodic lattice will have no resistance. Resistance is due to irregularities introduced by thermal motion, or by the presence of foreign atoms, which destroy the periodicity of the lattice. This is just what the experiments seem to demand.

F. Energy States

It is convenient to think of each electronic state as represented by a point in a three-dimensional k space. The coordinates of the point are the components (k_x, k_y, k_z) of the wave vector $\mathbf{k}$. This k space is exactly similar to the reciprocal lattice space, which has been of so much use in the theory of x-ray diffraction. Points representing allowed states are uniformly distributed in k space. The number in the element dk_x, dk_y, dk_z is $(V/8\pi^3)dk_x dk_y dk_z$ where V is the volume of the crystal.

The energy of an electron is not in general a continuous function of the wave vector. From

the theory of the motion of an electron in a periodic potential field, it is found that the whole of k space is divided up into regions or zones in each of which the energy is a continuous function of k. Across the boundary between two zones, the energy jumps discontinuously from one value to another. Each zone corresponds to a band of allowed energies which may be separated by a gap of forbidden energies from the next higher band. On the other hand, the energy bands may overlap, the lowest level of the upper band being lower than the highest level of the lower band.

The zones or energy bands may be correlated with the states of electrons in the free atom. One may imagine that the lattice constant of the crystal is continuously increased until the atoms are so far apart that there is little interaction between them. The energy bands will become narrower and narrower, until finally they go over to the discrete levels of the free atom. Thus one speaks of the s band of a monovalent metal which arises from the s level of the valence electron of the free atom. The d levels of the transition elements break up into several distinct d bands in the metal. There can be two s electrons in the free atom, and the total number of states in the s band is such that it will accommodate two electrons per atom. Similarly, the total number of states in the d bands corresponds to ten electrons per atom.

G. Metals and Insulators

If every allowed state in a band is occupied by an electron, the total current is zero, because for every electron traveling in one direction there will be another going in the opposite direction with the same velocity. If a band is only partially full, more electrons may be going in one direction than the opposite, giving a resultant current. The first case is characteristic of insulators, the second of metals. In an insulator any band which contains any electrons at all is full, and there is a gap of forbidden energies to the higher, unoccupied bands. An insulator must have an even number of valence electrons per unit cell. A metal contains bands in which only a fraction of the states are occupied. The divalent metals (Be, Ca, etc.) have just enough electrons to fill the lowest (s) band, i.e., two per atom. Since they are good conductors, it must be concluded that a higher band overlaps the lowest, so that there are electrons in two different bands, each partially full.

H. Acceleration of Electrons

The configuration of electrons in a metal may be described by giving the distribution of over the occupied states in k space. If an electric field acts on the metal, the distribution will no longer be symmetric about the origin, but will be displaced in the direction of the field, giving a resultant current. The new distribution results from an equilibrium between transitions among the states due to acceleration by the field and those due to the scattering which gives rise to the resistance.

The classical expression for the acceleration of an electron by an electric field F is

$$m(dv/dt) = -eF. \tag{19}$$

If we use the relation $mv = hk/2\pi$, appropriate for free electrons, it is found that the rate of change of the wave vector k with time is

$$dk/dt = -2\pi eF/h. \tag{20}$$

What effect will the periodic field of the crystal lattice have on the acceleration? It is not difficult to show that (20) will still be valid, even though Eq. (19) can no longer be used, and even though the velocity is no longer proportional to k.

The energy of an electron as a function of k along the direction of the applied field is illustrated schematically in Fig. 8a. The wave vector, k, according to Eq. (20) increases uniformly with time, so that a point which represents the state of an electron will move to the right with constant velocity. We have seen (Eq. 18) that the velocity of the electron itself is proportional to the slope, dE/dk. The velocity of an electron whose state is represented by the point A_1 where the curvature is positive, increases with time, since dE/dk increases as k increases. On the other hand, the velocity of an electron whose state is represented by A_2 decreases with time, since dE/dk is decreasing in this region. The electron then acts like a particle with negative mass. When the state reaches the point A_3, the velocity is zero. At this point there is a very

small probability that the electron will jump to the next higher band. Normally, the electron will reappear at A_3' (which really represents the same state as A_3) and then retrace its course over the lower band. The electron suffers Bragg reflection at A_3, and starts moving in the opposite direction.

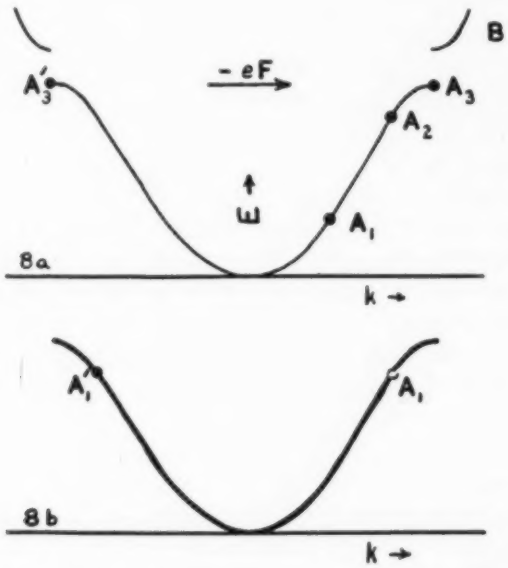

FIG. 8. (a) Motion of electron in a band under the influence of an applied electric field. (b) Motion of positive hole in band.

Let us now suppose that all the states are occupied except one, which is represented by the point A_1 in Fig. 8b. If all the states were occupied, the resultant current would be zero; the total current is therefore the negative of the current carried by an electron in the state A_1. This is equal to the current carried by an electron with velocity equal and opposite to that at A_1, i.e., just the current of an electron in the state A_1'. Under the influence of an electric field, F, the whole distribution of electrons, and therefore also the position of the unoccupied state or "hole" will move to the right with uniform velocity. Correspondingly, the point A_1' will move to the left in the direction in which a positively charged particle would move. If, as shown in the figure, the point A_1' is in the region of negative curvature, the velocity and current will increase with time. Thus the "hole" in the otherwise filled band acts like a particle of positive charge and positive mass in the region of negative curvature, and like a particle of positive charge and negative mass in the region of positive curvature near the bottom of the band. We shall see (Section V) that the above considerations may be used to give an explanation of the anomalous sign of the Hall coefficient.

In a normal metal, all the states with energies below some maximum energy, E_{max}, will be occupied, and those with energies greater than E_{max} will be unoccupied. (We neglect, for the moment, the small dispersion due to thermal agitation.) All these electrons will be accelerated by the applied field, so that the whole distribution in k space will move in the direction of the field. At first the density of electrons is changed only in those states which lie near the surface of the Fermi distribution, i.e., those with energies near E_{max}. A plot of the density of the occupied states in k space for a normal metal, and also after an electric field has been applied for a short time, is shown in Fig. 9.

Let J be the total current, as obtained by summing the contribution from each electron, j_k, (Eq. (18)) over all occupied states. We may define the effective number of free electrons per unit volume by means of the equation[8]

$$dJ/dt = e^2 F N_{eff}/m. \tag{21}$$

In case the lattice field vanishes, so that the electrons actually are free, N_{eff} is equal to N, the actual number of electrons per unit volume. In general N_{eff} may be either greater or smaller than N. The expression for N_{eff} is particularly simple if the surfaces of constant energy are spheres, so that E depends on the magnitude but not the direction of $\mathbf{k}$. In this case

$$N_{eff} = \frac{4\pi^2 m N}{h^2}\left(\frac{1}{k}\frac{dE}{dk}\right)_{E=E_{max}}. \tag{22}$$

Thus N_{eff} is large for a wide band and small for a narrow band. It is a measure of the relative ease with which an electron may travel from one atom to another in the crystal. If a zone is completely occupied by electrons, $N_{eff}=0$, since dE/dk vanishes at the surface of the zone.

I. CONDUCTIVITY

In a metal with finite resistance, the distribution in k space will shift in the direction of

the applied field until an equilibrium has been reached when the effect of the field will be just balanced by collision processes. The equilibrium distribution will be just that which would be obtained if the electrons had been accelerated for a time $t=\tau$ in the absence of resistance. Here τ is called the time of relaxation (cf. Section III). For fields of ordinary magnitude, the equilibrium distribution will differ but slightly from the normal distribution in zero field.

The conductivity may be expressed in the Drude-Lorentz form, we merely need to insert N_{eff}, as defined by Eq. (21) in place of N,

$$\sigma=(N_{eff}e^2/m)\tau. \tag{23}$$

The factors which determine τ will be discussed later; we first wish to give an explanation of the anomalous sign of the Hall coefficient exhibited by some metals.

J. Hall Coefficient

If the conduction band is only partially full, so that the states near the top of the Fermi distribution lie in the region where the curvature (d^2E/dk^2) is positive, the electrons behave normally; i.e., as particles of negative charge and positive mass. The sign of the Hall coefficient will be that which is expected for electrons. Let us now suppose that the band is nearly full, so that the electrons near the top of the Fermi distribution (which are those important for conductivity) have states in the region of negative curvature. It is then better to think of conduction by the unoccupied states or "holes" near the top of the band. These behave (cf. Section V, H) as particles of positive charge and positive mass. They give rise to a Hall coefficient of anomalous sign. In many metals, electrons occupy two unfilled bands, in one of which conduction is by "holes" and in the other by "ordinary" electrons. The sign will then depend on which of these gives the predominant effect. Conduction by "holes" is the quantum-mechanical analog of conduction by associated electrons, as visualized by Hall (Section IV).

The magnitude of the Hall coefficient can be worked out, and the correct order of magnitude is found. Numerical agreement is obtained for the alkali metals.

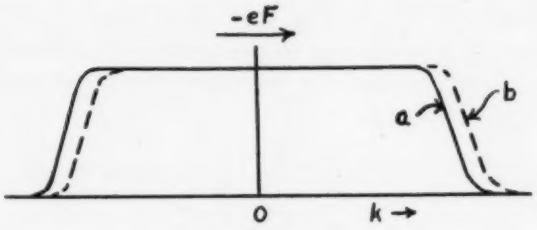

Fig. 9. Shift of the electron distribution due to an applied field.

VI. Resistance of Pure Metals

A. High Temperatures

The resistance of pure metals is due to the thermal motion of the atoms. A time of relaxation, τ, may be defined for collisions due to thermal motion only at high temperatures. At low temperatures, the quantization of the different modes of vibration of the lattice is important. At each collision a vibrational quantum of energy, $h\nu$ (ν is the vibrational frequency) is either taken from or given to the lattice, so that the collisions are inelastic. If the energy of the quantum is small compared with κT, as it will be if the temperature is well above the Debye characteristic temperature for the metal, it is possible to neglect this quantization, and to treat the vibrations classically. It then turns out that the probability of a collision of an electron with the lattice, and consequently $1/\tau$, is proportional to the mean square amplitude of motion of the ions in confirmation of Wien's hypothesis. The mean square amplitude is proportional to the absolute temperature, and is inversely proportional to the mass of the atom, M, and to the square of the vibrational frequency, ν,

$$(x^2)_{ave}=\kappa T/4\pi^2M\nu^2. \tag{24}$$

Thus the resistance should be proportional to the absolute temperature, in agreement with experiment. The vibrational frequency is proportional to the characteristic temperature, Θ, so that

$$1/\tau\sim(x^2)_{ave}\sim T/M\Theta^2. \tag{25}$$

A second factor of importance in $(1/\tau)$ is the density of states in energy near the top of the Fermi distribution. A large density means that there are a large number of states into which the electrons can be scattered, and so a large

value for $(1/\tau)$. The scattering probability is directly proportional to the density. The density is, of course, high for a narrow band and small for a wide band.

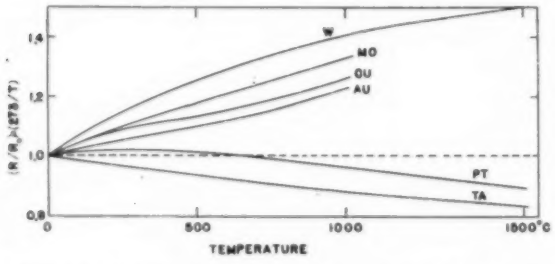

FIG. 10. Plot of the relative resistance of various metals divided by the absolute temperature, T, illustrating deviations from proportionality of resistance with T at high temperatures. Data from values quoted by Gruneisen and by Meissner (cf. Bibliography).

Deviations from the proportionality of resistance with absolute temperature at very high temperatures ($\sim$1000°C) have been explained by Mott as due to the change in Θ as a result of thermal expansion. As the metal expands, Θ decreases, so that R/T increases as the temperature rises. This is the normal behavior, but for some metals, in particular for those in the transition group, R/T decreases with increasing temperature. In this group of metals there is a narrow d band, and at high temperatures the density of states changes appreciably in the range of energies of width κT at the top of the Fermi distribution. The effective density decreases as T increases, which explains the decrease in R/T observed for these metals. Fig. 10 gives a plot of R/T as a function of T for various metals.

B. Low Temperatures

In order to discuss the temperature variation of resistance at low temperatures, it will be necessary to investigate the interactions of the electrons with the lattice vibrations in somewhat more detail. Following Debye, we may analyze the vibrations into a system of independent waves. The very long waves are just the ordinary sound waves; the shortest waves correspond to adjacent atoms vibrating in opposite directions. Each wave is described by the propagation vector $\mathbf{q}$. The direction of $\mathbf{q}$ gives the direction of propagation of the wave, and its magnitude is $2\pi/\lambda$, where λ is the wave-length. There are three independent vibrations for each $\mathbf{q}$, corresponding to the transverse and longitudinal sound waves. If the velocity of the wave is c, the frequency is

$$\nu = c/\lambda = cq/2\pi \tag{26}$$

and the energy of the vibrational quantum is $h\nu = hcq/2\pi$.

In each collision of an electron with the lattice a vibrational quantum is either emitted from or absorbed by the lattice. The selection rules for the transition of an electron from the state $\mathbf{k}$ to the state $\mathbf{k}'$ are as follows

$$\begin{aligned} \mathbf{k}' &= \mathbf{k}+\mathbf{q} \quad \text{(emission)} \\ \mathbf{k}' &= \mathbf{k}-\mathbf{q} \quad \text{(absorption)}. \end{aligned} \tag{27}$$

The vector relations are illustrated in Fig. 11. The angle, θ, between k and k' is the angle through which the electron is deflected by the collision. In addition to these rules, there is the requirement of conservation of energy. Thus, for absorption, the energy of the electron in the final state, k', must be equal to the energy of the electron in the initial state, minus the energy of the vibrational quantum.

At low temperatures, the only vibrations which will be excited are those with low energies, and these have long wave-lengths and therefore small values of q. The low resistance is due not only to the fact that the amplitudes of vibration are small, but also to the fact that the electrons are deflected through small angles (cf. Fig. 11). A quantum can be absorbed by the lattice even though no quanta are originally present. Thus it would appear that a metal has resistance at the absolute zero of temperature. However, a quantum can be absorbed only if the electron can lose an equivalent amount of energy. The average excitation energy of the electrons near the top of the Fermi distribution is of the order κT. An electron cannot lose more than this amount, because all the lower states are occupied.

Bloch's derivation of the formula for the temperature dependence of resistance involved a number of assumptions and approximations, among which are: (1) Debye theory for the thermal vibrations. (2) Thermal equilibrium of vibrations. (3) $E(k)$ a function of $|k|$. In addition, certain assumptions about the form of the

interaction between the electrons and lattice vibrations were made. The function giving the distribution of electrons in k space, which was used in calculating the conductivity, is only an approximate solution of the Boltzmann equation. The formula derived states that the resistance is proportional to[9]

$$R \sim \left(\frac{T}{\Theta}\right)^5 \int_0^{\Theta/T} \frac{x^5 e^x dx}{(e^x-1)^2}. \qquad (28)$$

This formula was used by Gruneisen, and is plotted in Fig. 1, together with the experimental points for a number of metals. The check is extremely good, especially when one takes into account the approximate nature of the theoretical derivation. In this respect the theory is somewhat analogous to the Debye theory of specific heats.

The formula shows that the resistance at very low temperatures should be proportional to T^5. This law can be derived independently, and is on a firmer theoretical foundation. Most metals seem to follow this law fairly well,[10] but there are some deviations. In particular, the resistance of some of the transition metals at extremely low temperatures ($<10°$K) seem to follow a T^2 law. Baber[11] finds a term proportional to T^2 in the resistance arising from collisions between electrons. The effect is never large, but should be most pronounced in metals having a very narrow conduction band, such as the d band of the transition metals.

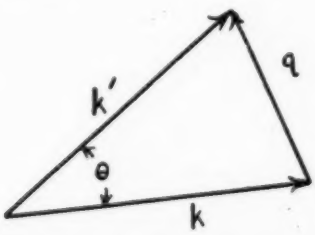

FIG. 11. Illustrating the vector relations for the scattering of an electron wave by a lattice wave.

C. Pressure Variation of Resistance

We have seen that the conductivity may be expressed in the form

$$\sigma = N_{\text{eff}} e^2 \tau / m \qquad (23)$$

and that $(1/\tau)$ is proportional to (1) the mean square amplitude of the thermal motion of the atoms, which, according to the Debye theory, is proportional to $T/M\Theta^2$, and (2) the density of the electronic states in energy at the top of the Fermi distribution, which is inversely proportional to dE/dk.

TABLE I. *Pressure coefficient of resistivity of various metals.*

METAL	$-(d \log R/dp)10^{12}$ (c.g.s.)	$(2\beta V_0/C_v)10^{12}$ (c.g.s.)
Li	−4.0	21.
Na	73.	40.
Mg	5.9	9.
Al	4.8	6.
K	190.	91.
Ca	−8.9	
Fe	2.7	2.0
Co	1.1	2.0
Ni	2.1	2.0
Cu	2.3	3.0
Rb	200.	120.
Sr	−47.	
Mo	1.5	1.1
Ag	4.0	4.8
Cs	220.	157.
Ta	1.7	1.8
Pt	2.1	1.9
Au	3.4	3.3
Pb	15.4	12.5

As we have mentioned earlier, the normal decrease of resistance with increasing pressure is accounted for by the increase in Θ with pressure, which results from the stronger binding forces as the atoms are brought closer together. The relative change in resistance with pressure due to the change in Θ is

$$d \log R/dp = -2d \log \Theta/dp. \qquad (29)$$

The dependence of Θ on pressure can be estimated from Gruneisen's formula[12]

$$\beta V_0/KC_v = -d \log \Theta/d \log V,$$

where β is the volume coefficient of expansion, K is the compressibility,* V_0 is the volume occupied by one gram of the substance, and C_v is the specific heat. Since the compressibility $K = -d \log V/dp$,

$$d \log \Theta/dp = \beta V_0/C_v. \qquad (30)$$

Values of $-2d \log \Theta/dp$ as calculated from (30) are compared with the observed values of $d \log R/dp$ for a number of metals in Table I.

* We have also used K to denote the heat conductivity. There should be no confusion.

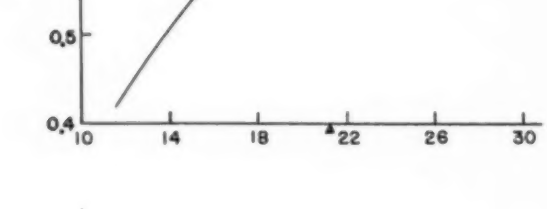

FIG. 12. Plot of α (Eq. (31)) for sodium and lithium as a function of volume.

The agreement, at least as to order of magnitude, is in general good, but there are some notable exceptions, e.g., Li, Ca and Sr, for which the resistance increases with pressure. Since Θ certainly increases with pressure, these anomalous values must be attributed to electronic factors. We will first discuss the monovalent metals and then give a possible explanation, due to Mott, of the anomalous behavior of some of the divalent metals.

A plot of the variation of the resistance of the alkali metals with pressure, as observed by Bridgman, is shown in Fig. 2. Na behaves normally, the resistance decreasing with increase of pressure. The resistance of Li increases with pressure, while K, Pb, and Cs show a minimum, the resistance at first decreases and then, with further increase in pressure, the curve reverses and the resistance increases.

To a first approximation the electrons in a monovalent metal may be treated as free electrons. The energy is then

$$E = \tfrac{1}{2}mv^2 = h^2k^2/8\pi^2m.$$

A better approximation for E is

$$E = \alpha h^2k^2/8\pi^2m, \tag{31}$$

where α is the effective number of free electrons per atom. Values of α which have been computed for Li and Na from fundamental principles[14] are plotted as a function of the atomic volume in Fig. 12. It is found that α is about 0.65 for lithium and decreases as the volume decreases. It is nearly equal to unity for sodium and increases slightly as the volume decreases. To make a very rough calculation of the variation of resistance with pressure, we may assume that the characteristic temperature, Θ, is inversely proportional to the square root of the compressibility, K (Einstein's formula). Since τ is proportional not only to Θ^2, but also to dE/dk, or α, we find that the resistance is proportional to

$$R \sim N_{eff}^{-2}\Theta^{-2} \sim K/\alpha^2 \tag{32}$$

or

$$R_p/R_0 = (K/\alpha^2)_p/(K/\alpha^2)_0. \tag{33}$$

The subscript zero refers to the values at zero pressure. Values of R_p/R_0 for sodium as computed from Eq. (33) are compared with the experimental values in Fig. 13. The agreement is fairly good.

Similar calculations can be made for lithium. The decrease in α with pressure would tend to

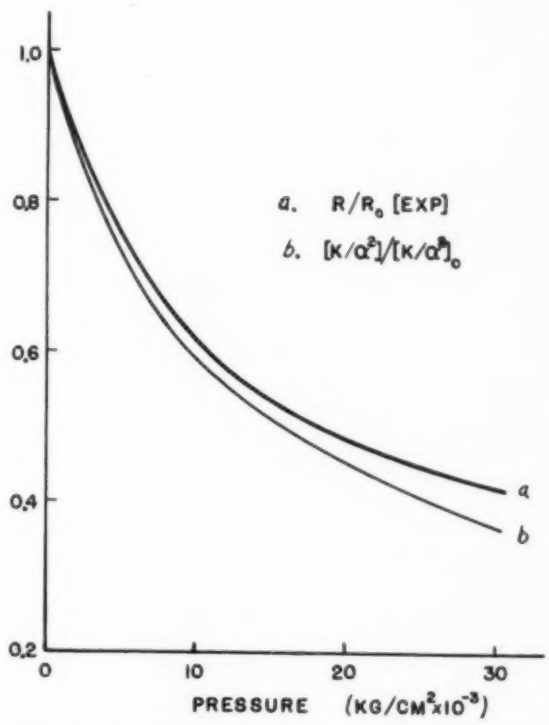

FIG. 13. Comparison of experimental and theoretical values of the relative change of resistance of sodium with pressure.

make the resistance increase. Frank[13] has attributed the observed rise in resistance to a decrease in N_{eff}. However, the decrease in α shown in Fig. 12 is not sufficiently great to counter-balance the effect of the increase in Θ, so that Eq. (33) gives a net decrease in resistance, in contradiction with experiment. Of course, the factors given in Eq. (32) are not the only ones which affect the resistance. Another important one is the term which represents the interaction between the electrons and lattice waves. Unpublished calculations by I. Weiner on the basis of the author's theory[17] indicate that the further terms have little effect on the pressure variation of resistance of sodium. They act in such a direction as to increase the resistance of lithium at high pressures, but the effect is not very large, so that there is still a small net decrease in the calculated resistance as the pressure is increased. There is some evidence that the conduction electrons in lithium lie in two overlapping bands, and it may be necessary to take this into account to obtain complete agreement between theory and experiment.

A discussion of the conductivity of divalent metals, where two Brillouin zones are of importance, has been given by Mott.[15] An excellent qualitative discussion of his general method is given in the introduction to the second of the papers listed.[16] If there are two overlapping energy bands, which we may designate by a and b, the conductivity is

$$\sigma=(Ne^2/m)(\alpha\tau_a+\beta\tau_b). \qquad (34)$$

Here τ_a and τ_b are the times of relaxation of the electrons in bands a and b, respectively, and α and β are the corresponding effective members of free electrons per atom. Mott shows that τ_a and τ_b will be of the same order of magnitude, but that α and β may be very different. If there is a low density of states in band a and a high density in band b, then α will be very much larger than β, and most of the current will be carried by electrons in band a. The resistance will then be due largely to transitions which send electrons from band a to band b, and the times of relaxation, τ_a and τ_b, will be inversely proportional to the density of states at the top of the Fermi distribution in band b. If, as the pressure is increased, the overlap is increased so that the density of states at the top of the Fermi is increased, the resistance will increase, since τ_a and τ_b will decrease. This will occur if either a or b has lower energy. A schematic diagram of two such overlapping bands is shown in Fig. 14.

Manning and Krutter[17] have made approximate calculations of the energy bands of Ca. They find a dense d band lying above and overlapping the normal s band (which contains nearly two electrons per atom). They find that the overlap increases with pressure, so that the resistance should increase with pressure, in qualitative agreement with experiment.

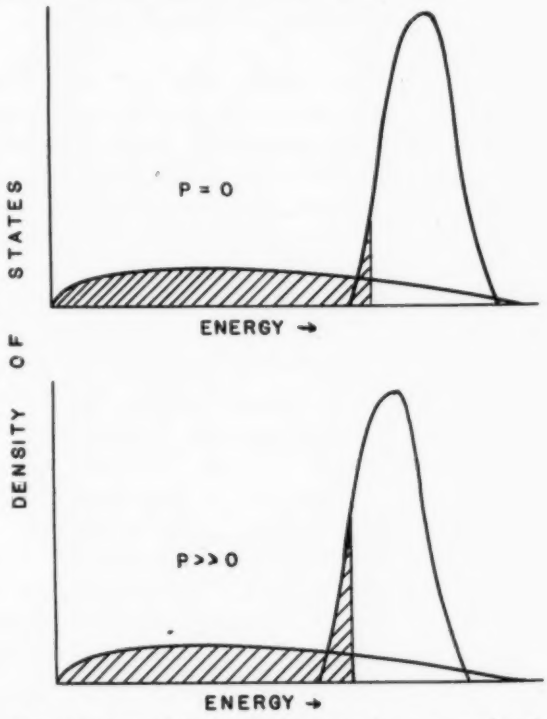

FIG. 14. Occupied electronic states in two overlapping bands at (a) zero pressure, (b) some high pressure (schematic).

D. Absolute Value of the Conductivity

We have seen that one of the important factors which determine the resistance of a metal is the square of the amplitude of vibration of the atoms. Due to this cause alone, the conductivity would be proportional to $M\Theta^2$, where Θ is the Debye characteristic temperature and M is the atomic weight. In Fig. 15 we give a plot of $\sigma/M\Theta^2$, which should depend on purely electronic factors, as a function of the atomic number of the element. The most striking features are

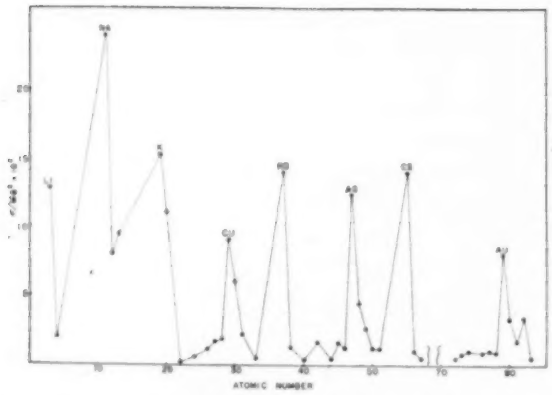

FIG. 15. Values of $\sigma/M\Theta^2$ plotted as a function of the atomic number. There is a gap for the rare earth metals.

the relatively high values for the monovalent metals, and the low values for the transition elements. Note, for example, the large difference in the values of $\sigma/M\Theta^2$ for the neighboring pairs (Ni, Cu), (Pd, Ag) and (Pt, Au). In the transition metals there is an incomplete d band which is overlapped by an s band which is similar to the s bands of the monovalent metals. (Cf. Fig. 16.) The current is carried mainly by electrons in the s band but the large resistance is due to scattering from the s band to the narrow d band. The probability of transitions of this type is large because of the high density of states in the d band. Such transitions cannot occur in the monovalent metals, because the d band is fully occupied.

The comparatively high resistances of the divalent metals is probably due to the small effective number of free electrons for these metals. This is true to a much greater extent for such semi-metallic elements as Bi, Sb, and As.

A calculation of the absolute value of the conductivity of a metal from fundamental principles is very difficult because little is known about either the electronic wave functions or the vibrational spectrum of most metals. Such calculations have been attempted only for the monovalent metals. To illustrate the degree of agreement that is obtained, results of a calculation by the author[18] are given in Table II. This calculation was based on the following assumptions: (1) The wave functions of the electrons were assumed to be nearly the same as those for free electrons throughout the major part of the volume. (2) The Debye theory was used for the lattice vibrations. (3) The perturbation potential, which gives the scattering of electrons by the lattice vibrations, consisted of two parts: (*a*) the change in the potential of the ions, and (*b*) the change in the potential of the self-consistent field of the valence electrons when the ions are moved from their equilibrium positions by the lattice waves.

The agreement is fairly good for Na and K (the metals for which the assumptions are probably best justified), but the calculated conductivities of the remaining monovalent metals are too large.

E. Ferromagnetic Metals

The resistance of the ferromagnetic metals rises rapidly as the Curie temperature is approached. There is a discontinuity in the slope of the resistance-temperature curve at the Curie point, and above the curve is much like that of a normal metal. The curve for nickel, which has been investigated more extensively than any other ferromagnetic metal, is shown in Fig. 17. Gerlach[19] has suggested that the resistance in the neighborhood of the Curie point can be given as

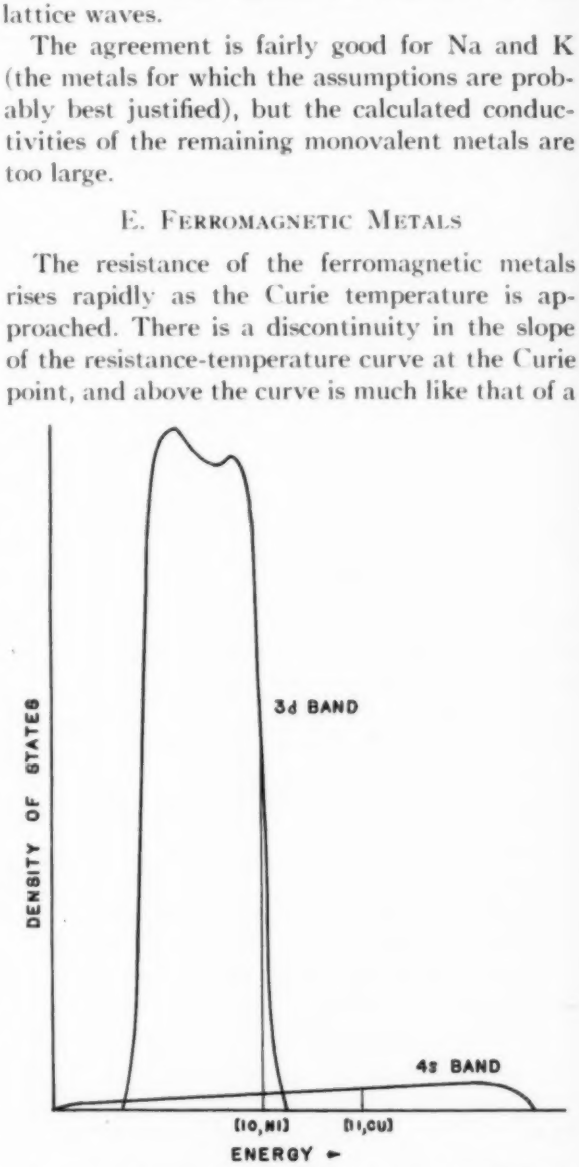

FIG. 16. Schematic picture of wide s band overlapping narrow d band.

the sum of a normal resistance, R_n, which is given by the Bloch-Gruneisen function, and a second term, R_F, which is a function of the spontaneous magnetization:

$$R = R_n + R_F = R_n + C(I_0^2 - I^2). \qquad (35)$$

Here I_0 is the intensity of the spontaneous magnetization at the absolute zero, I the actual magnetization at the temperature T, and C is a constant independent of temperature.

The subject has been treated theoretically by Mott.[20] The resistance of nickel is due largely to transitions which take electrons from the s to the d band. Each state in the d band can accommodate two electrons, one of each spin. At low temperatures, when the spontaneous magnetization reaches the saturation value, all the states in the d band are occupied by electrons whose spins are parallel to the direction of the magnetization. The remaining electrons have spins antiparallel but there are not enough to completely fill the band. The chance that an electron changes its spin during a collision is rather small, so that only half of the electrons in the s band, namely those with antiparallel spin, can make transitions to the d band. At higher temperatures, when the magnetization is not complete, electrons of either spin can make these transitions, so the resistance rises. The curves a and c in Fig. 17 are suggested resistance curves for paramagnetic nickel and for nickel magnetized to saturation. The three points shown give the resistances as computed by Mott for the actual magnetizations at the given temperatures. The calculations are rather complicated, and do not yield the simple form suggested by Gerlach. The agreement with the experimental curve is fairly good.

The resistance decreases when the specimen is magnetized by an external magnetic field. It is not as yet certain whether this effect can be quantitatively explained as simply due to the change in magnetization.

TABLE II. *Electrical conductivity of monovalent metals.* $T = 0°C$ ($ohm^{-1}\ cm^{-1} \times 10^{-4}$).

METAL	EXPERIMENTAL	CALCULATED
Li	11.8	28
Na	23.4	23
K	16.4	20
Rb	8.6	33
Cs	5.3	22
Cu	64.	174
Ag	66.	143
Au	49.	142

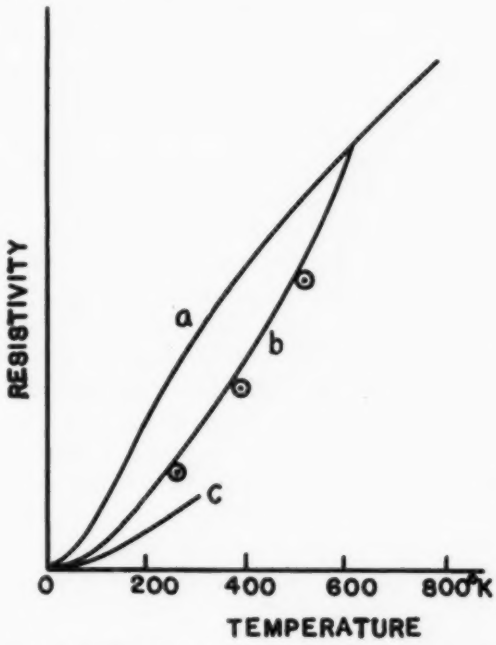

FIG. 17. Resistivity of nickel as a function of temperature. (*a*) Calculated for hypothetical paramagnetic nickel. (*b*) Experimental curve. (*c*) Calculated for magnetization at 0°K. (⊙) Calculated for observed magnetizations at given temperatures. (After Mott, reference 19.)

VII. Conductivity of Alloys

A. DILUTE SOLUTIONS

We have already discussed Matthiessen's rule (Section II, D) which gives the increase in resistance due to a small concentration of a foreign metal in solid solution. This rule receives a simple explanation according to the quantum theory of metals. A perfect periodic lattice has no resistance. In a pure metal, resistance is due to thermal motion, which destroys the periodicity of the lattice. In a solid solution electron waves may also be scattered from the foreign atoms present. For small concentrations, the resistances due to these two causes are additive. Matthiessen's rule will apply if the temperature dependent part, resulting from the thermal vibrations of the lattice, is independent of the concentration.

The increase in resistance due to the dissolved metal is usually very large. At room temperature, the resistivity of a metal may be doubled

by the presence of one atomic percent of impurity. Resistance measurements are often used as a test of the purity of a specimen.

The effects of different solute metals may vary over a considerable range, and for the most part have not been amenable to theoretical treatment. Some interesting relationships have, however, been pointed out by Norbury.[21] By comparing the increase in resistance caused by one atomic percent of different metals dissolved in a common solvent, he showed a marked dependence on the valencies of the solvent and solute metals. In general, the greater the difference in valencies (or in the horizontal position in the periodic table), the greater is the additional resistance. The effect is most pronounced for metals dissolved in Cu, Ag, and Au. In later work, Linde[22] has found that, for these metals, the increase in resistance varies approximately with the square of the difference in valencies. If $Z+1$ is the number of electrons outside of a closed d shell (so that $Z=0$ for Cu, $Z=1$ for Zn, $Z=2$ for Ga, etc.) the additional resistance varies with Z^2, as shown in Fig. 18. A simple explanation has been given by Mott.[23] All electrons outside of the closed d shells, from the dissolved as well as from the solvent metals, go to make up the conduction electrons which are free to travel throughout the metal. The core of a dissolved atom has an excess charge over a solvent atom of amount Ze. Electrons are scattered by the field of this excess charge. It follows from the Rutherford law that the scattering is proportional to the square of the charge (Ze) and it is this factor which makes the additional resistance proportional to Z^2. Quantitative calculations, taking into account the screening of the excess charge by the conduction electrons, give the correct order of magnitude for the effect.

Mott[24] has also investigated the additional resistance due to one atomic percent of metal A dissolved in metal B as compared with that of one atomic percent of B dissolved in A, and found that under certain conditions, these should be approximately equal.

B. Random Solid Solutions

In the present article we will be concerned only with the conductivity of a single homogeneous phase. (Many alloys consist of a mechanical mixture of two phases; in this case the conductivity is roughly the weighted average of the conductivities of the individual phases.) We first limit the discussion to the case of a disordered alloy; i.e., we assume that the atoms of the metals making up the alloy are distributed at random over the lattice points. Ordered alloys will be discussed in the next section. The resistance of an alloy may be expressed as the sum of two terms

$$R=R_0+R_T, \tag{36}$$

a temperature dependent term, R_T, which results from the thermal motion of the atoms, and is much the same as the resistance of a pure metal, and a second term, R_0, which is the resistance at the absolute zero of temperature. The second part represents the resistance caused by the fact that the lattice is not perfectly periodic due to the random distribution of the different atoms which make up the alloy.

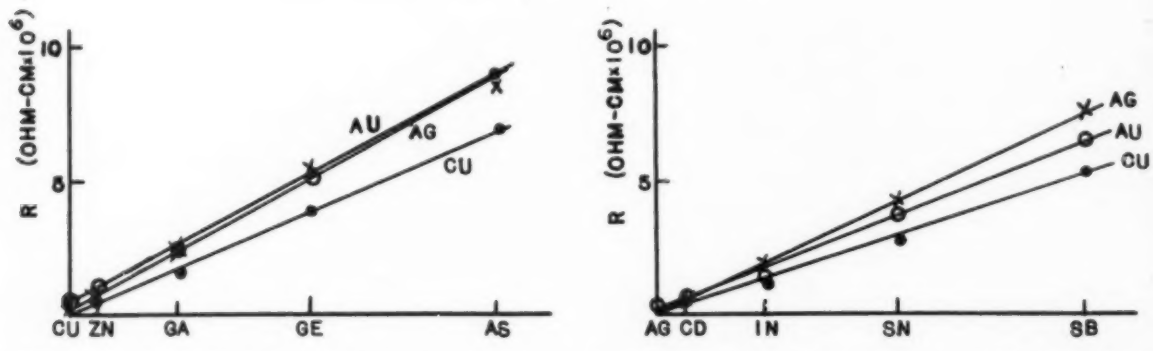

FIG. 18. Increase in resistance due to one atomic percent of various metals dissolved in Cu, Ag, and Au. The abscissa are proportional to the squares of the difference in valency between the solvent and solute metals. Similar results are obtained if the solute metals come from other rows of the periodic table. Data from Linde (reference 21).

A theory of the resistance of binary mixtures on the basis of the Bloch theory has been given by Nordheim. He finds that if x is the concentration of atom A, so that $(1-x)$ is that of atom B, the resistance, R_0, is proportional to $x(1-x)$. A plot of R_0 as a function of the concentration x is a simple bell-shaped curve with a maximum at a concentration of 50 percent. As we have seen (Fig. 4) this is just the type of curve which is found experimentally for the Ag-Au alloys. Similar curves are found for other binary alloys, the component metals of which are mutually soluble in all proportions, and which exist in but a single phase, e.g., K−Rb; Pt−Pd; In−Pb. (Cf. Fig. 19.)

A somewhat different type of curve is found for alloys of the noble metals with the transition metals, as illustrated in Fig. 20 for the case of alloys of Cu, Ag, and Au with Pd. The maximum resistance is shifted toward the Pd end of the curve. The explanation of Mott is briefly as follows. As we have already mentioned, the relatively high resistance of the transition metals, including Pd, is due to the presence of an incomplete d shell, so that transitions from the s band, which carries most of the current, to the

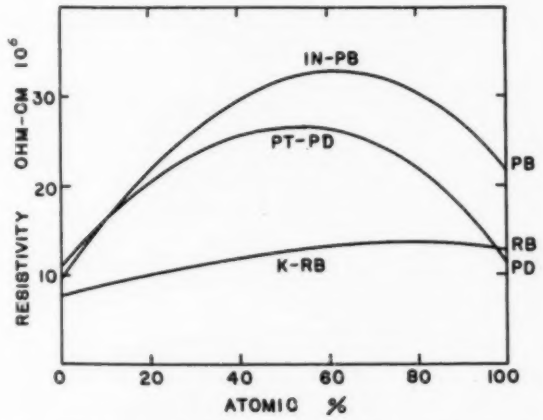

FIG. 19. Resistivity of K-Rb, Pt-Pd, and In-Pb alloys as a function of the atomic concentration. $T=25°C$ for all curves. Data from *International Critical Tables*.

d band are possible. In the alloys under consideration the d band is incomplete for all concentrations of Pd above about 40 percent. The abnormally high values of the resistances of the alloys above this concentration are due to s-d transitions.

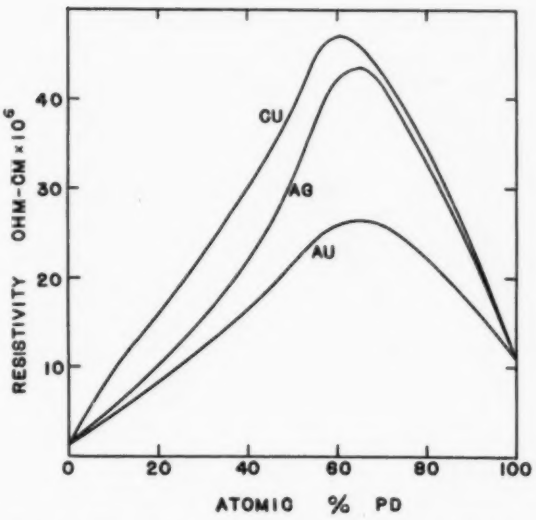

FIG. 20. Resistivity of Cu-Pd, Ag-Pd, and Au-Pd alloys as a function of the atomic percent Pd. Cu-Pd and Ag-Pd from Svensson,* and Au-Pd from Geibel (*International Critical Tables*).

In Fig. 21 we give a plot of the resistivity of the Cu-Ni alloys at several temperatures, according to the measurements of Svensson. These alloys are ferromagnetic for concentrations of nickel above about 40 atomic percent. Constantan, with the approximate composition CuNi, is a member of this series. Svensson attempts to correlate his results by expressing the resistance as the sum of three terms: (1) R_T, resulting from thermal motion, (2) R_0, which gives the resistance due to the random distribution of the different types of atoms, and (3) R_F, a ferromagnetic part which is a function of the magnetization. A qualitative theoretical discussion has been given by Mott.[20a]

C. Order-Disorder Alloys[25]

We have shown (Fig. 5) the resistance-concentration diagram for the copper-gold alloys. The quenched alloys give a simple bell-shaped curve similar to that of the silver-gold alloys. If the alloys are annealed at temperatures below 400°C, the resistance drops sharply in the neighborhood of the compositions CuAu and Cu_3Au. On the basis of chemical and resistivity measurements, Tammann suggested that the atoms take up more or less regular ordered positions at these concentrations. The ordered structure was

* Ann. d. Physik **14**, 699 (1932).

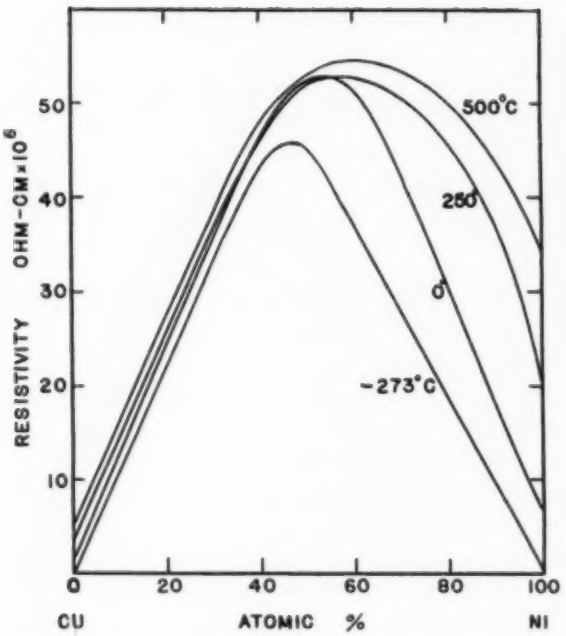

FIG. 21. Resistivity of Cu-Ni alloys. At 0, 250 and 500°C from Svensson.* At −273°C from Krupkowski and de Haas.†

later definitely proved for the Cu_3Au alloy by analysis of the "superstructure" lines in the x-ray pattern by Johansson and Linde.[26] Since that time, many other ordered alloys have been found. Resistivity measurements have played an important role in both their discovery and investigation, supplementing x-ray and specific heat data. The copper-gold alloys have perhaps been investigated more thoroughly than any other system, and much of our discussion will be confined to Cu_3Au as a typical example.

The face-centered lattice of the copper-gold system can be considered to be a superposition of four interpenetrating simple cubic lattices. At high temperatures, the atoms are distributed at random over the lattice points, but somewhat below 400°C the gold atoms of Cu_3Au tend to congregate on but one of these simple cubic lattices, forming an ordered structure. At the composition CuAu, below a certain critical temperature, the copper and gold atoms segregate on alternate planes. The spacing between these planes changes, and the structure changes from cubic to tetragonal.

* Ann. d. Physik **25**, 263 (1936).
† Comm. Leiden No. **194**, 1 (1928).

The equilibrium degree of order depends on the temperature. The distribution is random above the critical temperature, T_c, and order gradually takes place as the temperature falls below T_c. A number of different definitions of the degree of order existing in a crystal have been suggested, perhaps the best known being that of Bragg and Williams.[27] Let us designate the two types of atoms in the alloy by A and B. When perfect order exists, the A atoms will occupy a subsidiary lattice, and positions on this lattice will be called α-sites. Similarly, the B atoms will occupy β-sites. In the partially ordered crystal, let the probability that an A atom be on an α-site be p_A. Finally let r_A be the value of p_A for a completely random distribution (e.g., $r_A=\frac{1}{4}$ for Cu_3Au, if A refers to gold). The degree of (long distance) order is defined as:

$$S=\frac{p_A-r_A}{1-r_A}, \tag{37}$$

so that $S=1$ for perfect order, and $S=0$ for a random alloy. This definition has been criticized in that no account is taken of any ordering of neighbors that may exist, and attempts to take the local ordering into account have been made by Bethe,[28] Peierls,[29] Kirkwood,[30] and others. The most suitable definition of order for considerations of resistivity measurements is not known. The two critical distances are the electronic wave-length (~10A) and the mean free path

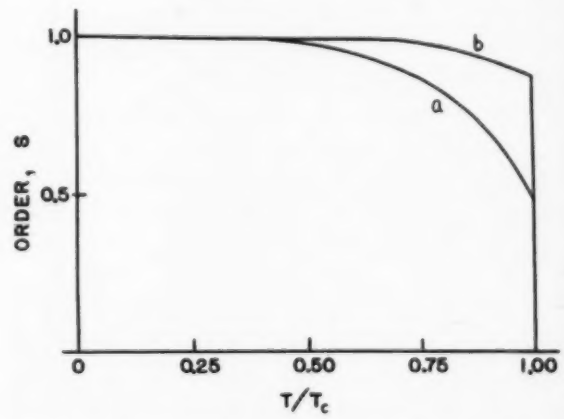

FIG. 22. Theoretical curves of long distance order, S, as a function of T/T_c for an alloy of the type A_3B. (*a*) Bragg-Williams. (*b*) Peierls (for face-centered cubic lattice).

(~100A); the amount of order existing in regions of each of these dimensions probably plays a role.

Theoretical curves of Bragg and Williams and of Peierls giving the degree of order, S, as a function of temperature for an alloy of the type A_3B are shown in Fig. 22. The long distance order changes abruptly at the critical temperature, and there is a latent heat at the transition point. This is contrary to the behavior of alloys of the type AB, for which there is no latent heat, and the degree of order starts in at zero at the transition point and gradually rises as the temperature falls.

In Fig. 23 we show the resistivity-temperature curves for Cu_3Au as observed by Sykes and Evans.[31] Curve a is for the equilibrium state, which was obtained after long annealing. In curve b, the cooling rate was 30°C per hour. Curve c is extrapolated from above the critical temperature to the value obtained for an alloy quenched from 450°C, and represents the resistance curve for the completely random alloy. Due to the relatively slow rate at which different atoms in the crystal interchange places, the rate of approach to the equilibrium configuration is slow except at temperatures close to the transition point. At room temperature, the rate is so slow that the alloy will exist indefinitely in a metastable state. Measurements of the resistivity as a function of temperature for different rates of cooling or heating have been found extremely useful in determining the rates of approach to equilibrium.

Unfortunately, however, resistivity measurements cannot be used for exact quantitative work because the resistivity is not simply related to the degree of order. Following the general theory we have discussed earlier, we should expect that the resistance is the sum of two terms, a temperature dependent term, R_T, which arises from the thermal motion of the atoms, and a second term, R_0, giving the resistance due to the disordered arrangement of the atoms which will be dependent on the temperature only indirectly through its dependence on order. Purely for simplicity, Bragg and Williams assumed that the second term is a linear function of the degree of order, S, vanishing when the order is perfect. As may be seen from a comparison of Figs. 22 and 23, there is some justification for this assumption. The subject has been treated theoretically by Muto,[32] who extended Nordheim's treatment of random alloys to cover the order-disorder alloys. He finds a quadratic dependence of R_0 on S. The calculation assumed no correlations between the types of atoms on neighboring sites, and so neglected any local ordering that may be present.

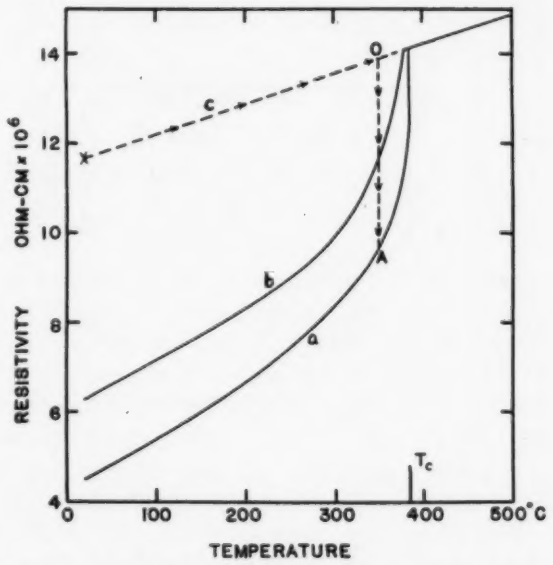

FIG. 23. Resistivity as a function of temperature for Cu_3Au. (a) Quenched; (b) Cooled at a rate of 30°C/hr. (c) Slow cooling, in equilibrium above 350°C. The path OA is discussed in the text. Data from Sykes and Evans (reference 30).

In a very interesting series of papers, Sykes and Jones[33] have investigated the formation of nuclei and their effect on the resistivity of Cu_3Au. The quenched alloy is heated rapidly to about 350°C, and the resistivity rises to the point 0 (Fig. 23), corresponding to a random alloy. Ordering has not had time to set in. If the alloy is kept at this temperature, the resistance gradually drops along the line OA until finally it reaches the equilibrium value. In each crystal, the gold atoms may segregate on any one of the four simple cubic lattices which make up the face-centered structure. Nuclei may start on any of these at random and grow until they meet one another. The crystal then consists of a large number of small regions in each of which the structure is ordered, but there is a discontinuity or jump in phase at the boundaries. Some of these

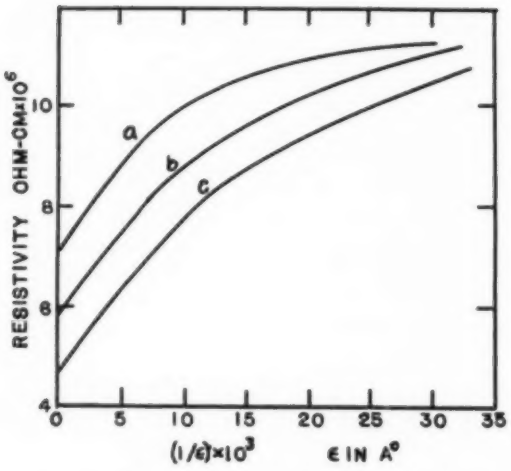

FIG. 24. Resistivity as a function of the apparent size of nuclei. Annealing temperatures: (*a*) 376°C; (*b*) 346°C; (*c*) 298°C. Data from Jones and Sykes (reference 22).

regions will gradually grow at the expense of the others, so that the nuclei increase in size. As this happens, the resistance drops. The average size of the nuclei during different stages of this process were estimated by Sykes and Jones from the widths of the superstructure lines in the x-ray powder diagram. Different times of anneal were taken, corresponding to about equal changes in the resistance, and then the alloys were quenched in water. In this way a whole series of metastable states, corresponding to different stages in the growth of the nuclei, were obtained for the study of the resistivity and its dependence on the size of the nuclei.

In Fig. 24 we give a plot of the resistivity as a function of the apparent nuclei size for three different temperatures of anneal as obtained by Jones and Sykes. The true size of the nuclei is estimated to be about one-half of the apparent size, ϵ, as determined by x-ray methods. The differences between the three curves are due to the differences in the degree of order in the individual nuclei at the various annealing temperatures. The curves become straight lines for values of $(1/\epsilon)$ below about 10^{-2} (ϵ in A). In this region the nuclei size is large compared with the width of the boundaries, and the change in resistance can be considered to be due to the reflection of electrons from the boundaries. Taking the effective number of free electrons per atom equal to unity, Jones and Sykes estimate that the reflection coefficient at a boundary is about one-tenth. Actually, it may be somewhat greater than this value.

There is an anomaly in the specific heat of the quenched alloy as it is heated between 100° and 200°C, long before there is any appreciable effect on the electrical resistance. This must represent a very early stage in the formation of nuclei. Probably a large amount of local ordering takes place which involves comparatively large energy changes, but which is confined to such small regions that it has little influence on the resistance.

The resistivity of an ordered alloy is changed markedly by cold work. In Fig. 25 we give the results of Dahl on the effect of plastic deformation on the resistivity of a Cu_3Au alloy. With sufficient deformation, the resistivity of the annealed alloy approaches that of the quenched alloy. As this occurs, the x-ray superstructure lines disappear, indicating the return of a random structure. A large change of resistance on cold work is often taken to be an indication (although not a certain one) of an ordered alloy.

As a second example of the effect of order on resistivity, we show in Fig. 26 the resistance of β-brass (CuZn) as a function of temperature. The

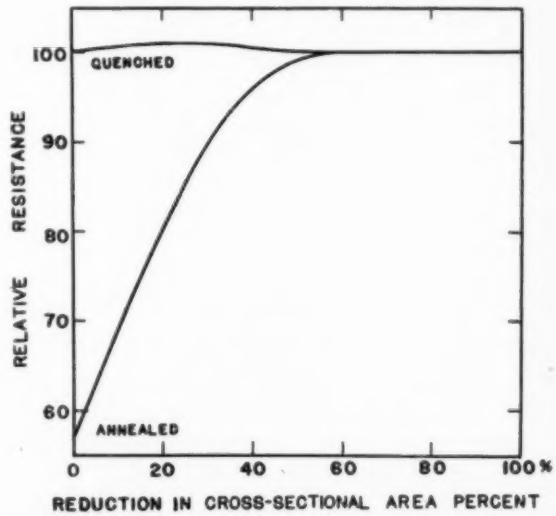

FIG. 25. Effect of plastic deformation on the resistance of Cu_3Au alloy. Data from O. Dahl.*

structure is body-centered cubic, and in the ordered state the Cu and Zn atoms tend to segregate on the two interpenetrating simple cubic lattices which make up the structure. Ac-

* Zeits. f. Metallkunde **28**, 133 (1936).

cording to the theory of Muto,[32] the resistance due to disorder, R_0, should be proportional to $(1-S^2)$ where S is the degree of order (Eq. (37)). Plots of $1-S^2$ as a function of temperature according to the theories of Bragg and Williams and of Bethe are shown below the resistivity curve.

D. Age-Hardening Alloys[34]

When a supersaturated alloy is quenched from a high temperature, one or more of the phases may begin to precipitate out of the solid solution, either at room temperature or after annealing. This causes a gradual change in the physical properties of the alloy. The hardness usually increases with time to a maximum, after which there is a gradual decrease. The electric and magnetic properties also change during the hardening process. The resistance sometimes decreases, but often there is an initial increase, followed by a decrease. The maximum in resistance usually comes before the maximum in hardness.

The resistance will depend, of course, on the distribution of atoms in the lattice. A random distribution yields a high resistance, and a conglomerate of crystals of individual pure metals or compounds a comparatively low resistance (cf. Figs. 3 and 4). Thus one might expect the resistance to decrease as a metal precipitates from solid solution. However, as Mott[35] has pointed out, the random distribution may not be the one which gives the highest resistance. If the atoms are distributed in very small clusters, such that the average size of a cluster is of the order of magnitude of an electron wave-length ($\sim$10A) they may be more effective in scattering the waves than if the clusters are larger or smaller. The maximum in resistance may therefore correspond to a very early stage in the precipitation.

VIII. The Weidemann-Franz Law

It is not our purpose to discuss heat conductivity, or such subjects as thermoelectricity and the various galvano- and thermomagnetic effects in metals, even though they are very closely related to our present study. We must, however, make some mention of the Weidemann-Franz law. As is well known, heat may be conducted in a metal either by the conduction electrons or through the lattice itself, by means of the thermal vibrations. In insulating crystals, only the latter is effective. In metals, conduction by electrons is usually much the greater of the two.

The Weidemann-Franz law can be derived under quite general considerations on the basis of the Bloch theory, and states that the ratio of the heat conductivity, K, to the electrical conductivity, σ, is

$$K/\sigma=(\pi^2/3)(\kappa^2/e^2)T.$$

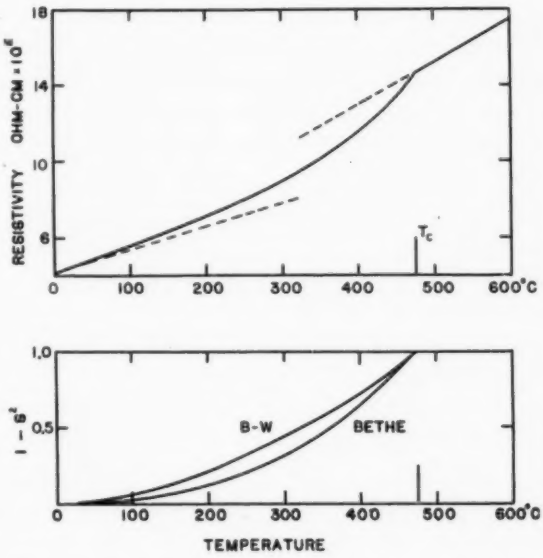

FIG. 26. Top. Resistance of β-brass (composition 51.25 atomic percent Cu, 48.75 percent Zn) as a function of temperature. Data from W. Webb.* Bottom: Plot of $1-S^2$, where S is the degree of long distance order, according to the theories of Bragg and Williams and of Bethe.

The numerical factor is slightly larger than that obtained from the Drude theory ($\pi^2/3$ in place of 3) and agrees somewhat better with the experimental values. The derivation applies only to conduction by electrons, and so neglects any contribution to the heat conductivity by the lattice vibrations. It is valid whether the resistance is due to disorder (as in alloys) or is due to thermal motion of the atoms, but in the latter case only for temperatures above the Debye characteristic temperature. Furthermore, it is supposed that κT is small compared with the width of the conduction band, so that deviations may be expected, for example, in the transition metals at high temperatures.

* Phys. Rev. **55**, 297 (1939).

IX. Conclusion

In this brief survey, no attempt has been made at completeness. We have merely attempted to give illustrative examples of some of the various types of problems connected with the conduction of electricity in metals and alloys, and, wherever possible, to correlate them on the basis of the Bloch theory. Among the subjects upon which we have not touched are (1) dependence of resistance on crystallographic directions, (2) resistance of liquid metals, (3) the effect of polymorphic transitions, (4) the influence of an external magnetic field on the resistance, (5) the temperature coefficient of the resistance of alloys, (6) the structure sensitive properties, such as the effect of cold work, and (7) the resistance of thin films.

With a deeper understanding of the fundamental causes of resistance in metals and alloys, resistivity measurements promise to play an increasing role in the study of other physical properties. This is especially true of problems connected with the arrangement of different types of atoms in an alloy. There is a great need for further study, of both an experimental and a theoretical nature, and if this article provides any stimulus for further activity in this direction, it will have served its purpose.

Before concluding, it might be well to point out some phenomena for which the Bloch theory has not as yet provided even a qualitative understanding. The best known of these is, of course, superconductivity. A second is the discovery of De Haas and co-workers[35] at Leiden that there is a minimum in the resistance-temperature curve of gold at liquid helium temperatures. The increase in resistance becomes very rapid at extremely low temperatures ($<1°K$). The curve suggests that the resistance may become infinite at the absolute zero. The position of the minimum depends on the purity of the gold, shifting to lower temperatures as the amount of impurity is reduced. No explanation of this phenomenon has been given. A third example is provided by the existence of a class of semi-conductors with incompletely filled d bands.[36] We have mentioned (Section V, G) that a necessary condition for an insulator is that there be an even number of valence electrons per unit cell; if the number is odd, one would expect a metal. Substances like MnO, CoO, Mn_3O_4, etc., violate this rule since they are not metallic, but are semi-conductors.

The Bloch theory is based on the assumption that each electron moves independently in a periodic potential field. The electrostatic interaction of the electrons is neglected, except insofar as it is taken into account through the potential of the average space charge of the electrons. The theory is extremely valuable because it provides a simple physical picture which gives explanations (in many cases, quantitative) of a very wide range of phenomena. It should be recognized, however, that it may be necessary in some cases to go beyond the Bloch picture to explain things which depend to a large extent on electron interaction, or on the cooperative action of a large number of electrons.

Bibliography

(*a*) *References to Books*

The references given below refer only to the few specific examples of various phenomena which have been discussed in the text. A fairly complete summary of the experimental literature extending up to about the year 1934 is given by W. Meissner, *Handbuch der Experimentalphysik*, Vol. XI/2. Other sources of experimental data are:

1. G. Gruneisen, *Handbuch der Physik*, **24**.
2. G. Borelius, *Handbuch der Metallphysik*, I/1 (Leipzig, 1935).
3. W. Hume-Rothery, *The Metallic State* (Oxford, 1931).

The following books and articles devoted mainly to the theory have been found useful:

1. A. Sommerfeld and H. Bethe, *Handbuch der Physik* **24/2** (1933).
2. N. F. Mott and H. Jones, *Theory of the Properties of Metals and Alloys* (Oxford, 1936).
3. A. H. Wilson, *Theory of Metals* (Cambridge, 1936).
4. H. Fröhlich, *Elektromentheorie der Metalle* (Berlin, 1936).
5. A. H. Wilson, *Semi-Conductors and Metals* (Cambridge, 1939).

(*b*) *References to Journal Articles*

1. R. D. Tolman and T. D. Stewart, Phys. Rev. **8**, 97 (1916); **9**, 164 (1917).
2. It has been shown by Darwin that the experiment should give the free electron value of e/m; the "effective" mass does not enter. C. G. Darwin, Proc. Roy. Soc. **A154**, 61 (1936).
3. E. Gruneisen, Verh. d. D. Phys. Ges. **15**, 186 (1913); Leipziger Vortrage, **46** (1930); Ann d. Physik **16**, 530 (1933).
4. P. W. Bridgman, Proc. Am. Acad. **72**, 157 (1938).
5. P. Drude, Ann. d. Physik **1**, 566 (1900); **3**, 370, 869 (1900); **7**, 687 (1902); **14**, 936 (1904). H. A. Lorentz, *Electromentheorie der Metalle* (Leipzig, 1909).
6. The theory is summarized in a recent book: E. H. Hall, *A Dual Theory of Conduction in Metals* (Cambridge, 1938).
7. F. Seitz and R. P. Johnson, J. App. Phys. **8**, 84, 186, 246 (1937).
8. Cf. Mott and Jones, p. 96.
9. F. Bloch, Zeits. f. Physik **59**, 208 (1930). See also Gruneisen, reference 3. A simplified derivation has been given by F. Sauter, Naturwiss. **7**, 109 (1930).
10. W. J. de Haas and G. J. Van den Berg, K. Onnes Lab. Leiden Comm. Nos. 241–252, Suppt. No. 82A (1936), have measured the resistivities of a number of metals between 1° K and 20° K. The results can be expressed in the form CT^b with b usually between 4 and 5, but for Pt, $b=2$.
11. W. G. Baber, Proc. Roy. Soc. **A158**, 383 (1937).
12. See, for example, J. K. Roberts, *Heat and Thermodynamics* (Blackie, 1933), p. 437.
13. N. H. Frank, Phys. Rev. **47**, 282 (1935).
14. J. Bardeen, J. Chem. Phys. **6**, 369 (1938).
15. N. F. Mott, Proc. Phys. Soc. Lond. **46**, 680 (1934); Proc. Roy. Soc. **A153**, 699 (1936). See also the theoretical discussion by A. H. Wilson, Proc. Roy. Soc. **A167**, 580 (1938).
16. Cf. also Mott and Jones, p. 265.
17. M. F. Manning and H. M. Krutter, Phys. Rev. **51**, 761 (1937).
18. J. Bardeen, Phys. Rev. **52**, 688 (1937). Similar calculations have been made by E. L. Peterson and L. W. Nordheim, Phys. Rev. **51**, 355 (1937).
19. W. Gerlach, Zeits. f. Physik **59**, 847 (1930).
20. (a) N. F. Mott, Proc. Roy. Soc. **A153**, 699 (1936); (b) **A156**, 368 (1936). See also A. H. Wilson, reference 15.
21. A. L. Norbury, Trans. Faraday Soc. **16**, 570 (1921).
22. J. O. Linde, Ann. d. Physik **10**, 52 (1931); **14**, 353 (1932); **15**, 219 (1932).
23. N. F. Mott, Proc. Camb. Phil. Soc. **32**, 281 (1936).
24. N. F. Mott, Proc. Phys. Soc. Lond. **46**, 680 (1934); also reference 22.
25. For a general review of this subject, see F. C. Nix and W. Shockley, Rev. Mod. Phys. **10**, 1 (1938). See also G. Borelius, Proc. Phys. Soc. **49E**, 77 (1937).
26. C. H. Johansson and J. O. Linde, Ann. d. Physik **78**, 439 (1925).
27. W. L. Bragg and E. J. Williams, Proc. Roy. Soc. **A145**, 699 (1934); **A151**, 540 (1935).
28. H. A. Bethe, Proc. Roy. Soc. **A150**, 552 (1935).
29. R. Peierls, Proc. Roy. Soc. **A154**, 207 (1936).
30. J. G. Kirkwood, J. Chem. Phys. **6**, 70 (1938).
31. C. Sykes and H. Evans, J. Inst. Metals **58**, 255 (1936).
32. T. Muto, Sci. Papers Inst Phys. Chem. Res. **30**, 99 (1936); **31**, 153 (1937).
33. C. Sykes and F. W. Jones, Proc. Roy. Soc. **A157**, 213 (1936); **A166**, 376 (1938).
34. For a brief review of this subject, see C. H. Desch, Proc. Phys. Soc. Lond. **49E**, 103 (1937).
35. Discussion following a paper by M. L. V. Gayler, J. Inst. Metals **60**, 55 (1937).
36. W. J. de Haas, H. B. G. Casimir and G. J. Van den Berg, Physica **5**, 225 (1938), where references to earlier work may be found.
37. J. H. de Boer and E. J. W. Berwey, Proc. Phys. Soc. Lond. **49E**, 59 (1937).

Stresses in Freely Falling Chimneys and Columns

FRANCIS P. BUNDY

Ohio University, Athens, Ohio

A chimney or column is considered as a rigid rod, initially in a vertical position, and hinged at its base. The internal forces and stresses which are developed as the rod falls freely from the vertical position are calculated. It is shown that the inertial reaction forces produce a bending moment which results in a tension on the leading side and a compression in the trailing side of the rod. This tension in the leading side has its maximum value at roughly 0.3 to 0.5 the height of the rod, depending upon its shape and the angle of inclination from the vertical. This tension usually produces a transverse rupture in large falling chimneys or columns, though not always. These transverse ruptures should occur at the point of maximum tension.

It is shown that in very tall columns or chimneys the vertical shear stress near the base is sufficient to produce a tension rupture there—and usually does. The positions of these latter ruptures cannot be predicted accurately in actual cases because of the greatly variable conditions which may exist at the point of support after dynamiting.

Calculations are given for the cases of solid columns of uniform cross section, solid columns of uniformly tapered cross section, and uniformly tapered chimneys of constant wall thickness. Photographs of actual falling chimneys are presented to check the theory.

Introduction

THE falling of a large tall chimney is a very spectacular and interesting sight. There is usually much speculation as to where the chimney should break as it falls. Sutton[1] has pointed out that any part of a chimney which lies above the center of percussion is forced to accelerate more rapidly than a particle free to move along the same path under the force of gravity, and consequently the part of the chimney above the center of percussion tends to lag behind the general motion of the chimney as a whole. From this he concludes that the chimney should break at the center of percussion or above. Reynolds[2] has shown that the above reasoning is correct except for the conclusion concerning the point of breaking. He calculated the bending moment and transverse shear at various points along the chimney. He found the bending moment to be maximum at one-third the height for a chimney of uniform cross section. He concluded that a falling chimney should break near the point of maximum bending moment and showed a drawing of a newspaper photograph from the *Philadelphia Recorder*, to support his conclusion.

These articles interested the author and led him to perform some experiments with models. The models acted more nearly in accordance with Reynolds' idea than Sutton's, but not exactly with either. This discrepancy showed the necessity of a more complete analysis of the stresses. In this paper a rather detailed analysis is made of the stresses which are developed in a freely falling chimney. The results are shown to be accurately consistent with data from actual large falling chimneys.

General Theory

Before rupture occurs, a falling chimney may be considered as a rigid body rotating in a vertical plane about its base. The notation which will be used in this paper is as shown in Fig. 1, and as follows: h = total height, I = mass moment of inertia about 0, k = radius of gyration, $\bar{r}$ = distance from 0 to the center of gravity, $k^2/\bar{r}$ = distance from 0 to the center of percussion, θ = angle of inclination from the vertical, A_r = cross-sectional area at distance r from 0, J_r = area moment of inertia of cross section about the neutral axis at distance r from 0, V = total volume of walls, and W = total weight of chimney.

The equations of motion show that if the chimney starts from rest in a vertical position the angular acceleration is:

$$\alpha=\frac{\bar{r}}{k^2}g\sin\theta, \tag{1}$$

and the angular velocity is

$$\omega=\frac{1}{k}(2g\bar{r}(1-\cos\theta))^{\frac{1}{2}}. \tag{2}$$

Any particular element of length dr of the chimney must be in equilibrium under the inertial reaction forces and the external forces acting on it. Part of the external force *on a particular element* is provided by gravity, and part by the force transmitted from the adjacent parts of the chimney. The part contributed by the transmitted forces is determined by subtracting the gravitational forces from the inertial reaction forces. It is found that the net transverse force exerted by the element of length dr on the adjacent parts of the chimney is

$$dF\text{ (transverse)}=\frac{A_r}{V}\left(1-\frac{\bar{r}}{k^2}r\right)W\sin\theta dr, \tag{3}$$

where the direction of fall is considered positive. The transverse shear at any cross section at distance r from 0 is the sum of the transverse forces on the elements from r to the top. That is,

$$S_r=\int_r^h dF\text{ (transverse)}$$

$$=\frac{W\sin\theta}{V}\int_r^h A_r\left(1-\frac{\bar{r}}{k^2}r\right)dr. \tag{4}$$

The net longitudinal force exerted by the element dr on the neighboring parts is

$$dF\text{ (longitudinal)}$$

$$=dr\frac{A_r}{V}W\left[\cos\theta-2r\frac{\bar{r}}{k^2}(1-\cos\theta)\right], \tag{5}$$

where the inward radial direction is assumed positive. The "regular" longitudinal force at any transverse cross section is then,

$$P_r=\int_r^h dF\text{ (longitudinal)}$$

$$=\frac{W}{V}\int_r^h A_r\left[\cos\theta-2r\frac{\bar{r}}{k^2}(1-\cos\theta)\right]dr. \tag{6}$$

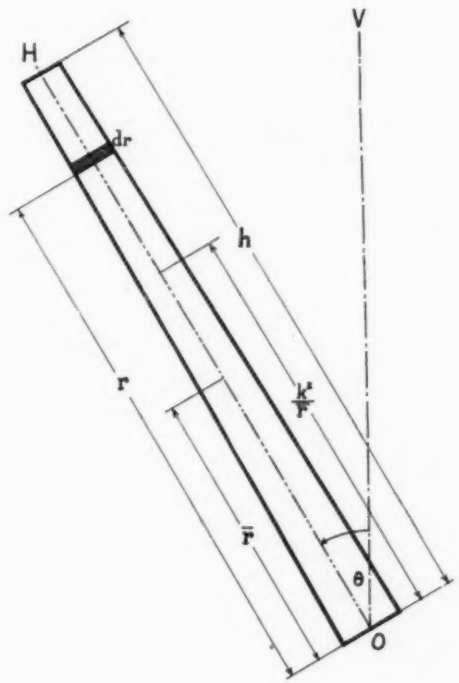

FIG. 1. Falling chimney as a rigid body.

The bending moment about a transverse axis normal to the plane of motion at height r is given by,

$$L_r=\int_{x=r}^{x=h}(x-r)dF\text{ (transverse)},$$

$$=\frac{W\sin\theta}{V}\int_{x=r}^{x=h}(x-r)A_x\left(1-\frac{\bar{r}}{k^2}x\right)dx. \tag{7}$$

This bending moment is in such a direction as to produce a tension in the leading side of the falling chimney.

The *total longitudinal stress* at any point in the chimney will be the sum of that due to the "regular" longitudinal force, P_r, and that caused by the bending moment. The longitudinal stress caused by the bending moment is maximum at

the leading and trailing sides and has the magnitude

$$s(BM)_r = \frac{L_r}{J_r} y_r, \tag{8}$$

where y_r is the distance from the "neutral surface" to the leading or trailing sides. This will be a tension on the leading side and a compression

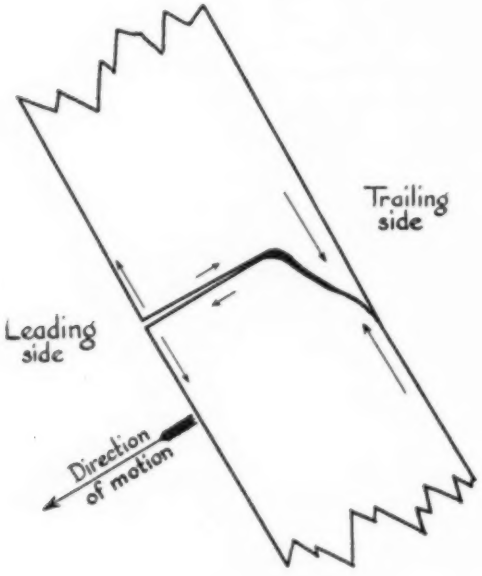

FIG. 2. General form of rupture started on leading side by longitudinal tension.

on the trailing side. The total stress at the leading side will be then,

$$s_L = P_r/A_r - L_r y_r/J_r, \tag{9}$$

while that at the trailing side will be

$$s_T = P_r/A_r + L_r y_r/J_r. \tag{10}$$

Brick-and-mortar work usually ruptures because of tension. A chimney would be expected to break on the leading side at the point where s_L has its maximum negative value. Such a break should be in a transverse plane and its position should be quite predictable if the chimney construction is homogeneous. A transverse rupture that starts on the leading side usually spalls off in the downward direction on the trailing side as shown in Fig. 2. This spalling effect is due to the combined action of the transverse shear and compressive stresses acting there when the break is impending. The emphasis of this paper is placed on the prediction of the location of this transverse rupture caused by excessive tension on the leading side.

Another type of break which is often observed takes place quite near the bottom, shown in Fig. 3(b) as *RR*. This type of rupture is due essentially to the tension produced by the vertical shear as shown in Fig. 3(a). The vertical shear s_v induces the horizontal shear s_v'; the two shears combine to produce a tension, T, normal to *RR*. This form of rupture is most likely to occur in very tall chimneys in which the vertical shear is large near the base—even for small angles of inclination. There are two such ruptures visible in Fig. 8(a), which portrays the fall of a 258-ft. chimney. The upper rupture is in a very advanced stage. These vertical shear ruptures near the base cannot be predicted accurately because of the

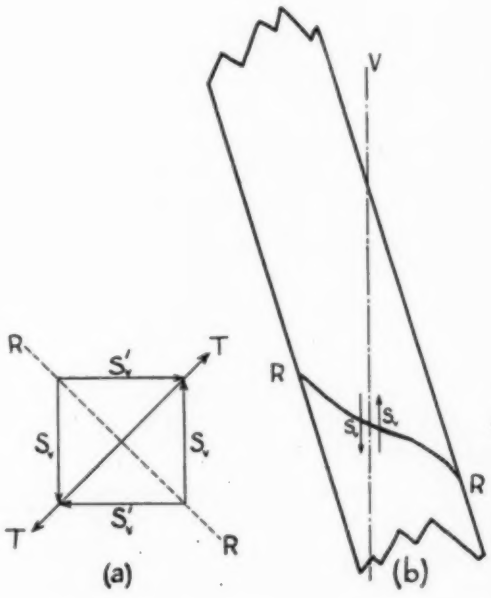

FIG. 3. General form of ruptures near base caused by vertical shear.

variable conditions at the base. For instance, the main point of support after blasting may be near the center or near the trailing side. No attempt

will be made in this paper to predict the exact location of these ruptures.

Any given falling chimney may not develop both types of ruptures described above. If the longitudinal tension rupture develops first, the probability of the development of vertical shear ruptures near the base is diminished very little because the forces near the base remain about the same. However, if vertical shear ruptures develop first, the probability of a longitudinal tension rupture in the leading side is very much reduced because the chimney buckles at the rupture point and the angular acceleration of the upper part of the structure is greatly reduced. Occasionally a chimney falls which develops vertical shear ruptures near the base without developing a longitudinal tension rupture.

In the following sections the theory which has been developed above will be applied to some special cases which approximate real chimneys. To calculate accurately the stresses in any particular chimney it is necessary to know all of its dimensions.

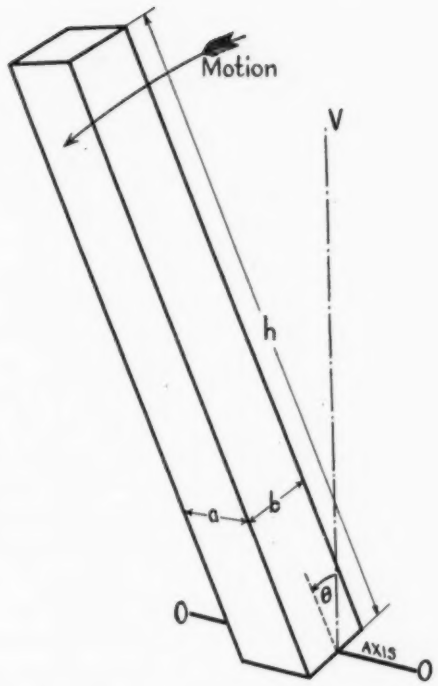

FIG. 4. Long solid column of uniform rectangular cross section.

Special Cases

I. LONG SOLID COLUMN OF UNIFORM RECTANGULAR CROSS SECTION

The dimensions will be taken as shown in Fig. 4. In this case, $I=\frac{1}{3}Wh^2/g$, $k=h/\sqrt{3}$, $\bar{r}=\frac{1}{2}h$, $k^2/\bar{r}=\frac{2}{3}h$, $A_r=\text{constant}=ab$, and $J_r=\text{constant}=ab^3/12$.

The transverse shear force at any height r is found to be

$$S_r=\frac{W\sin\theta}{4h^2}(h^2-4hr+3r^2). \tag{11}$$

This force is zero at $\frac{1}{3}h$; maximum in the negative direction at $\frac{2}{3}h$; maximum in the positive direction at $r=0$. The value at $r=0$ is three times that at $\frac{2}{3}h$. The values of this force at various heights and angles of inclination are shown graphically in Fig. 5(a).

The longitudinal force transmitted through a transverse cross section at height r above the base is in this case

$$P_r=\frac{W(h-r)}{2h^2}[(5h+3r)\cos\theta-3(h+r)]. \tag{12}$$

This force is portrayed graphically in Fig. 5(b). The force at the base becomes zero when the angle of inclination is about 50°, and becomes negative for angles greater than 50°. This effect is demonstrated by a tree or column "hopping" off its base when the angle of inclination becomes large.

The bending moment at any height r is

$$L_r=\frac{W\sin\theta}{4h^2}(-r^3+2hr^2-h^2r). \tag{13}$$

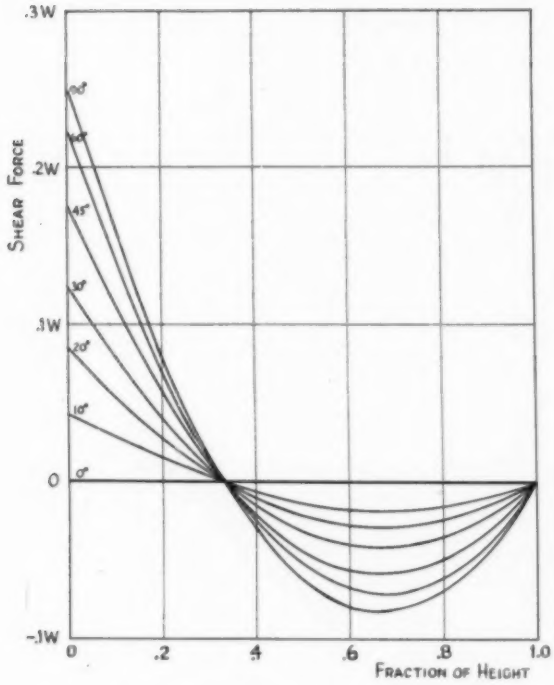

(a) Transverse shear force.

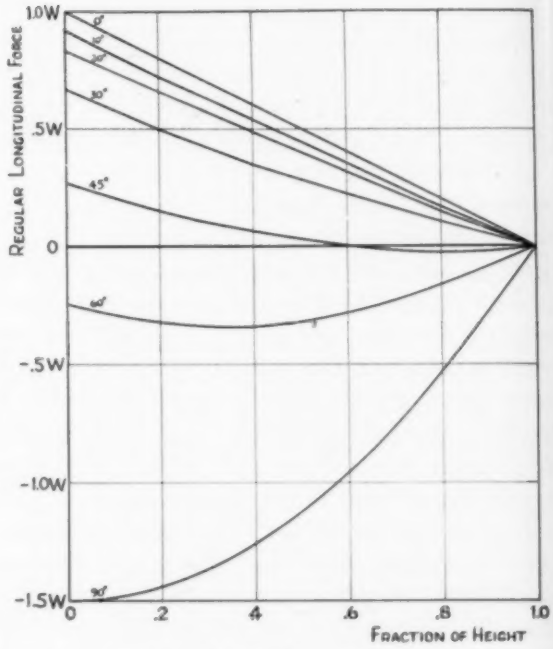

(b) Regular longitudinal force.

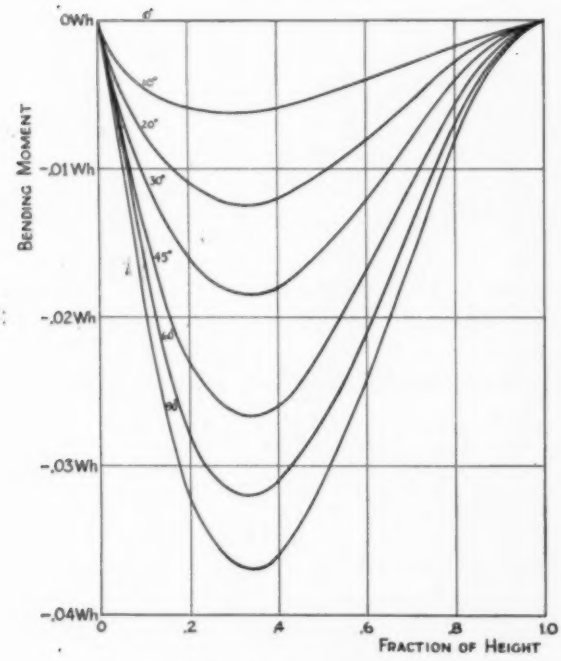

(c) Bending moment.

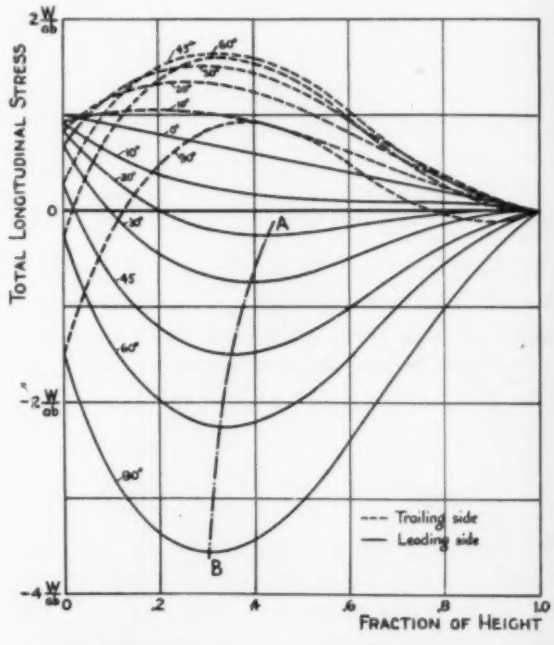

(d) Total longitudinal stresses in leading and trailing sides for the special case of rectangular cross section where $h = 10b$.

FIG. 5. Forces and stresses developed in a freely falling solid column of uniform cross section.

The bending moment is zero at $r=0$ and $r=h$. It has its maximum value at $r=\frac{1}{3}h$. Fig. 5(c) shows the values for various values of r and θ.

The total longitudinal stresses on the leading side and trailing side are, respectively,

$$s_L=\frac{W(h-r)}{2h^2ab}[(5h+3r)\cos\theta-3(h+r)]-\frac{3W\sin\theta}{2h^2ab^2}[r^3-2hr^2+h^2r], \tag{14}$$

$$s_T=\frac{W(h-r)}{2h^2ab}[(5h+3r)\cos\theta-3(h+r)]+\frac{3W\sin\theta}{2h^2ab^2}[r^3-2hr^2+h^2r]. \tag{15}$$

Fig. 5(d) shows the values of the total longitudinal stresses in the leading and trailing sides for various values of r and θ *for the special case of* $h=10b$. The full lines refer to the leading side and the dotted lines to the trailing side. It is interesting to note that a tension does not exist at any point along the leading side until the angle of inclination exceeds about 15°. The line AB is the locus of the point of maximum tension. If the column should break very early in its fall the most probable point of rupture would be about $0.42h$ while if it should not break until late in its fall it would be about $0.33h$. If the dimensions of a column, and the r and θ at which rupture occurs, are known, the tensile strength of the material may be determined. Fig. 6 is a drawing from a photograph of a falling chimney of uniform cross section. The photograph was printed in the *Philadelphia Recorder* of October 8, 1937. This chimney ruptured at $0.42h$ when at an angle of 20° from the vertical. This is precisely as predicted by the theory.

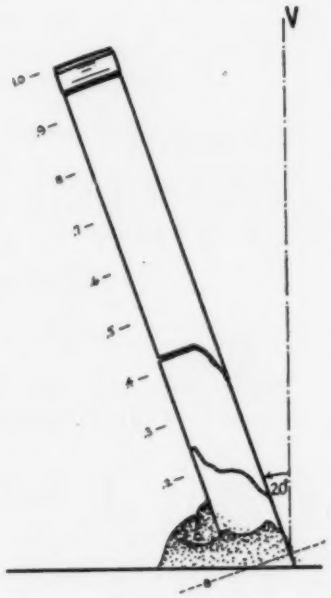

FIG. 6. Drawing taken from a photograph of a falling chimney of uniform cross section. (Photo from *Philadelphia Recorder* of October 8, 1937; drawing from J. B. Reynolds, reference 2.)

II. Long Solid Column with Uniform Taper and Circular Cross Section

Let the radius of cross section at the base be n times that at the top. Then if ρ_t = radius of cross section at top,

$$\rho_r=\rho_t\left[n+(1-n)\frac{r}{h}\right],$$

$$A_r=\pi\rho_t^2\left[n^2+2n(1-n)\frac{r}{h}+(1-n)^2\left(\frac{r}{h}\right)^2\right],$$

$$V=\tfrac{1}{3}\pi\rho_t^2h(1+n+n^2),$$

$$\bar{r}=\frac{h(n^2+2n+3)}{4(n^2+n+1)},$$

$$k^2=\frac{h^2(n^2+3n+6)}{10(n^2+n+1)},$$

$$\frac{k^2}{\bar{r}}=\frac{2h(n^2+3n+6)}{5(n^2+2n+3)}.$$

The transverse shear force is found to be

$$S_r=\frac{W\sin\theta}{n^2+n+1}\left\{(n^2+n+1)-\frac{5(n^2+2n+3)^2}{8(n^2+3n+6)}-\frac{3}{h}\left[\left[n^2r+\left[\frac{n(1-n)}{h}-\frac{5n^2(n^2+2n+3)}{4h(n^2+3n+6)}\right]r^2\right.\right.\right.$$
$$\left.\left.\left.+\left[\frac{(1-n)^2}{3h^2}-\frac{5n(1-n)(n^2+2n+3)}{3h^2(n^2+3n+6)}\right]r^3-\frac{5(n^2+2n+3)(1-n)^2}{8h^3(n^2+3n+6)}r^4\right]\right]\right\}. \tag{16}$$

The bending moment about the transverse axis normal to the plane of motion is

$$L_r=\frac{3W\sin\theta}{h(n^2+n+1)}\left\{r\frac{h}{3}\left[\frac{5(n^2+2n+3)^2}{8(n^2+3n+6)}-(n^2+n+1)\right]+r^2\frac{n^2}{2}+r^3\frac{1}{3h}\left[n(1-n)-\frac{5n^2(n^2+2n+3)}{4(n^2+3n+6)}\right]\right.$$
$$\left.+r^4\frac{1}{12h^2}\left[(1-n)^2-\frac{5n(1-n)(n^2+2n+3)}{(n^2+3n+6)}\right]-r^5\frac{(1-n)^2(n^2+2n+3)}{8h^3(n^2+3n+6)}\right\}. \quad (17)$$

The longitudinal force is

$$P_r=\frac{3W\cos\theta}{h(n^2+n+1)}\left[\left[\frac{h}{3}(n^2+n+1)-rn^2-r^2\frac{n(1-n)}{h}-r^3\frac{(1-n)^2}{3h^2}\right]\right]$$
$$-\frac{15W(1-\cos\theta)(n^2+2n+3)}{h^2(n^2+n+1)(n^2+3n+6)}\left[\left[\frac{h^2}{12}(n^2+2n+3)-r^2\frac{n^2}{2}-r^3\frac{2n(1-n)}{3h}-r^4\frac{(1-n)^2}{4h^2}\right]\right]. \quad (18)$$

To illustrate this case the detailed results for the special case of $n=1.5$ and $\rho_t=0.03h$ will be presented. In this particular case,

$$\rho_r=0.015h\left(3-\frac{r}{h}\right);\quad A_r=0.00283h^2\left[2.25-1.5\frac{r}{h}+0.25\left(\frac{r}{h}\right)^2\right];\quad \bar{r}=0.435h;\quad k=0.518h;\quad \frac{k^2}{\bar{r}}=0.617h.$$

The transverse shear force is

$$S_r=W\sin\theta\left[0.297-1.42\frac{r}{h}+1.62\left(\frac{r}{h}\right)^2-0.562\left(\frac{r}{h}\right)^3+0.064\left(\frac{r}{h}\right)^4\right]. \quad (19)$$

This function is shown graphically in Fig. 7(a). It is zero at $r=h$ and $r=0.304h$. Thus the bending moment must have its maximum value at $r=0.304h$.

The bending moment is

$$L_r=Wh\sin\theta\left[-0.297\frac{r}{h}+0.711\left(\frac{r}{h}\right)^2-0.542\left(\frac{r}{h}\right)^3+0.141\left(\frac{r}{h}\right)^4-0.0123\left(\frac{r}{h}\right)^5\right]. \quad (20)$$

This function is portrayed graphically in Fig. 7(b).

The longitudinal force is

$$P_r=-W\left[1.403-2.300\left(\frac{r}{h}\right)^2+1.021\left(\frac{r}{h}\right)^3-0.128\left(\frac{r}{h}\right)^4\right]$$
$$+W\cos\theta\left[2.403-1.423\frac{r}{h}-1.826\left(\frac{r}{h}\right)^2+0.969\left(\frac{r}{h}\right)^3-0.128\left(\frac{r}{h}\right)^4\right]. \quad (21)$$

This is shown graphically in Fig. 7(c). The upper part of the column begins to be under tension at about $\theta=45°$. The net longitudinal force at the base becomes zero when θ becomes slightly greater than 50°. At this inclination the transverse shear becomes effective in sliding the column off its base. This effect is clearly seen in Fig. 8(d).

Figure 7(d) portrays graphically the total longitudinal stress (due to longitudinal force and bending moment together) at various heights on the column and at various angles of inclination from the vertical. The earliest possible tension break on the leading side would occur at about $0.5h$ or slightly above, while delayed breaks would occur as low as $0.36h$.

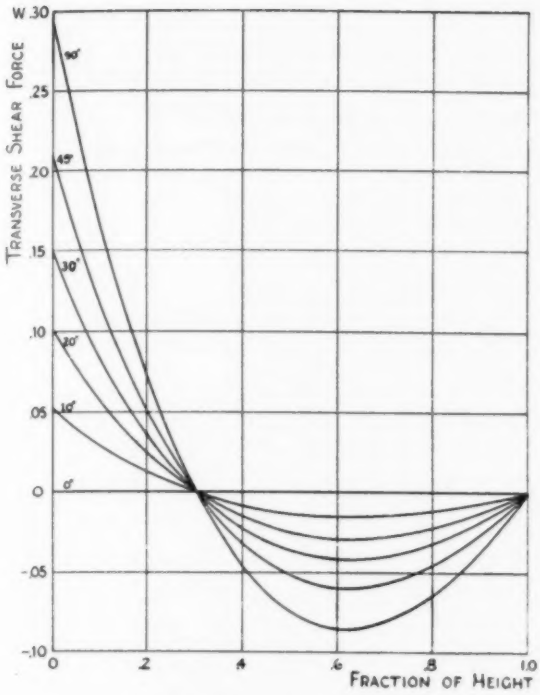

(a) Transverse shear force.

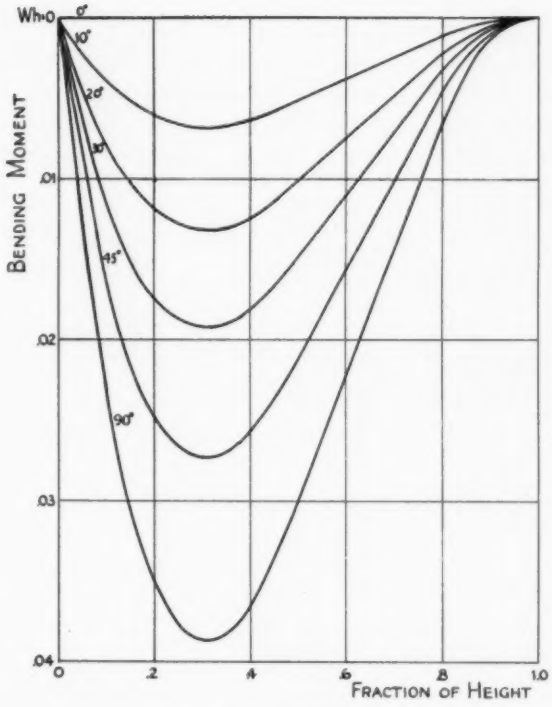

(b) Bending moment.

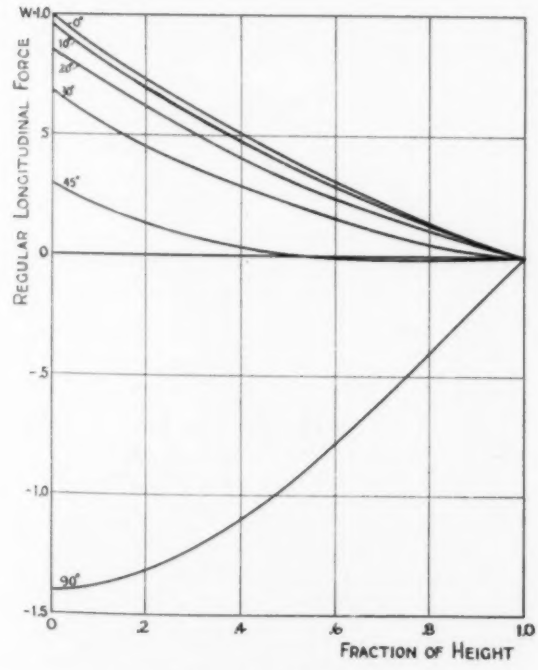

(c) Regular longitudinal force.

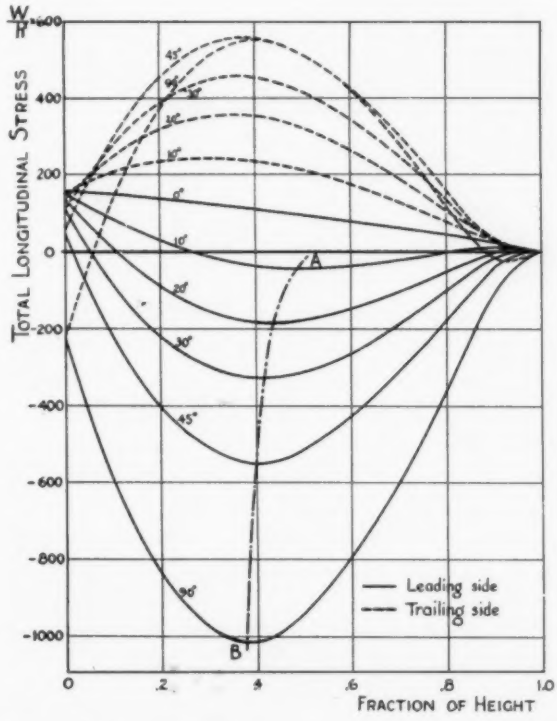

(d) Total longitudinal stresses in leading and trailing sides for the special case of $n=1.5$ and $\rho_1=0.03h$.

FIG. 7. Forces and stresses developed in a freely falling solid column with uniform taper and circular cross section.

III. Tapered Chimney of Uniform Wall Thickness

The general expressions for the forces and stresses in a chimney of uniform taper and uniform wall thickness in terms of the general dimensions are so complicated as to be of little use. Therefore, to illustrate, a chimney of definite dimensions will be considered. Let the chimney be 150 feet high, 15 feet outside diameter at base, 10 feet outside diameter at top, and let it have a wall thickness of 2 feet. Then,

$$A_r=\pi(\rho_1^2-\rho_2^2)=\left(66-31.4\frac{r}{h}\right)\text{ sq. ft.},$$

$$J_r=\frac{\pi}{4}(\rho_1^4-\rho_2^4)=\left[1770-2013\frac{r}{h}+618\left(\frac{r}{h}\right)^2-98.2\left(\frac{r}{h}\right)^3\right]\text{ ft.}^4,$$

$$V=7550\text{ cu. ft.},\quad k=0.531h,\quad \bar{r}=0.447h,\quad \frac{k^2}{\bar{r}}=0.637h.$$

The transverse shear force is,

$$S_r=W\sin\theta\left[0.286-1.312\frac{r}{h}+1.356\left(\frac{r}{h}\right)^2-0.330\left(\frac{r}{h}\right)^3\right]. \tag{22}$$

The values of this force for various values of r and θ are shown in Fig. 9(a).

The bending moment at height r is,

$$L_r=2.98W\sin\theta\left[-14.4\frac{r}{h}+33.0\left(\frac{r}{h}\right)^2-22.7\left(\frac{r}{h}\right)^3+4.1\left(\frac{r}{h}\right)^4\right]. \tag{23}$$

The values are shown in Fig. 9(b).

The "regular" longitudinal force is

$$P_r=W\cos\theta\left[2.42-1.31\frac{r}{h}-1.77\left(\frac{r}{h}\right)^2+0.66\left(\frac{r}{h}\right)^3\right]-W\left[1.43-2.09\left(\frac{r}{h}\right)^2+0.66\left(\frac{r}{h}\right)^3\right]. \tag{24}$$

The values are shown in Fig. 9(c).

The total longitudinal stresses in the leading and trailing sides are shown graphically in Fig. 9(d). The locus of the point of maximum tension in the leading side is shown by the line AB. Tension first develops in the leading side at approximately $0.52h$ when θ is about 15°. If the chimney remains intact until $\theta=90°$ the most probable breaking point is at $0.35h$. It is interesting to note that the locus of the point of maximum tension in this chimney is very nearly the same as that for the case of the *solid* tapered column [Fig. 7(d)].

In Fig. 8 the 258-ft. chimney at Detroit, the 120-ft. chimney at Firhill, Glasgow, and the 150-ft. chimney at Philadelphia approximate the conditions assumed in the last calculation. Therefore, the points of maximum tension in Fig. 9(d) should correspond to the points of rupture in these chimneys. Although the effect of perspective in these photographs slightly reduces the accuracy with which measurements can be made, they should give fair agreement with the theory. In the 258-ft. chimney the rupture was at about $0.47h$ and θ was about 20° or 25° when rupture occurred. This rupture is indicated in Fig. 9(d) as point P. The agreement with the theory is close.

The 120-ft. chimney seemed to pull apart quite easily, so the rupture probably occurred when tension first developed. The rupture was already in an advanced stage at $\theta=30°$. It was located at $0.51h$. The position of this rupture, which is

indicated by point Q in Fig. 9(d), is in good agreement with the prediction of the line AB.

The 150-ft. chimney was quite strong. It remained intact until θ was about 60°. The break occurred just before the photograph was taken and was at $0.39h$. This rupture is indicated by the point R in Fig. 9(d) and its position shows good agreement with the theory. This chimney was also beginning to "hop" off its base when the photo was taken. This effect is in agreement

(a) 258-ft. chimney at Detroit.

(b) 120-ft. chimney at Firhill, Glasgow.

(c) 20-ton rectangular chimney at Philadelphia.

(d) 150-ft. chimney at Philadelphia.

FIG. 8. Photographs of falling chimneys. (Wide World Photos, New York.)

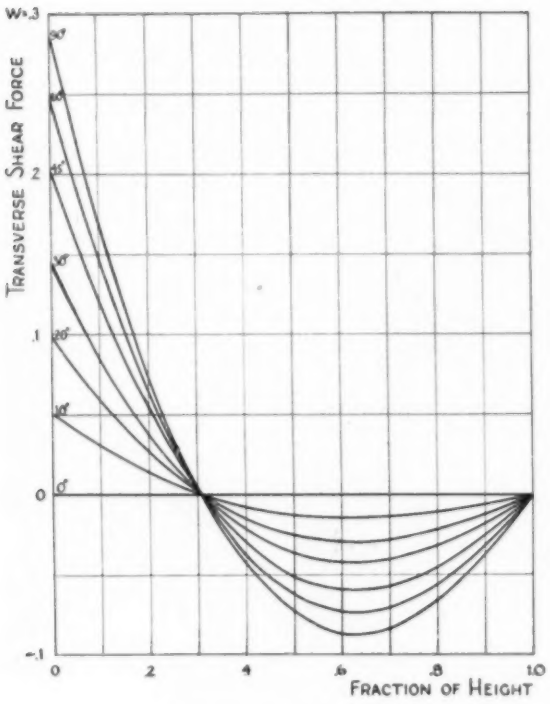

(a) Transverse shear force.

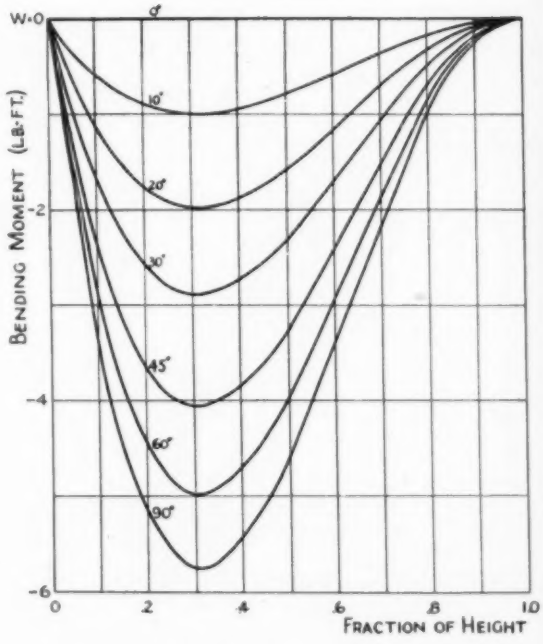

(b) Bending moment.

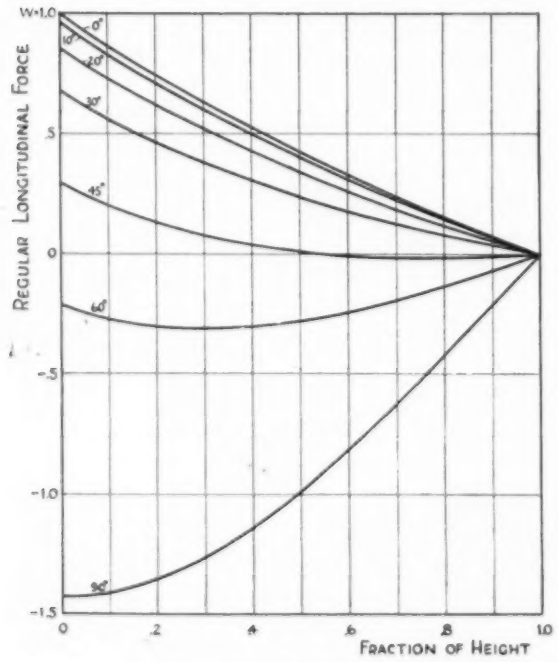

(c) Regular longitudinal force.

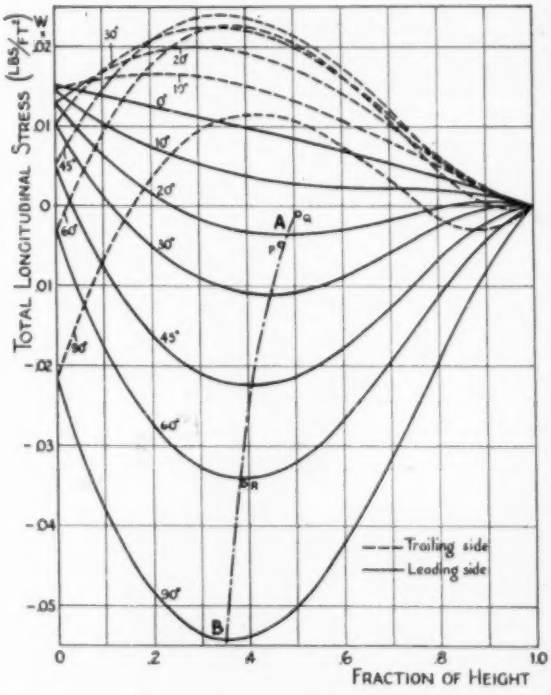

(d) Total longitudinal stress in the leading and trailing sides.

FIG. 9. Forces and stresses in a freely falling chimney with uniform taper and uniform wall thickness. (Radius base, 7.5 ft.; radius top, 5.0 ft.; wall thickness, 2 ft.; height 150 ft.)

with the prediction of Fig. 9(c) which shows that the longitudinal force at the base should become negative for angles of inclination greater than 50°.

The rupture in the chimney shown in Fig. 8(c) was at 0.63h and took place when θ was about 35°. This chimney was obviously much heavier in the lower part than in the upper. Calculations cannot be made for it because the details of its construction are not known. However, in general, the heavier the chimney at the base in comparison to the top, the higher will be the point of maximum tension in the leading side. Thus this chimney should have been expected to break at a rather high point.

Scale Effect

The mass of an object varies as the cube of its dimensions whereas its area varies as the square of its dimensions. Thus, the stresses set up by gravity and by inertial reactions in objects of the same proportions but of different sizes will be in proportion to their size. For this reason the stresses developed in a very large chimney are much greater than those in a smaller one of the same proportions. Consequently, if a large and a small chimney are made of the same material and the same proportions, the larger one would rupture earlier in its fall than the smaller one. This explains why the 258-ft. chimney in Fig. 9 is the only one of the four which developed a rupture due to vertical shear near the base.

Because of this "scale effect" it is not very practical to study small scale models in the laboratory. Such small models do not develop very large stresses while falling and do not rupture until quite late in their fall, if at all. The models mentioned at the beginning of this paper were made of small wood blocks built up without any adhesive material between them. Even these models did not break until the angle of inclination became about 60° or 70°. Long, very slender, brick-and-mortar models 10 or 15 ft. in height might be used to make tensile strength measurements by this method, although far more simple methods are obvious.

The theory developed here could be rather easily modified to determine the forces and stresses in an airplane propeller which is subject to angular acceleration, or in other similar rotating parts. It could also be modified to apply to such moving parts as connecting rods in an engine.

The author wishes to express his appreciation to Dean W. M. Young and Mr. C. W. Bankes for valuable discussions and assistance with regard to this problem.

---

[1] R. M. Sutton, Science **84**, 246 (1936).
[2] J. B. Reynolds, Science **87**, 186 (1938).

THE following mnemonic poem, designed to assist one in remembering the value of pi out to thirty decimal places, is quoted in the December issue of the *Cenco News Chats*, publication of the Central Scientific Company, Chicago, Illinois.

Now I, even I, would celebrate
 3 1 4 1 5 9
In rhymes inept the great
2 6 5 3 5
Immortal Syracusan, unknown nevermore,
 8 9 7 9
Who in his wondrous lore
 3 2 3 8 4
Passed on before,
 6 2 6
Gave men his teaching how to circles mensurate.
 4 3 3 8 3 2 7 9

Resumés of Recent Research

Synthesizing Speech Investigators of the physical nature of speech have from time to time artificially produced phonetic elements and simple speech sounds.[1] Recent articles[2] by Homer Dudley describe the Vocoder (Voice Coder) developed to remake connected speech automatically with a full range of phonetic elements and inflection. A synthesizer forms this speech from two basic sources; a buzzer-like tone consisting of a fundamental frequency and its harmonics, and a hiss-like sound with components of random frequency distribution. Suitable controls switch between these two sources of energy and regulate the pitch of the buzzer when used. At the same time controls of the energy in partial frequency bands determine the spectrum of the energy used. Substituting manual controls for the automatic ones of the Vocoder led to the Voder[3] or Voice Operation DEmonstratoR shown in the Bell System exhibits at the World's Fairs of this year. (See Fig. 1.)

FIG. 1. Apparatus used for synthesizing speech.

The Vocoder contains an analyzer which derives the necessary control information from the voice of a talker and supplies it to the synthesizer. While the synthesizer may thus reproduce the speech of the original talker, it is also possible to remake completely the character of the original by modifying the action of the control channels. Thus it may be degenerated to a dead monotone or a whisper; it may be transposed to any pitch register even below the deepest basso or above a childish treble; its inflection range may be increased, decreased or reversed, and pitch effects such as vibrato and quaver may be added. If the artificial pitch source is replaced by instrumental music or characteristic noises, it is possible to impress the speech spectrum upon them. Remarkable effects are thus produced ranging from a celestial choir to a whispering locomotive.

The synthesizing of speech provides a new tool for the better understanding of the nature of speech. Possible applications for this device are foreseen in the talkies and in transmitting speech with improved privacy and economy of frequency range.

Order-Disorder Transformations If the order-disorder transformation is regarded as a rearrangement of different sized atoms taking place in such a way that the ordered structure assumes a minimum volume, one would expect high hydrostatic pressure to promote an ordered condition in alloys partially or wholly disordered. One may actually predict the magnitude of such a pressure effect on thermodynamic considerations from a knowledge of the thermal expansion coefficient of the alloy.

Using electrical resistance as an index of order, the predictions of the theory have been tested

[1] See, for example, Fletcher, *Speech and Hearing*, pp. 10–11, and numerous references in Paget, *Human Speech*.

[2] H. Dudley, Proc. Nat. Acad. Sci. **25**, 377 (1939); J. Acous. Soc. Am. **11**, 169 (1939).

[3] J. Frank. Inst. **227**, 739 (1939); Dudley, Riesz, Watkins.

with the three alloys Cu_3Au, CuAu and beta-brass (CuZn) in a recent paper "The Effect of High Pressure on the Order-Disorder Transformation in Alloys."[1] Over a range of pressures up to 10,000 kg/cm² and a range of temperatures 50°C–425°C, the author's results are in fair agreement with the approximate theory developed.

Several observations are also reported on the shift of the critical point of the alloys Cu_3Au and CuAu with pressure. It is suggested that the observed shifts in conjunction with accurate thermal expansion data may be useful in elucidating the exact nature of the transition at the critical temperature.

Along with the three alloys mentioned above, the behavior of the electrical resistance of a fourth alloy, alpha-brass (Cu_3Zn), is also described. The author suggests that the similarity in the behavior of this alloy to that of the others examined may be due to a slight ordering of the constituents of the alloy under pressure.

Logarithmic Amplifier for Direct Currents In many electrical circuits it is desirable to use a stage of logarithmic amplification. Such cases occur when a scale of intensities is to be compressed or when the properties of the logarithmic function are necessary, as in logarithmic plots, or in multiplication and division by means of the addition and subtraction of logarithms.

A method of obtaining a quantity proportional to the logarithm of a direct current is described in a paper by R. E. Meagher and E. P. Bentley.* The device consists of a 77 radio tube with all three of its grids maintained at a positive potential of 45 volts with respect to a low temperature cathode. Under these conditions the cathode to plate potential V is a logarithmic function of the cathode to plate current i, according to the equation $V=0.226 \log_{10} i+\text{constant}$, where V is in volts. The equation was found to be strictly true for a current input range from less than 10^{-7} to 10^{-5} ampere, and to hold approximately for currents up to 10^{-3} ampere.

The circuit depends for its operation on the Maxwellian distribution of velocities of electrons emitted by a hot cathode, so that it can be shown theoretically that the proportionality constant between output and log input (0.226 volt) is a constant dependent only upon the temperature of the cathode. This temperature, characteristic of the Maxwellian distribution, was found to be about 1140°F, when the filament voltage was 4.4 volts.

When two similar circuits are made and properly balanced, it is possible to add or subtract logarithms and thereby to perform electrical multiplications or divisions. In this way the authors found it possible to obtain the ratio of intensities of radioactive sources by the subtraction of logarithms.

Separation of Bromine Isotopes by Centrifugation Of the more practical methods in use today for obtaining partial separation of isotopes the most conspicuous feature is a dependence either on molecular force laws or on molecular weight or on both. As a consequence those methods involving molecular force laws have been applied to only a few isotopes for which the force laws happen to be favorable; those dependent on mass have been found useful for only the light isotopes. It was pointed out long ago that the separation of isotopes in a high centrifugal field gradient would be independent of the mass and hence applicable as an enrichment method for the heavier elements.

The feasibility of centrifugation of isotopes was investigated recently by Richard F. Humphreys[1] using a Beams vacuum ultracentrifuge to obtain a partial separation of the bromine isotopes. The technique of "evaporative centrifuging" was used, in which ten cc of ethyl bromide were distilled into a four-inch hollow Duralumin rotor. When the rotor was set in motion the liquid formed a thin layer at the periphery, its vapor filling the entire volume of the rotor. Under the centrifugal field gradient the isotopic molecules of the vapor underwent partial separation. Consequently, the vapor that

[1] Thomas C. Wilson, Phys. Rev. **56**, 598 (1939).
* R. E. Meagher and E. P. Bentley, Rev. Sci. Inst. **10**, 336 (1939).

[1] R. F. Humphreys, Phys. Rev. **56**, 684 (1939).

was slowly removed at the center was enriched in ethyl bromide molecules containing Br^{79}, while the residue in the rotor was enriched in Br^{81}. Theory was set up with which the separation could be predicted for a given rate of removal.

With a speed of 1500 r.p.s. the centrifugal field at the periphery was 388,000 times gravity. By performing two successive fractionations on the first fractions of material removed, one cc of ethyl bromide was obtained in which Br^{79} was enriched 11 percent relative to Br^{81}. This corresponded well to the predicted enrichment. It was pointed out that though such an enrichment was not as large as one would desire, it was still much larger than obtained heretofore by any other enrichment method. Hence centrifugation shows some promise as a means of separating heavy isotopes.

Here and There

Midwest Power Conference

Armour Institute of Technology, in cooperation with seven middle western universities and colleges and several local and national technical societies, is again sponsoring the annual Midwest Power Conference to be held in Chicago, April 9 and 10, in the Palmer House Hotel, under the direction of Stanton E. Winston, 401 South Quincy Street, Hinsdale, Illinois, Associate Professor of Mechanical Engineering at the Institute. Charles A. Nash, 4715 North Spaulding Avenue, Associate Professor of Electrical Engineering at the Institute, is Secretary of the 1940 Conference.

The several midwestern colleges cooperating with Armour Institute in the sponsoring of the Midwest Power Conference, and their representatives are: Dr. L. E. Grinter, Vice President, Armour Institute; Professor M. P. Cleghorn, Head of the Department of Mechanical Engineering, Iowa State College; Professor F. L. Foltz, Head of the Department of Electrical Engineering, Michigan State College; Professor C. Francis Harding, Head of the School of Electrical Engineering, Purdue University; and Professor H. O. Croft, Head of the Department of Mechanical Engineering, State University of Iowa.

The purpose of the Power Conference has been established as that of offering an opportunity for all persons interested in power production, transmission or consumption to meet together annually for the study of mutual problems free from the restrictions of required memberships in technical or social organizations. The tentative program for the conference includes some twenty-five important subjects to be discussed by authorities from educational and industrial fields in all parts of the country. Such a central conference provides the only opportunity for full correlation of all the technical and social phases of power production, distribution, and utilization. Academic sponsorship permits the freest possible discussion ranging from the technical through the economic and into the social aspects of the subject.

The twenty-five or so speeches tentatively scheduled to be discussed by authorities from educational and industrial fields will place special emphasis on steam, Diesel, electric and hydraulic power. In each of these fields, papers will be presented which will discuss the best modern practice, while other papers will venture into the picture of the future as indicated in the investigations of our great research laboratories.

★

Research in Industry

Appointment of Raymond Stevens, Vice President of Arthur D. Little, Inc., of Cambridge, Massachusetts, as Director of a nation-wide survey of research in industry, was announced December 6 by Dr. Ross G. Harrison, Chairman of the National Research Council. The announcement followed the first meeting of a special committee held at the Engineers' Club in New York to formulate initial plans for the survey.

Dr. Harrison stated that, while funds for the work had been made available by the National Resources Planning Board, of which Mr. Frederic A. Delano is Chairman, the survey would be conducted and the report prepared by the National Research Council, in accordance with plans approved by an Advisory Committee of leading scientists, industrial research directors and executives. Mr. F. W. Willard, President of the Nassau Smelting and Refining Company, New York, is Chairman of the Council's Advisory Committee. Dr. Harrison said that the report will be submitted in printed form by the Council this year and will present an objective study of industrial research as a national resource, as a means of aiding in its further development and utilization.

★

Ohio Physics Club

The Ohio Physics Club, member of the Ohio Physics Association, announces an attendance of approximately 100 teachers and industrialists from Ohio and adjoining states at its fall meeting held at Findlay College, Findlay, Ohio, on Saturday, November 4. The guest speaker was Dr. K. K. Darrow of the Bell Telephone Laboratories of New York City. Dr. Darrow's subject was "The Fission of Uranium."

Westinghouse Research Fellowships

Announcements of the Westinghouse Research Fellowships for 1940 have been mailed to university officers throughout the country. Founded at the Westinghouse Research Laboratories in 1938, these fellowships provide an opportunity each year for five men of Ph.D. standing to work on fundamental research problems of their own selection. The appointments are for one year at a stipend of $2400 with possibility of one reappointment. At present there are ten Westinghouse Fellows working at the Laboratories in East Pittsburgh. Three are working on nuclear physics with the large electrostatic generator, and the others are working on mass spectroscopy for molecular structure studies, elastic constants of single crystals of copper-gold alloys, internal friction of metal single crystals, diffusion of metals by means of artificial radioactive tracers, ultra-high frequency oscillation generators and chemical applications of radioactive tracers. The fellowships are open to physicists, chemists, mechanical and electrical engineers, and metallurgists. To receive consideration applications must be received by March 1, 1940. Further information is obtainable from the Manager of Technical Employment and Training, Westinghouse Electric & Manufacturing Company, Pittsburgh, Pennsylvania.

★

Graduate School Appointment

Professor Alpheus W. Smith, Chairman of the Department of Physics at the Ohio State University, has been appointed Dean of the Graduate School. Dr. Smith succeeds Dr. George F. Arps, who died on September 16.

★

Modern Pioneers' Award

The National Association of Manufacturers is planning to extend specific recognition to science, in the form of awards to "outstanding contemporary scientists who will be selected as modern pioneers." The first occasion on which these awards will be bestowed is at the celebration of the one hundred and fiftieth anniversary of the American Patent System on February 27. Dr. Karl T. Compton, President of Massachusetts Institute of Technology, has been elected Chairman of a committee of six scientific men who will make the selection. The other members are Dr. Forest R. Moulton, permanent secretary of the American Association for the Advancement of Science; Professor George B. Pegram, Dean of the Graduate School, Columbia University; Professor John T. Tate, Professor of Physics and Dean of the College of Science, Literature and Art and Director of University College of the University of Minnesota; Dr. Edward R. Weidlein, Director of the Mellon Institute for Industrial Research, Pittsburgh; and Professor Frank C. Whitmore, Research Professor of Organic Chemistry and Dean of the School of Chemistry and Physics at the Pennsylvania State College. A special committee of eighty industrialists has been appointed to promote the search for "modern pioneers." The Chairman is Robert L. Lund, executive Vice President of the Lambert Pharmacal Company.—*Science*

Debye Lectures at Cornell

Professor P. Debye, Nobel prize winner in chemistry, 1936, and Director of the famous Kaiser Wilhelm Institute of Physics at Berlin-Dahlem, has accepted the call as George F. Baker nonresident lecturer in chemistry at Cornell University for four months, beginning with the second term of this academic year, it was announced by President Edmund Ezra Day. Professor Debye will discuss the determination of molecular structure by the method of interferences.

The 1936 Nobel prize in chemistry was awarded Dr. Debye in recognition of his contributions to the knowledge of molecular structure through his investigations on dipole moments and on the diffraction of x-rays and electrons in gases. Other recent honors accorded him are honorary memberships in the Indian Academy of Sciences at Bangalore, the Chemical Society of the Netherlands and the Physical Society, London.

★

Officers Elected

Filling the places left vacant by the retirement of Gerard Swope and Owen D. Young, Charles E. Wilson is now President and Philip D. Reed, Chairman of the Board of Directors of the General Electric Company. The new officers were elected at a meeting of the directors of the Company in New York City, November 17 and took over their new responsibilities January 1. Mr. Swope and Mr. Young are Honorary President and Honorary Chairman of the Board, respectively.

★

Dr. Henry Norris Russell, Director of the observatory at Princeton University, was elected to honorary membership in the New York Academy of Sciences at the recent annual meeting.—*Science*

★

Necrology

Mr. George L. Crosby, Vice President and general sales manager of Roller-Smith Company, died quite suddenly at his home in Bethlehem, Pennsylvania, on December 2, 1939. Mr. Crosby had been connected with the Roller-Smith Company since 1910.

★

Dr. Oliver E. Buckley, Executive Vice President of the Bell Telephone Laboratories, New York City, with which he has been associated since 1925, has been elected President of the Engineering Foundation to succeed the late Professor George E. Beggs. F. F. Colcord, Vice President of the United States Smelting Company, has been made Vice Chairman of the Foundation; Kenneth H. Condit has become Chairman of the research procedure committee, and E. M. T. Ryder, a member of that committee. Professor Walter I. Slichter, of Columbia University, has been elected a member of the executive committee.—*Science*

Contributors to This Issue

A. J. Wells

John Bardeen was graduated from Princeton University in 1936 with a Ph.D. degree in mathematical physics. He spent the years 1930 to 1933 doing geophysical work for the Gulf Research and Development Corporation, and 1935 to 1938 as a Junior Fellow of the Society of Fellows of Harvard University. Dr. Bardeen is at present assistant Professor of Physics at the University of Minnesota.

A. Judson Wells was graduated from Harvard College in 1938 with the degree of B.S., and is now engaged in graduate work in physical chemistry at Harvard. Mr. Wells has also been connected with the research staffs of the Monsanto Chemical Company and the BB Chemical Company of Cambridge, Massachusetts.

J. Bardeen

C. M. Slack

Charles H. Bachman received his B.S. in E.E. in 1932, M.S. in physics in 1933, and Ph.D. in 1935 from Iowa State College. He was with the Hygrade Sylvania Corporation as physicist from 1935 to 1939 and is now with the General Electric Company in Schenectady. (Dr. Bachman's paper, "Ring Focusing of Negative Ions in a Cathode-Ray Beam," appeared in the January issue.)

Charles M. Slack received his B.S. degree from the University of Georgia in 1922 and his Ph.D. from Columbia University in 1926. Since 1927 he has been a Research Physicist with Westinghouse Electric and Manufacturing Company.

C. H. Bachman

E. R. Piore

Louis F. Ehrke received the degree of M.E. from Stevens Institute of Technology in 1924 and has since been a member of the research staff of the Westinghouse Electric and Manufacturing Company.

E. R. Piore is engaged in research work at the Television Laboratory of the Columbia Broadcasting System, New York City. He received his training from the University of Wisconsin, receiving the B.A. degree there in 1930 and the Ph.D. degree in 1935. From 1935–1938 Dr. Piore was with the Electronic Research Laboratories, RCA Manufacturing Company.

L. F. Ehrke

F. P. Bundy

Francis P. Bundy has served as Instructor in Physics at Ohio University, Athens, Ohio, since 1937, in which year he received the Ph.D. degree from Ohio State University. Dr. Bundy's fields of major interest have been spectroscopy and mechanics.

Pictures and biographical sketches of the following contributors have appeared in previous issues of the *Journal of Applied Physics:*

F. Morgan, p. 391, Vol. 9, No. 6, 1938.
Morris Muskat, p. 391, Vol. 9, No. 6, 1938.
George A. Morton, p. 496, Vol. 10, No. 7, 1939.

Contributed Original Research

An Investigation into the Gettering Powers of Various Metals for the Gases Hydrogen, Oxygen, Nitrogen, Carbon Dioxide and Air

LOUIS F. EHRKE AND CHARLES M. SLACK
Research Department, Lamp Division, Westinghouse Electric & Manufacturing Company, Bloomfield, New Jersey
(Received May 6, 1939)

Measurements of the "gettering" or clean-up ability of aluminum, magnesium, thorium, uranium, misch metal, zirconium and barium for the common gases were made. In most cases the measurements were quantitative and represent gettering powers unassisted by an electric discharge or other source of ions. The effect of temperature conditions on the gettering and keeping properties of several of the getters is given. The superior gettering powers of the diffuse layers produced by vaporizing the getters in the presence of a gas, as compared to those of the bright getter deposits produced in a high vacuum were confirmed. Barium and misch metal were found to be the most active of the materials tried, and the convenient forms which barium is now commercially obtainable would seem to make it first choice for most work, though it is not effective in the presence of Hg vapor. Magnesium and aluminum showed little activity without the presence of a discharge. Thorium and uranium showed considerable activity for H_2 and O_2, but the high temperatures needed for flashing, make them rather inconvenient to use.

INTRODUCTION

THE list of readily available articles concerning getters in the recent literature is not large, and most of the work covers only a limited portion of the field. This paper describes an investigation of various materials which have been used or suggested as getters. The work was carried on in such a manner that a direct quantitative comparison of the gettering powers of most of the materials investigated could be determined for various gases.

The word "getter" is generally applied to any material introduced into a lamp or other evacuated vessel for the purpose of improving or maintaining the degree of vacuum therein. The use of suitable getter materials may be of advantage in one or more of the following ways:

1. The tube may be subjected to a less rigorous exhaust treatment and the remaining gas immobilized or taken up by the getter material.
2. Gas evolved from the tube parts during the running life of the tube may be taken up by the getter and thus the original high degree of vacuum may be maintained and the tube life extended.
3. In the case of devices in which a filling of inert gas such as argon or neon is used, the purity of the gas must be maintained throughout the life of the tube.

This result may be obtained by the use of a getter which exercises a selective power, absorbing the gaseous impurities evolved from the tube parts, but not cleaning up the inert gas filling.

Gettering action may conveniently be separated into two general types:

1. "Dispersal gettering," in which clean-up takes place while the getter is being dispersed or volatilized in the presence of the gas to be cleaned up and
2. "Contact gettering," in which a previously vaporized getter acts to clean up any gas which may be introduced into its presence. This term is also applied to the getter action which may continue after volatilization ceases in cases of dispersal gettering.

With few exceptions, the results here given are for contact gettering without the accelerated action produced by a discharge or other source of ionization.

MATERIALS INVESTIGATED

The following materials were investigated as getters: magnesium, aluminum, barium, misch metal (active constituents are largely cerium and lanthanum), thorium, uranium, and zirconium. Several samples of barium derived from different sources were investigated. The barium samples were derived from two types of "Batalum" obtained from the RCA, barium-aluminum alloy pellets, copper clad barium cartridges, and type KIC getter wire obtained from the Kemet Laboratories, and the regular Ba-Sr emission mixture.

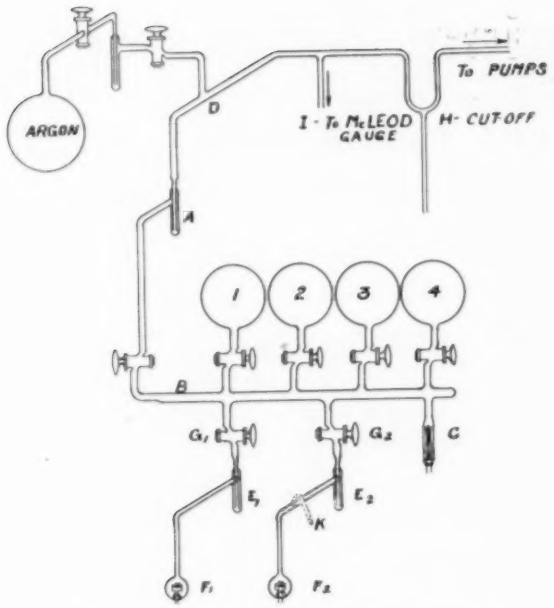

FIG. 1. Apparatus used in the later stages of the investigation.

The gases investigated included hydrogen, nitrogen, air, oxygen, carbon dioxide, and argon.

APPARATUS AND EXPERIMENTAL PROCEDURE

The apparatus as used in the later stages of the investigation is illustrated in the sketch, Fig. 1. A set of mercury diffusion pumps connected through the liquid-air trap "*A*" to the manifold "*B*." Four gas reservoir bulbs No. 1–4, containing the gases under investigation were sealed to the manifold through stopcocks. Two small liquid-air traps E_1 and E_2 were sealed through stopcocks G_1 and G_2 to the lower side of the manifold and the tubes containing the getters were sealed on the other side of these traps. These small traps were found necessary to avoid the contamination of the getter layer by vapors arising from the stopcock lubricant. A Pirani gauge "C" was also sealed to the manifold as shown. Frequent outgassing of the Pirani gauge filament and constant use of a refrigerating medium on the traps were found to be necessary to avoid inaccuracies in the gauge readings caused by the vapors from the stopcock lubricant. The system was also provided with a McLeod gauge "I" located on the pump side of the maintrap "A." With the exception of the experiments on carbon dioxide, in which case the refrigerant on the traps was CO_2 snow in acetone, liquid air was used on all three traps. A reservoir containing argon, and a liquid-air trap which acted as an auxiliary reservoir, permitting the argon to remain at liquid air temperatures for extended periods, was sealed to the system at "*D*."

The general procedure was to seal one or more small bulbs containing the getters to the system at F_1 and F_2. These bulbs were of Nonex glass and were 5 cm inside diameter. This provided an area of about 75 sq. cm which was normally covered by the getter deposit. The system was then evacuated and the getter bulbs baked to 450°C for one hour. After the bulbs had cooled, the getters were outgassed as completely as possible without starting vaporization. After the bulb had cooled again, the getter was flashed in the manner indicated under the sections devoted to individual getters. A zero reading for the Pirani gauge was established at this point. The system was then trapped off at "*H*." Some of the gas under investigation was admitted from the appropriate reservoir bulb, and the pressure read on both the Pirani and McLeod gauges. When an equilibrium value had been reached, the stopcock "G" leading to the getter tube was opened and the clean-up action followed by the Pirani gauge readings with an occasional check and a final determination by the McLeod gauge. If complete, or nearly complete clean-up occurred, a new sample of gas was admitted by the same procedure.

In several cases quantitative determinations were made of the amount of getter evaporated as well as the quantity of gas cleaned up. In the case of those getters which were flashed by putting the getter material into the turns of a tungsten coil and then heating the coil to produce evaporization of the getter, the quantity evaporated was determined by weighing the combined coil and getter before and after flashing. The values for the Kemet KIC wire were obtained by making several determinations using a specially constructed quartz fiber spring balance in vacuum. The quartz spiral carried a very light mica cylinder which was suspended so as to surround a measured length of the getter wire. When the

wire was heated to flash the getter, the barium deposited on the mica cylinder and the weight of barium could be determined from the extension of the calibrated quartz spring. Several determinations established the uniformity of the samples and it was assumed that the same length of wire yielded the same weight of barium in the actual gettering experiments. The use of Batalum permitted the calculation of the approximate amount of getter obtained from the weight of the coating, as will be further explained in the section on barium.

Since the gettering power of a deposited layer is, in most cases, much higher when the layer is diffuse in character, rather than the bright shiny type produced when the getter is thoroughly degassed and then flashed in a high vacuum, both types were examined. While the diffuse layer produced by flashing the getter in the gas to be cleaned up possesses the above-mentioned characteristic, the gas cleaned up during flashing and the possibility of gas being given off from the getter support of the getter itself make it undesirable to work in this manner.

Recourse was therefore had to a procedure which makes use of the fact that inert gases are not appreciably cleaned up when a getter such as barium is flashed in their presence although the deposited getter layer has the diffuse character and enhanced clean-up power cited above. The procedure, which has been described in British patent No. 471, 409 issued to the Philips Company is briefly as follows: After thorough de-gassing of the getter, the tube is filled with argon or other inert gas to a pressure of 1–3 mm. The getter is then flashed, producing the characteristic diffuse layer and the argon is pumped out, leaving an uncontaminated getter layer of high activity. In the case of barium, such a layer is black and the exposed side resembles a layer of lamp black when viewed by the naked eye. Magnesium and aluminum treated in this way yielded layers of varying shades of gray. Those examples which were produced by this means are marked "diffuse" in the tabular summary of results at the end of the paper.

The getters investigated will be discussed below and a brief summary of the more important results obtained will be found at the end of the paper.

Aluminum

Aluminum was evaporated from tungsten filament coils. The aluminum was in the form of wire twisted around the turns of the tungsten coil or a small piece of aluminum placed within the tungsten coil. Heating the tungsten by passing current through it vaporized the aluminum. Both bright and diffuse deposits were employed and produced no apparent clean-up of nitrogen, carbon dioxide, hydrogen or air. Oxygen was cleaned up to some extent by both the bright and diffuse aluminum deposits. It was difficult to de-gas thoroughly the material without causing some vaporization, and the gas content of the aluminum itself may be responsible for the fact that there was a slow evolution of gas after attempting to getter air, even though there has been no measurable clean-up. This evolution took place at room temperatures and was accelerated by even slightly heating the deposited layer. It is possible that, in this particular case, some contamination of the getter layer took place, since there was no liquid air between the stopcock and the getter tube.

Magnesium

Both bright and diffuse magnesium were investigated. The magnesium was in the form of wire and was vaporized from tungsten filaments as described for aluminum. Here again there was great difficulty in properly de-gassing the material before vaporization sets in. Heating the deposited layer sometimes caused an evolution of gas even in cases where there had been no appreciable clean-up. Bright magnesium showed no clean-up with hydrogen with the getter cold or at 200°C or upon torching to some higher temperature. No clean-up was shown for nitrogen, carbon dioxide, or air for bright magnesium. Oxygen was cleaned up to some extent with a cold bright deposit. Heating the surface produced no further effect until the temperature reached 175°C. Between this value and 265°C about 25 percent more gas cleaned up in about thirty minutes. There was no subsequent evolution of gas on cooling.

Diffuse magnesium layers showed negligible clean-up for nitrogen. Hydrogen was not cleaned up by a cold deposit, but showed some evidence

of clean-up when the deposit was torched sufficiently to re-vaporize some of the getter layer. Carbon dioxide cleaned up initially, but later some noncondensible gas was evolved. Placing liquid air on the traps in place of the CO_2 snow after clean-up slowed down this evolution but did not entirely stop it. It is thought that at the temperature of CO_2 snow, there is sufficient water vapor present to break down and furnish the noncondensible gas. The vapor pressure of water at CO_2 snow in acetone temperature is about 0.7 micron.

The diffuse magnesium layer exercised considerable clean-up power for oxygen, cleaning up 9–10 times the amount cleaned up by a comparable amount of bright magnesium. This clean-up appears to be permanent since no evolution took place on baking the bulb to 265°C or upon allowing it to stand at room temperature over night. MacRae and Snow[1] working in this laboratory about 1923, found that magnesium did not clean up hydrogen when simply vaporized in a tube containing about 1,000 microns of the gas, but that the deposited layer will clean up if the gas is activated by an electric discharge or the presence of a hot tungsten filament. Reimann[2] found some clean-up for hydrogen both for contact and dispersal gettering with magnesium and found that the effect was greatly increased when the gas was ionized by the electric discharge. It is probable that the use of magnesium in radio tubes and similar devices has been successful largely because of the presence of ionization in such devices. Bombardment of a magnesium layer which has gettered some hydrogen results in rapid evolution of gas if the bombarding particles are of considerable energy. This effect was also noted by Reimann.

Zirconium

Zirconium has been suggested for use as a getter, in powder form, as a paste to be painted on the anode of a tube such as a radio tube, and in solid sheet form so located as to be maintained at a suitably high temperature through the operation of the tube. Dushman[3] mentions a patent issued to Coolidge in 1919 dealing with the use of the powder form of zirconium and thorium as getters, and a more recent article by Fast[4] deals with the use of zirconium in solid form. In the arrangement used here, the zirconium was in the form of a ribbon filament mounted on a stem and sealed into a small bulb. Current passed through the ribbon raised it to the desired temperature which was determined by means of an optical pyrometer. The ribbon was thoroughly de-gassed at temperatures of 1500°C or more and allowed to cool. A sample of the gas under investigation was then admitted to the getter bulb and the temperature of the zirconium ribbon slowly raised until clean-up started. The pressure changes were observed on the Pirani gauge and checked on the McLeod gauge. After a determination had been made, the ribbon was heated and any evolution of gas noted. Then the tube was pumped out, and the getter ribbon degassed again, after which the set-up was ready for another gas sample.

Nitrogen was not detectably cleaned up at temperatures below 1527°C at which point a slight clean-up occurred. After pumping out the bulb, no evolution of gas was produced by heating the filament to 1500°C.

Oxygen showed a slow steady clean-up which set in about 885°C and proceeded more rapidly as the temperature was raised through 1070°C to a high value of 1142°C. A total of about 18.1 microns at a volume of 1 liter was cleaned up during the time the filament was heated. After pumping out the tube, the filament was re-heated to 1452°C with a consequent evolution of 0.7 micron of gas.

Hydrogen showed a clean-up which set in at 760°C. At 984°C the clean-up was accelerated and about 6.5 microns at a 1-liter volume was cleaned up in 17 minutes. The temperature was raised to 1020°C at which point 4 microns cleaned up in about 26 minutes. The temperature was then increased to 1210°C at which point a further clean-up of 3.5 microns took placed in 18 minutes.

[1] MacRae and Snow, unpublished.

[2] A. L. Reimann, "The Clean-up of Hydrogen by Magnesium" Phil. Mag. **16**, 673–686 (1933): "The Clean-up of Various Gases by Magnesium Calcium and Barium," Phil. Mag. **18**, 1117–1132 (1935).

[3] Saul Dushman, "High Vacuum," U. S. Patent No. 1,323,386, p. 153: "Recent Advances in the Production and Measurement of High Vacua." Section II deals with getters. J. Frank. Inst. **211**, 689 (1931).

[4] J. D. Fast, "Zirconium," Foote Prints on Chemicals, Metals, Alloys, and Ores **10**, 1–24 December, 1937.

Clean-up ceased at a residual pressure of about 0.3 micron even though the temperature was raised to 1350°C. This apparently represented some impurity in the gas which the zirconium refused to clean up since a fresh batch of gas was cleaned up to the extent of 7.1 microns in seven minutes at 1400°C after pumping out the above residue.

Fast[5] states that the optimum temperature for hydrogen clean-up is about 300° to 400°C and that at temperatures in the neighborhood of 1400°C an equilibrium pressure is established, much of the absorbed hydrogen being given off again.

Carbon dioxide showed no clean-up effects at temperatures ranging from 1371° to 1500°C.

Thorium

The thorium was used in the form of small pieces of wire about 0.030-inch diameter slipped into a tungsten filament (coiled). Because of the high melting point and low vapor pressure of thorium, considerable difficulty was experienced in vaporizing a satisfactory amount of this getter, particularly in argon. It was evident in most cases that there were traces of other materials evaporated from the leads and support wires in addition to the evaporated thorium. For this reason it is probable that pure thorium would be somewhat more effective than our results indicate. Both bright and diffuse thorium layers cleaned up air to some extent, the diffuse layer being about three times as effective as the bright layer. Bright thorium did not clean up carbon dioxide at room temperatures but upon torching the deposit, some rise in pressure was first observed, but rapid clean-up set in at a temperature which softened the glass, probably about 650°C. Diffuse material showed some clean-up effect for CO_2 at room temperature and accelerated action upon torching as above.

Oxygen was cleaned up by both forms of getter deposit. The bright deposit accounted for 7.45 microns of a 1-liter volume, and the diffuse layer cleaned 33.1 microns of a 1-liter volume per mg of thorium evaporated.

Hydrogen cleaned up to the extent of 19.4 microns of a liter volume per mg thorium for the bright deposit, and 53.7 microns for a 1-liter volume per mg thorium evaporated for the diffuse layer.

Uranium

Uranium metal in the form of small pieces of rod about 0.030-inch diameter was slipped into tungsten coils and evaporated by heating the tungsten. Both bright and diffuse layers showed clean-up powers for hydrogen and oxygen. The clean-up was 8.9 microns of hydrogen for a 1-liter volume per mg uranium evaporated for a bright deposit and the corresponding figure for a diffuse layer was 21.5 microns or about $2\frac{1}{2}$ times as much.

For oxygen, the figures are about 10 microns of gas for a 1-liter volume per mg uranium evaporated for both the bright and diffused layers.

Misch Metal

This material, which consists of rare earths, derived from monazite and alloyed with iron, shows marked gettering powers. The active material is chiefly cerium and lanthanum. In the measurements made in this investigation the material consisted of small pieces sawed from a slug and carefully cleaned. The pieces of misch metal were inserted into tungsten coils and sealed in before the atmosphere acted on them to any great extent. Vaporization was accomplished in the usual way by passing current through the filament. Both bright and diffuse layers were tested.

Oxygen was cleaned up to the extent of 21 microns of a 1-liter volume per mg evaporated material for bright layers and 50 microns per mg for diffuse layers.

Hydrogen showed less difference for the bright and diffuse layers, cleaning 46 microns for a 1-liter volume per mg evaporated material for the bright deposit as compared with 63 microns per mg for the diffuse layer.

Carbon dioxide was only sparsely cleaned by the bright form while the diffuse layer cleaned about twenty times as much. The figure for the diffuse layer was 45 microns for a 1-liter volume per mg evaporated getter material.

Nitrogen was less active cleaning up 16.1 microns per mg evaporated material at 1-liter volume for the diffuse layer and 3 microns for the bright layer.

[5] J. D. Fast, "Zirconium and Its Compounds with High Melting Points," Philips Tech. Rev. **3**, 346–352 (1938).

Both bright and diffuse layers cleaned up air, the diffuse layer being about nine times as effective in this case as the bright layer.

Torching the getter deposit in the case of CO_2 accelerated the clean-up action. This was also true in the case of hydrogen provided only a small amount had cleaned up. If the getter deposit was heavily loaded with hydrogen, torching caused an evolution of gas to occur.

Barium

As mentioned in an earlier section of the paper, the investigation into the gettering power of barium was carried on with samples derived from several sources. The work was begun by using barium obtained from Batalum, a form of barium getter developed by Lederer and Walmsley[6] of the RCA particularly for use in metal radio tubes, the manufacture of which presents some new getter problems. Essentially, Batalum consists of a coating of barium and strontium carbonates (a later version employs barium berylimate), coated or sprayed on a tantalum wire. Such a getter is stable and easy to handle. When the wire is heated by the passage of current to about 800°–1100°C the carbonates break down and the oxides are reduced by the tantalum to produce metallic barium and strontium.

This getter was found to exert a very powerful clean-up action when vaporized in the presence of air. On the other hand, when flashed in a high vacuum after careful de-gassing, its gettering powers were much diminished. This difference was so marked that the use of argon to produce the diffuse type of getter coating was begun as previously described. No detectable clean-up for argon itself was noted either for dispersal or contact gettering. The weight of the coating applied to the tantalum wire was found to affect the gettering power as expressed in gas cleaned up per mg barium available. It was found that light weight or thin coatings yielded deposits of greater efficiency, on this basis, than those obtained from heavier coatings. This is probably due to the fact that much of the material in the heavier coatings was prevented from coming into contact with the tantalum and that consequently all the barium oxide was not reduced. Thus less barium metal was produced per gram of coating than was the case with a thin coating in which complete reduction took place and the theoretical yield of barium was more closely approached. There is also the difficulty of thoroughly degassing the coating before breaking down the oxides. While these points in no way affect the value of Batalum as a practical and powerful getter, it was felt that uniform conditions for quantitative measurements could be attained more easily by the use of the KIC getter wire made by the Kemet Laboratories. Accordingly, the quantitative measurements were carried on with this material. KIC wire is manufactured by filling an 0.080-inch iron tube with liquid barium in vacuum, drawing down the composite wire thus formed to 0.020 inch or 0.030 inch and then grinding one side flat to a thickness of about 0.003 inch of iron over the barium core. This wire may be heated by the passage of current through it, or if suitably disposed, by high frequency heating. The getter is degassed by heating to about 750°C and the barium diffuses through the thin side of the wire when the temperature reaches about 850°C.

It was decided to flash the getter samples by passing current through them. Accordingly a standard length of 1 cm of getter wire 0.020-inch diameter mounted on 0.020-inch nickel leads was chosen. Several samples were made up and flashed in the quartz spiral spring balance previously mentioned. The average yield of barium from such a mount was found to be 2.35 mg under the flashing conditions used. This value was assumed to hold for similar filament mounts sealed into the getter tubes used in the clean-up measurements. It was difficult in this case also to be sure that the specimen was completely degassed before flashing some of the getter, and a part of the activity displayed by vacuum flashed specimens may be due to dispersal effect caused by further gas liberation from the getter itself or the supporting lead wires. Therefore it is probable that the difference in activity displayed by a sample flashed in vacuum and one flashed in argon, is even greater than indicated in our results. Similar considerations apply to all the getters flashed in this way, particularly to the cartridge type in which the barium is enclosed

[6] Lederer and Walmsley, "Batalum, a Barium Getter for Metal Tubes," RCA Review, July, 1937.

TABLE I. *Clean-up results.*

GETTER	GAS	BRIGHT DEPOSIT	DIFFUSE DEPOSIT
Aluminum	O_2	1 liter at 7.5 μ Hg pressure	1 liter at 38.6 μ Hg pressure
	N_2, H_2, CO_2	None	None
Magnesium	O_2	1 liter at 20 μ Hg pressure	1 liter at 202 μ Hg pressure
	CO_2	None	Slight, not permanent cf. text
	N_2, H_2 cf. test	None at room temperature	None at room temperature
Thorium	O_2	1 liter at 7.45 μ/mg Th	1 liter at 33.15 μ/mg Th
	H_2	1 liter at 19.45 μ/mg Th	1 liter at 53.7 μ/mg Th
Uranium	O_2	1 liter at 10.56 μ/mg U	1 liter at 9.26 μ/mg U
	H_2	1 liter at 8.9 μ/mg U	1 liter at 21.5 μ/mg U
Misch Metal	O_2	1 liter at 21.2 μ/mg misch metal	1 liter at 50.9 μ/mg misch metal
	H_2	1 liter at 46.1 μ/mg misch metal	1 liter at 63.9 μ/mg misch metal
	N_2	1 liter at 3.18 μ/mg misch metal	1 liter at 16.1 μ/mg misch metal
	CO_2	1 liter at 2.2 μ/mg misch metal	1 liter at 44.8 μ/mg misch metal
Barium	O_2 (Room temp. cf. text)	1 liter at 15.2 μ/mg Ba	1 liter at 45 μ/mg Ba
	H_2 (Room temp. cf. text)	1 liter at 87.5 μ/mg Ba	1 liter at 73.0 μ/mg Ba
	N_2 (Room temp. cf. text)	1 liter at 9.5 μ/mg Ba	1 liter at 36.1 μ/mg Ba
	CO_2 (Room temp. cf. text)	1 liter at 5.21 μ/mg Ba	1 liter at 59.5 μ/mg Ba
Zirconium	O_2, H_2, N_2, CO_2	cf. text	

in a pinched-off section of copper tube usually flashed by high frequency heating.

The effect of heating a getter layer deposited in vacuum was often to cause it to increase its gettering power and if the heating was carried to the vaporization point of barium, the activity approached that of the argon flashed type.

The approximate quantitative results obtained are given below (see also Table I). Where effects at greater than room temperatures are reported, the procedure was to place an electric oven over the getter tube and gradually to raise the temperature to the desired point, observing the pressure changes on the Pirani gauge. Unless otherwise stated the refrigerant on the traps was liquid air. The amount of clean-up is expressed in terms of microns of mercury pressure for a 1-liter volume per mg of barium vaporized.

Oxygen.—Bright or vacuum flashed barium cleaned up oxygen to the extent of 15.2 microns for a 1-liter volume per mg at room temperature. Heating to 200°C caused a further clean-up of 7.7 microns per mg which brought the total to 22.9 microns for a 1-liter volume per mg Ba. Further heating to 300°C caused an evolution of gas to begin. Diffuse or argon flashed material produced a clean-up averaging 45.1 microns at 1-liter volume per mg Ba at room temperature.

Nitrogen was cleaned up by a bright deposit to the extent of 9.6 microns for 1-liter volume per mg Ba at room temperature. Heating to 200°C caused an additional clean-up of 7.6 and heating to 300°C produced a further clean-up of 1.06 microns making a total of 18.25 microns at 1-liter volume per mg Ba. Diffuse barium layers cleaned up 36.1 microns for 1-liter volume per mg at room temperature.

Hydrogen.—The clean-up of hydrogen by the barium was 87 microns per 1-liter volume per mg Ba for the bright layer, and 73 microns for the diffuse layer. Probably because of the diffusive properties of hydrogen which permit the gas molecules to penetrate below the surface layer of a bright getter deposit, there does not appear to be much difference in the clean-up ability of the bright and diffuse deposits for this gas, even at room temperature.

On heating the vacuum flashed deposit to 300°C after cleaning up hydrogen, there was an evolution which caused the residual pressure to rise from 25 microns to 30 microns. A similar evolution occurred on heating a vacuum flashed deposit of barium from Batalum after hydrogen had been cleaned up.

Carbon dioxide.—Bright barium from KIC wire cleaned up CO_2 to the extent of 5.2 microns for a 1-liter volume per mg Ba at room temperature. Heating the bulb to 200°C caused an

additional clean-up of 19.6 microns, making a total clean-up of 24.8 microns for a 1-liter volume per mg Ba. Further heating to 300°C caused an evolution of gas which was not CO_2 since replacing the CO_2 snow on the traps by liquid air did not cause the gas to condense. A similar effect and a suggested explanation are noted under the section on magnesium. The diffuse barium deposit cleaned up CO_2 to the extent of 59.5 microns for a 1-liter volume per milligram of barium at room temperature.

General Considerations

When the gas is admitted to a flashed getter surface, the action is at first extremely rapid. Usually about 80 percent of the eventual clean-up occurs in the first fifteen seconds or less. The action then continues at a slower rate until all the gas is cleaned up, or until the getter is saturated and clean-up ceases. If successive batches of gas are introduced into the same getter tube and clean up, the start of the clean-up curves becomes less steep as the clean-up powers of the getter approach exhaustion. It was observed that in the case of air, clean-up was never complete, a residual pressure corresponding to the argon content of the air always remaining.

Two cases in which gettering was continued as long as any clean-up took place, and which resulted in apparently complete replacement of the getter deposit by a translucent, iridescent film, indicating practically complete utilization of the getter, give an interesting relationship between the amount of getter available and the gas cleaned up.

The first case, that of diffuse barium and oxygen, showed that for each oxygen molecule cleaned up, there was available 2.6 molecules of barium. Assuming the end product to be a BaO, which would require only 2.0 molecules of barium for each oxygen molecule, there was therefore an excess of barium which did not act, although there was no visible black deposit left on the bulb.

The second case, that of hydrogen and diffuse barium, showed a similar result. In this case there was available 1.6 molecules of barium for each hydrogen molecule cleaned up, whereas the formation of BaH_2 would require only 1.0 molecule of barium for each hydrogen molecule.

Later experiments dealing with the amount of gas given off by the getter in process of being flashed, make it seem most probable that the discrepancy noted above was caused by the use of some of the getter to clean up its own evolved gases.

Getter Action in the Presence of Mercury

The behavior of getters in the presence of mercury is of interest because of the existence of a number of tubes containing mixtures of mercury vapor and an inert gas, the purity of which should be maintained throughout the life of the tube. For these tubes, as well as those containing only mercury as a filling, the use of getters, if successful, would offer the same general advantages noted in the previous discussion. Unfortunately, the activity of most getters appears to be seriously affected if not entirely destroyed in the presence of mercury.

The getter materials investigated in the presence of mercury were barium, misch metal, thorium and magnesium. For this part of the investigation, the system was provided with two side tubes containing mercury and located as indicated by the dotted lines at "*K*" in Fig. 1. During the baking of the getter tubes, these side tubes were kept cool. After baking, the getter tubes were allowed to cool and the getters were then degassed in the usual manner. The getter could then be flashed with the getter tubes open to the mercury vapor pressure of approximately 1 micron in the side tube, or mercury could be distilled into the getter tube before flashing. Barium, which was found to be the best all-around getter in the absence of mercury, appeared to be most seriously affected by the mercury. Amalgamation of the getter deposit proceeded rapidly and the deposit refused to take up hydrogen. Oxygen was taken up in such small amounts that the effect would be of little practical value. If a barium getter deposit was laid down in a tube free from mercury, and hydrogen was cleaned up, and then mercury distilled into the getter tube, an evolution of gas took place as the getter deposit amalgamated with the mercury.

Misch metal seemed to be less affected by the presence of mercury than barium was. Quantitative measurements were not made, but a lighter

deposit than those produced in previous misch metal experiments cleaned up about 9 microns of oxygen in a 1-liter volume. Torching the getter tube produced further clean-up. No evolution took place during an eighteen hour period in which the getter deposit was left in contact with the mercury. This material, therefore, offers some help, but is much less effective than when free from mercury.

Magnesium also cleaned up and held oxygen in the presence of mercury. No clean-up of hydrogen was observed, although the same deposit took up oxygen when this gas replaced the hydrogen first tried.

Thorium behaved much as the magnesium did, cleaning up and holding oxygen but showing no activity for hydrogen.

In order to determine if any of the clean-up activity observed above was due to action by the mercury itself, a blank bulb containing no getter was sealed to the system. After torching the bulb, oxygen was admitted and then mercury was boiled into the bulb. Repeated heating of the tube walls and mercury failed to produce any clean-up. It is therefore probable that the mercury itself did not take up any appreciable part of the gases cleaned up in the above experiments.

These results would indicate that magnesium or misch metal would be more suitable than barium in cases involving the presence of mercury vapor, while in other cases, ease of handling (in its newly available forms), strong gettering powers for a variety of gases, and its low vapor pressure would seem to make barium the most suitable getter to use.

The Infra-Red Transmission of Thin Films of Various Organic Materials

A. J. Wells
Mallinckrodt Chemical Laboratory, Harvard University, Cambridge, Massachusetts
(Received March 23, 1939)

The transmission of thin films of the following materials has been measured between 400 cm^{-1} and 3000 cm^{-1}: Cellophane, ethyl cellulose, cellulose acetate, Duco household cement, polystyrene, glyptal, Pliofilm, rubber, Plexiglas, methyl methacrylate polymer, XYSG Vinylite, and Shawinigan V-15 resin. The possibility of using these materials for windows in spectroscopic experiments is discussed.

THIN films of certain materials have frequently been used for windows in investigations in the infra-red region.[1] With the recent development of many kinds of synthetic materials suitable for making films, it was thought desirable to make a rough, practical survey of the infra-red spectra of a number of these. The region covered was from 400 cm^{-1} to 3000 cm^{-1}, that is, the range conveniently covered with potassium bromide and rocksalt prisms. The results presented below are derived from readings taken at comparatively large frequency intervals so that they do not give a detailed picture of the spectra of these materials. However, they do show the main bands and should be sufficient for indicating which resins are most likely to be useful as windows or as lacquers for salt prisms, etc.

[1] J. Strong and S. C. Woo, Phys. Rev. **42**, 267 (1932).

The transmission of average thickness rocksalt and potassium bromide windows, recorded on the same spectrometer, is given for comparison.

Methods of Making Films

Some of the materials tested were available commercially as thin films. Others were available in solution or, if in solid form, were dissolved in suitable solvents. These solutions were diluted to the proper concentration and spread on the surface of mercury. The solvent was then allowed to evaporate, leaving a thin film of the material which could be removed on a metal ring. In other cases thin films of suspended liquid were formed by dipping wire rings into concentrated solutions of the material. The solvent was allowed to evaporate leaving a thin film of the solid. The rubber film was made from diluted

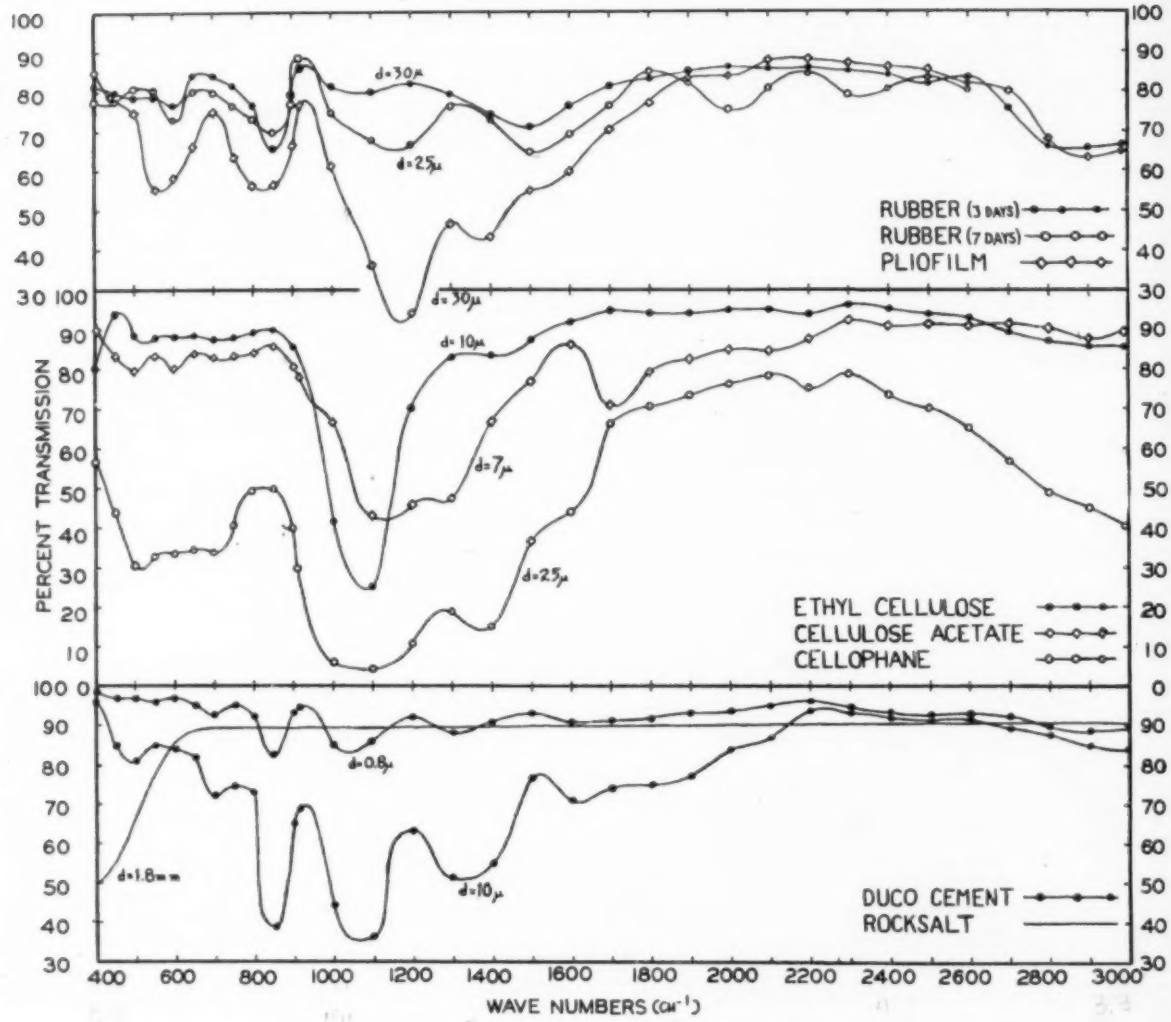

FIG. 1. Transmission of thin films. d = thickness.

latex by allowing a thin layer of the liquid to coagulate and dry on a glass plate. The rubber was stripped off and mounted on an iron ring. In general the films made by the mercury method were more constant in thickness, while those made by the dip method showed fewer surface imperfections and less image distortion with visible light. However, it was felt that the surface effects would be less important with light of longer wavelengths so that in the interests of uniformity the mercury method was used more extensively.

MATERIALS

Latex: obtainable from any latex importer. 60 percent Lotol from the Naugatuck Chemical Company was used in these experiments.

Pliofilm: a rubber hydrochloride obtainable in thin transparent sheets from the Goodyear Rubber Company.

Ethyl cellulose: obtainable from the Hercules Powder Company. Soluble in 80 percent benzene—20 percent alcohol. Films were made by both the mercury method and the dip method.

Cellophane: obtainable from the DuPont Company in convenient thicknesses. The particular sample used in this work had been used to wrap a package.

Cellulose acetate: obtainable in sheets from the Eastman Kodak Company. Soluble in acetone. Thin films were made by the mercury method.

Duco household cement: obtainable at hardware stores as a concentrated solution packaged in metal tubes. It can be thinned with amyl acetate. Films as thin as 1 micron were made by the mercury method.

Plexiglas: an acrylic resin obtainable in transparent sheets from the Röhm and Haas Company. Soluble in benzene. Films were made by the mercury method.

Methyl methacrylate polymer: obtainable from the DuPont Company as a powder. Soluble in toluene. Films were made by both the mercury method and the dip method.

Glyptal resin: obtainable in solution from the General Electric Company. They also furnish the thinner. No. 1276 was used in these experiments. Films were made by both methods.

Polystyrene: obtainable in transparent blocks from the DuPont Company. Soluble in benzene. Films were made by the mercury method.

XYSG Vinylite: a plasticized resin obtainable from the Union Carbide and Carbon Company. Soluble in alcohol. Thin films were made by the mercury method.

Shawinigan V-15 resin: obtainable as a powder from the Shawinigan Products Company. Soluble in acetone. Films were made by the mercury method.

Rocksalt: a single crystal plate of natural origin with cleaved faces.

Potassium bromide: a single plate crystal with cleaved faces cut from a large, artificially grown crystal obtained from the Harshaw Chemical Company.

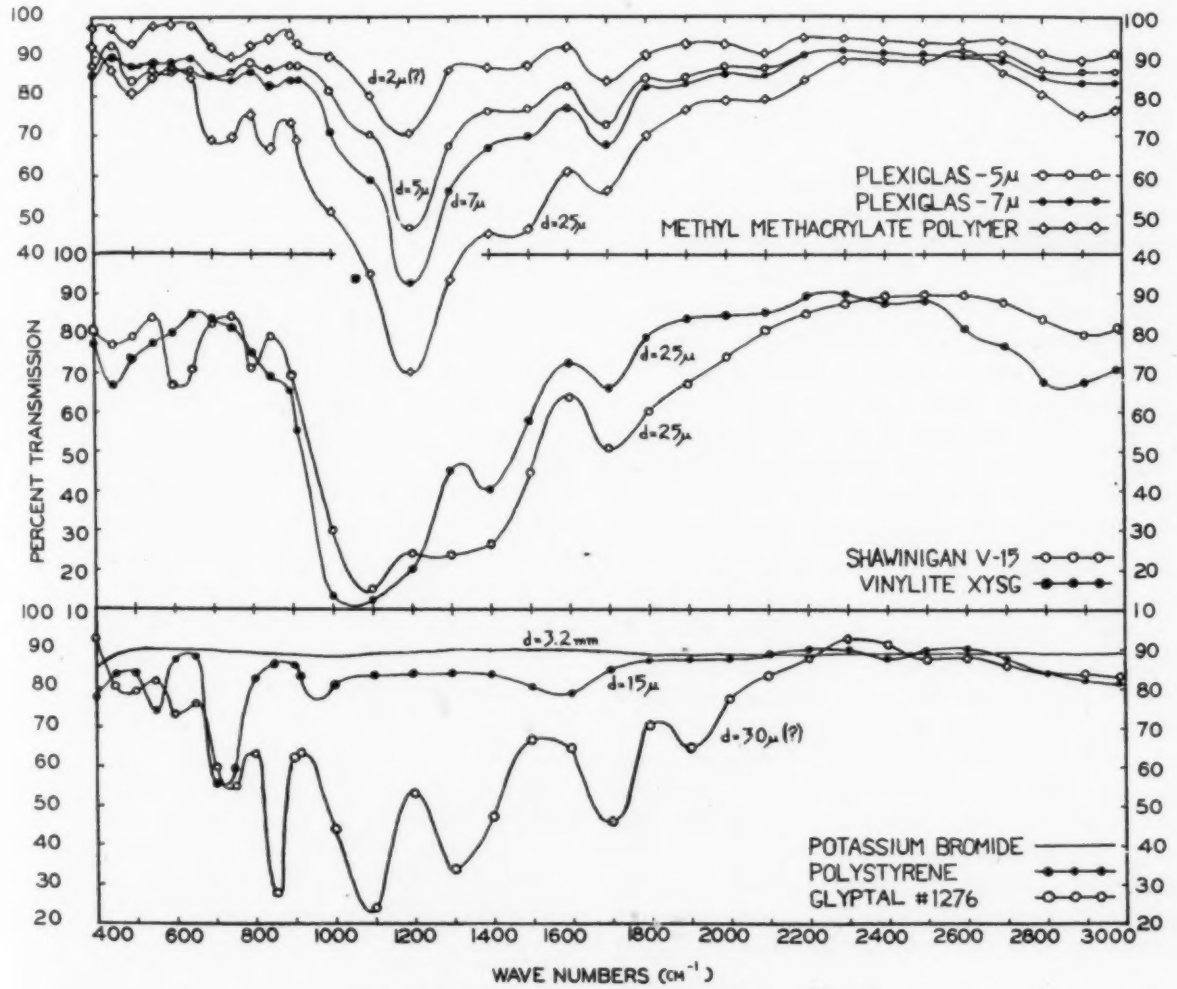

FIG. 2. Transmission of thin films. d = thickness.

Measurement of the Thickness of the Films

The thickness of a given film varied a good deal from point to point so that an average figure was the best that could be hoped for. Under these circumstances reasonably consistent results could be obtained with an ordinary micrometer on films thicker than 5 microns. Thinner films were measured by weighing a known area. The figures given below are correct to about 20 percent.

Measurement of the Transmission

The spectrometer used in these experiments has been described previously.[2] The automatic recording device was not used since it gave readings closer together than was necessary for the purposes of this investigation. Instead the deflected beam from the galvanometer was thrown upon a scale placed near the source of radiation. The samples were inserted by hand into the beam of radiation between the source and the first mirror while the deflection was read visually. The potassium bromide prism was used in the region from 400 cm^{-1} to 900 cm^{-1}, measurements being taken every 50 wave numbers. The rocksalt prism was used in the region from 900 cm^{-1} to 3000 cm^{-1}, measurements being taken every 100 wave numbers.

The results are plotted in Figs. 1 and 2 as percent transmission against wave numbers. There is a small amount of stray in the instrument for which no correction is made. There is also some loss by reflection from the surface of the films. The thicknesses are given on the curves. Where possible the results for two thicknesses are given.

Discussion

The results were not expressed as absorption coefficients because of the inaccuracies in the measurement of the thickness and because it was felt that the transmission of a film of practical thickness was a more pertinent property. The most interesting result is that in general the materials become more transparent in the potassium bromide region surpassing in some instances the transmission of the potassium bromide itself. They are useful, therefore, in extending the range of the spectrometer to longer wave-lengths.

From 400 cm^{-1} to 900 cm^{-1} the most transparent films are those made from Plexiglas, ethyl cellulose, and methyl methacrylate polymer. Very thin films of Duco cement are also quite transparent. R. Bowling Barnes[3] reports that films of celluloid 1 micron thick are transparent in the region from about 600 cm^{-1} out. Also thinner films of Shawinigan V-15 resin and of cellulose acetate might give satisfactory results.

Stair and Coblentz[4] have determined the absorption of rubber, polystyrene, Cellophane, and glyptal in the rocksalt region. Considering the qualitative nature of our work, the agreement is very good. Altogether, the best materials for transmission in this region (900 cm^{-1} to 1800 cm^{-1}) appear to be polystyrene and very thin films of Duco cement.

It is interesting to note that the observation of Stair and Coblentz,[4] that rubber on ageing gains bands around 1100 cm^{-1}, is substantiated by our curves for three-day old and seven-day old rubber films.

In studying the curves for the two samples of Plexiglas, one 5 microns thick, the other 7 microns thick, it was noted that the thinner film transmits better than the thicker one in every region except around 550 cm^{-1}. It would be expected that a film 7μ thick would reinforce light of wave-length twice 7μ multiplied by the index of refraction of the film. No data are available for the index of refraction of Plexiglas at 18μ, but if the not unreasonable value of 1.3 is used, reinforcement would be expected at 18μ corresponding to 550 cm^{-1}.

Since this work was completed very thin Duco cement films have been used as cell windows in the study of the absorption spectra of gases at 100°C in the region from 400 cm^{-1} to 1400 cm^{-1}.

Many thanks are due to Mr. John Brooke Gregory of the B. B. Chemical Company who helped obtain many of the materials and to Professor E. Bright Wilson, Jr., who suggested this study.

[2] H. Gershinowitz and E. B. Wilson, Jr., J. Chem. Phys. **6**, 197 (1938).

[3] R. B. Barnes, Phys. Rev. **39**, 562 (1932).

[4] R. Stair and W. W. Coblentz, Nat. Bur. Stand. J. Research **15**, 295 (1935).

Studies in Lubrication

VI. Electrolytic Models of Full Journal Bearings

F. Morgan, M. Muskat and D. W. Reed
Gulf Research & Development Company, Pittsburgh, Pennsylvania
(Received July 31, 1939)

An electrolytic model of a full journal bearing having a ratio of journal displacement to radial clearance of 0.1 has been constructed. The reliability of the model was established by comparing the results observed for the infinitely wide bearing with those predicted by the theory of Reynolds. The results obtained for models of journal bearings of finite width, bearings with circumferential grooves, and bearings with sources of lubricant are also in agreement with hydrodynamic theory.

Introduction

THE contributions of Sommerfeld[1] to the mathematical treatment of the Reynolds hydrodynamic theory[2] of lubrication paved the way to the practical application of the theory to the full journal bearing. Before the theory can be applied with confidence, however, and before comparison with experiment can be made, certain approximations must be investigated. Probably the most important of these arises from the fact that any actual journal bearing must necessarily be of finite width, while in the analysis of Sommerfeld (and of Reynolds) the width was assumed to be infinite in order that the motion could be treated as two-dimensional.

Perhaps the earliest case of a complete solution of a problem of lubrication in three dimensions was that of the treatment by Michell[3] in 1905 of a plane block of finite length and width sliding over a fixed plane surface which is copiously supplied with oil. The important features of the problem were shown to be essentially the same as in the two-dimensional system considered earlier by Reynolds except for the side leakage and lower film pressures obtaining in the block of finite width. Under such conditions the load carrying power, for the same film thickness, will obviously be greatly reduced.

Until very recently the extension of Michell's analysis to journal bearing systems had met with no success. To obtain some theoretical quantitative information about such bearings Kingsbury[4] introduced the analogy between the viscous flow of the lubricant film and the flow of electricity in a conductor. He applied it to various types of bearings, such as the square slide block, the sector-shaped surface, and partial journal bearings of 180 and 120 degrees of arc. This work was continued by Needs[5] who studied the journal bearing of 120 degrees for various values of the journal eccentricity.

A particularly valuable feature of the electrical analogy is that apparatus for such measurements has been developed to a high degree of perfection, and the measurements may usually be made without much difficulty. Moreover, it is especially convenient in case the effect of a source of lubricant or of bearing grooving is to be studied. It is, indeed, in the field of grooving that the electrical model seems to offer the greatest promise, because the number of types of grooves and of their modifications is so enormous and complex that no complete theoretical solution can reasonably be expected.

Besides possessing excellent possibilities for the study of grooving there are two other fields of possible usefulness for the electrical model of a complete journal bearing. In the first place, it is useful for checking the accuracy of solutions already existing. Secondly, by means of the model information in regard to the journal bearing may be obtained in a region where no solution is available.

The present model, in which the ratio of journal eccentricity to radial clearance is 0.1, was originally designed before a complete analytical solution was available. Since then a solution,

[1] A. Sommerfeld, Zeits. f. Math. Phys. **50**, 97 (1904).
[2] O. Reynolds, Phil. Trans. Roy. Soc. **177**, 157 (1886).
[3] A. G. M. Michell, Zeits. f. Math. Phys. **52**, 123 (1905).
[4] A. Kingsbury, Trans. A. S. M. E., PME–53–5, p. 59 (1931).
[5] S. J. Needs, Trans. A. S. M. E. **56**, 721 (1934).

satisfactory up to an eccentricity of about 0.5, has been developed.[6] The usefulness of this particular model has consequently been limited to the checking of this solution and of the Sommerfeld solution for the bearing of infinite width.

Although the model is similar to those of Kingsbury and Needs in that it also is based upon the analogy between viscous flow and the flow of electricity, it is nevertheless different in several important respects. For example, in all cases previously studied the problem was much simpler in that the pressures at the boundaries were always atmospheric so that the requirement that the pressure must be a periodic function of θ, as in a full journal bearing, did not arise. Furthermore, in the present case the labor involved in making measurements was considerably reduced both by the introduction of the current in a semi-continuous manner rather than in a stepwise order in the analog of the bearing of infinite width, and by the utilization of a potential divider by means of which the necessary boundary conditions could be established at once in the finite width case. As stated in an earlier paper,[7] information on the effects of an external source of lubricant and of various types of grooving has been largely of an empirical nature. Apparently no attempt has previously been made to adapt a model, electrolytic or otherwise, to the study of the associated phenomena.

Theory of the Model

The Reynolds differential equation, which is generally accepted as the fundamental basis of the theory of viscous lubrication, may be written:

$$\frac{\partial}{\partial x}\left(\frac{h^3}{12\mu}\frac{\partial p}{\partial x}\right)+\frac{\partial}{\partial z}\left(\frac{h^3}{12\mu}\frac{\partial p}{\partial z}\right)=\frac{U}{2}\frac{\partial h}{\partial x}, \qquad (1)$$

where h is the film thickness, μ the lubricant viscosity, p the pressure in the film, and U the relative velocity of the two surfaces. The coordinate x is measured in the direction of motion and z along the axis of the journal bearing.

In deriving this equation Reynolds made the assumptions that the thickness of the film is very small, that the pressure variation across the film may be neglected, and that fluid flow will consequently take place only in the x and z directions. With the same assumption of a small film thickness its form may be expressed as:

$$h=c+e\cos\theta, \qquad (2)$$

where the origin of coordinates is taken at the position of maximum film thickness, c is the radial clearance, and e is the journal displacement (cf. Fig. 1).

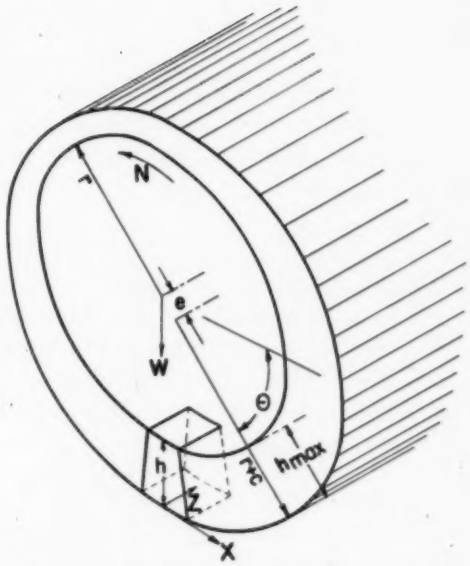

Fig. 1. Section of a lubricating film in a full journal bearing.

If we now introduce the notation:

$$\eta=e/c; \quad w=z/r; \quad x=r\theta, \qquad (3)$$

where r is the journal radius, and assume that μ is constant everywhere, Eq. (1) assumes the dimensionless form:

$$\frac{\partial}{\partial\theta}\left\{(1+\eta\cos\theta)^3\frac{\partial p}{\partial\theta}\right\}+(1+\eta\cos\theta)^3\frac{\partial^2 p}{\partial w^2}=-\beta\eta\sin\theta, \qquad (4)$$

where

$$\beta=6\mu Ur/c^2. \qquad (5)$$

For the problem of electrical conduction in two dimensions the basic differential equation corresponding to Eq. (1) is

$$\frac{\partial}{\partial x}\left(\sigma\frac{\partial V}{\partial x}\right)+\frac{\partial}{\partial z}\left(\sigma\frac{\partial V}{\partial z}\right)=q, \qquad (6)$$

where V is the potential, σ the conductivity, and

[6] M. Muskat and F. Morgan, J. App. Phys. **10**, 46 (1939).
[7] F. Morgan and M. Muskat, J. App. Phys. **10**, 327 (1939).

q the distributed current source strength. If now we change the coordinate scales in the electrical system according to the relations:

$$x = L\theta/2\pi; \quad z = wL/2\pi, \tag{7}$$

and suppose the conductivity σ to vary with x, or θ, as defined by

$$\sigma = \alpha(1+\eta \cos \theta)^3, \tag{8}$$

the potential will have to obey the equation:

$$\frac{\partial}{\partial\theta}\left\{(1+\eta\cos\theta)^3\frac{\partial V}{\partial\theta}\right\} + (1+\eta\cos\theta)^3\frac{\partial^2 V}{\partial w^2} = \frac{L^2}{4\pi^2\alpha}q. \tag{9}$$

If now, finally, the current source strength q be chosen so that:

$$L^2q/4\pi^2\alpha = -\gamma\beta\eta \sin \theta, \tag{10}$$

the distribution of potential V will be formally analogous to the film pressure p, with a numerical ratio of:

$$p = V/\gamma. \tag{11}$$

Of the transformation Eqs. (7), (8), and (10), Eq. (8) clearly represents the crux of the analogy. To achieve such a conductivity variation in a strictly two-dimensional system would be a problem even more difficult than the direct empirical solution of Eq. (4). Fortunately, however, the same result can be attained with reasonable accuracy by permitting the conductor itself to remain homogeneous—a uniform electrolyte—but changing its thickness, along x or θ, so that the *effective* two-dimensional conductivity will vary according to Eq. (8). In particular, by forcing the electrolyte thickness to vary as:

$$t = t_0(1+\eta \cos \theta)^3, \tag{12}$$

Eq. (8) will be satisfied on taking $\alpha = \sigma_0 t_0$, where σ_0 is the conductivity of the electrolyte.

Equation (12) implies, of course, that for a full journal bearing the over-all thickness of the electrolytic layer will vary by the factor $\{(1+\eta)/(1-\eta)\}^3$. For increasing values of the eccentricity η, the current flow will show increasing deviations from the strictly two-dimensional character, and the equivalence between Eqs. (8) and (12) will become increasingly less exact. This fact presents the major limitation to the use of the electrolytic model. However, for moderate values of the eccentricity, or for partial bearings of limited arc, the model should be sufficiently accurate for all practical purposes.

Equation (11) will give the pressure that is produced by the shear in the lubricant due to the relative motion of the bearing surfaces. If there are other pressures due to sources of lubricant or external effects, they may be treated separately and the resultant pressure found by the principle of superposition.

Theoretically the current supplied to the conducting layer should be a continuous function of the distance from the position of maximum thickness as determined by Eq. (10). In practice, however, it is more convenient to divide the surface into a number of equal areas and to supply current, as given by Eq. (10), at definite points in each element in turn. Corresponding to each value of the current, series of voltage readings are taken at definite intervals and the resulting voltage at any point is found by superposing the separately determined values. On the other hand, it should be noted that even this stepwise superposition procedure is only necessary when checking the model for the infinitely wide bearing. For bearings of finite width the use of the distributed sources given by Eq. (10) can be completely dispensed with by suitably manipulating the boundary conditions, as will be seen below.

Journal bearings of infinite width

In case the flow takes place only in the direction of relative motion of the two surfaces, which is the situation in the journal bearing of infinite width as treated by Reynolds and Sommerfeld, both the equations and the experimental arrangement become greatly simplified. In the above equations all terms that involve w may simply be dropped, and in the resulting ordinary differential equation p is a function of θ alone. This situation may be satisfied experimentally by insulating those sides of the conducting sheet which correspond to the infinitely distant ends of the journal bearing, and supplying current to electrodes which run axially from one insulated side to the other.

The resulting ordinary differential equation for this case, namely,

$$\frac{d}{d\theta}\left\{(1+\eta\cos\theta)^3\frac{dp}{d\theta}\right\}=-\beta\eta\sin\theta, \qquad (13)$$

has the solution

$$p=\frac{\beta\eta}{2+\eta^2}\frac{(2+\eta\cos\theta)\sin\theta}{(1+\eta\cos\theta)^2}. \qquad (14)$$

To compare the experimental results directly with Eq. (14), a considerable number of data must be obtained, because the voltage equivalent of p will be given by adding algebraically the contributions due to the current supplied to the various elements of area according to Eq. (10). A simpler test was therefore devised which involved only the comparison of the voltages obtained experimentally for any individual setting of the current electrodes with those predicted by the Reynolds theory. These theoretical values were obtained by integrating the equation

$$\frac{d}{d\theta}\left\{(1+\eta\cos\theta)^3\frac{dV}{d\theta}\right\}=0, \qquad (15)$$

subject to the conditions that at the position of maximum film thickness the voltage shall be zero and at the electrode at which current is supplied the voltage shall be determined by the input current which in turn was determined by Eq. (10). The solution of Eq. (15) is given by:

$$\begin{aligned}V&=\frac{Ia}{\sigma}\int_0^\theta\frac{d\theta}{(1+\eta\cos\theta)^3}\\&=\frac{Ia\eta}{\sigma}\left[\frac{2+\eta^2}{\eta(1-\eta^2)^{5/2}}\tan^{-1}\left(\frac{1-\eta}{1+\eta}\right)^{\frac{1}{2}}\tan\frac{\theta}{2}\right.\\&\qquad-\frac{3}{2}\frac{\sin\theta}{(1-\eta^2)^2(1+\eta\cos\theta)}\\&\qquad\left.-\frac{1}{2(1-\eta^2)}\frac{\sin\theta}{(1+\eta\cos\theta)^2}\right], \qquad (16)\end{aligned}$$

where I is the current supplied, σ the conductivity, and a is a scale factor depending upon the units of measurement.

The theoretical potential distribution for any position of the current electrode may easily be found from Eq. (16) by a method that will be described below. The individual curves for the various settings of the current electrode may then be superposed after being given the proper weight in accordance with the right side of Eq. (10), and the resultant curve may be compared with that plotted from Eq. (14).

Flooded journal bearing of finite width

The journal bearing of finite width may be represented by the electrical model in either of two ways. The first method involves the introduction of current at every point in accordance with Eq. (10), the maintenance of zero potential (atmospheric pressure) at all the boundaries, and the measurement of the voltage at representative points. The second method, which will be described below, can be applied only to the case in which the film thickness does not vary in the direction of the bearing width and the solution for the bearing of infinite width is available. As these conditions are fulfilled in the case of the complete journal bearing, and as the experimental work is thereby greatly reduced, this method was adopted for the present study.

For the simple case in which $h=h(x)$ and μ is a constant, a particular solution (independent of z) of the generalized Reynolds equation:

$$\frac{\partial}{\partial x}\left(h^3\frac{\partial p}{\partial x}\right)+\frac{\partial}{\partial z}\left(h^3\frac{\partial p}{\partial z}\right)=6\mu U\frac{\partial h}{\partial x}, \qquad (17)$$

is given by $p_0=p_0(x)$, where p_0 is the solution of the two-dimensional equation:

$$\frac{\partial}{\partial x}\left(h^3\frac{\partial p}{\partial x}\right)=6\mu U\frac{\partial h}{\partial x}. \qquad (18)$$

The general solution of Eq. (17) may then be represented as:

$$p=p_0-q, \qquad (19)$$

where q must satisfy the equation:

$$\frac{\partial}{\partial x}\left(h^3\frac{\partial q}{\partial x}\right)+\frac{\partial}{\partial z}\left(h^3\frac{\partial q}{\partial z}\right)=0. \qquad (20)$$

The condition that $p=0$ at the edges of the bearing then requires that $q=p_0$ at these boundaries.

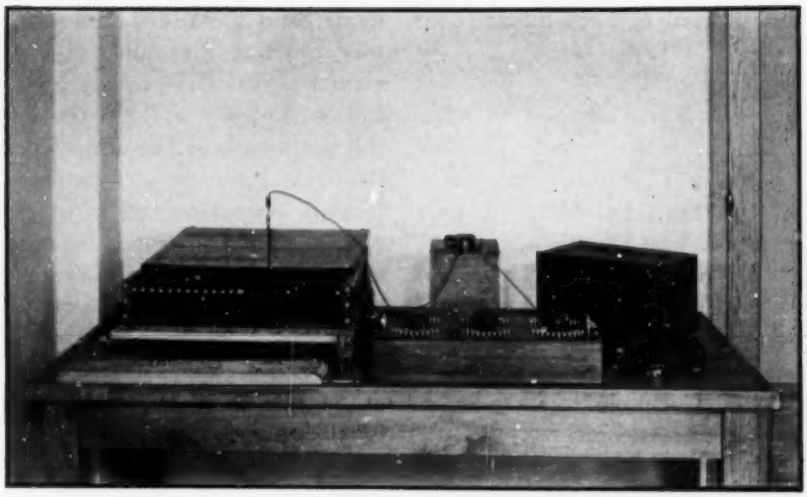

FIG. 2. Electrolytic model of journal and bearing.

The pressure at any point in the film of a bearing of finite width may thus be determined by Eq. (19), in which p_0 is the Sommerfeld value for the bearing of infinite width, and q is the pressure at the given point resulting from an impressed pressure at the ends of the bearing corresponding to the Sommerfeld distribution.

Likewise in the case of the electrical model a potential distribution, corresponding to that of the analogue of the bearing of infinite width, is applied to the end boundaries, and the potential at any point is found by substituting potentials for pressures in Eq. (19).

Journal bearing with circumferential groove

In case the dimension of the groove in the direction of the journal radius is large in comparison to the film thickness, the pressure drop in the groove may be neglected. In the electrical model this case is treated quite simply by applying a uniformly high potential at one end of the conducting layer, grounding the other, and determining the resulting intervening potential distribution. A circumferential groove,[5] of course, effectively cuts the bearing into two equal parts as far as load carrying power is concerned. So the data secured are applicable to a grooved bearing of width twice the actual width of the model.

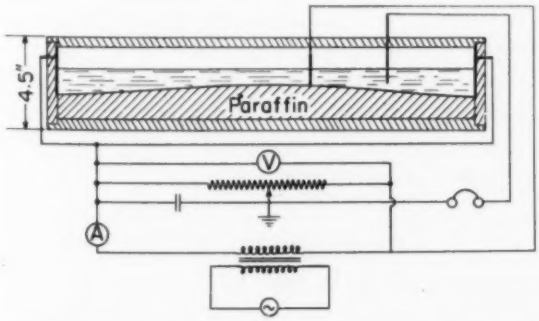

FIG. 3. Diagram of model of a bearing of infinite width together with the electrical circuit for determining the potential distribution.

Point source of lubricant in a complete bearing

The theoretical pressure distribution in a journal bearing with a fluid source has been treated in the third paper[6] of this series. In the electrical model the effects of the source and of rotation may conveniently be treated separately, and the combined results found by superposition.

CONSTRUCTION AND OPERATION OF THE MODEL

A photograph of the model as actually constructed is shown in Fig. 2. A diagrammatic sketch of the model and of the electrical circuit for the analog of the bearing of infinite width is shown in Fig. 3. The conductor consisted of a liquid of relatively low electrical conductivity, with a free upper surface and variable depth, contained in a box having a shape corresponding

[5] M. Muskat and F. Morgan, J. App. Phys. **10**, 398 (1939).

to that of the bearing surface. The liquid depth, which conforms to Eq. (12), was determined by a form consisting of a solid block of paraffin, the top surface of which was shaped to fit a template. The narrow space between the paraffin block and the Bakelite container was quite effectively sealed with Gulf Petrowax. A thin layer of the same material on the surface served to seal the small cavities formed when the paraffin cooled after being poured into the box. In the analog of the journal bearing of infinite width the liquid consisted of a dilute solution of copper sulfate in water. Distilled water later proved to be more satisfactory and was used in all the other cases. The first electrodes were made of copper. This material was later replaced by stainless steel; a deposit was observed to form on the copper, while the steel, when once cleaned, remained untarnished for many days. Special precautions were found to be necessary in the preparation of these materials, as the potential distribution as well as the behavior of the potential as a function of the frequency was found to depend upon the state of cleanliness of the electrodes. The most effective method of conditioning the electrodes was found to be to scour them, while wet, with emery cloth, and then to wash them with distilled water. As long as they remained under water no difficulty was experienced with further contamination. Holes drilled in the cover of the box controlled the position of the rods carrying the movable electrodes. The depth of liquid in the tank was determined by a micrometer gauge. Electrical contact, completed through the liquid itself, established one point of measurement while contact with the upper surface of the paraffin base determined the other. The depth reading was further checked by direct measurement of the total volume of electrolyte.

The model was 22 inches long (θ or x dimension) and 19.5 inches wide. The maximum depth of the liquid was 1.331 inches; the minimum depth was 0.729 inch.

The source of power was a Leeds and Northrup vacuum tube oscillator which operates at a frequency of 500, 1000, or 2000 cycles per second. In order to reduce the effect of unknown capacities a General Radio shielded transformer was connected between the oscillator and the model, and one side of the telephones, which were used to detect the null point, was grounded. An attempt was made to use a single dry cell as a source of current and a potentiometer to measure the voltage, but, because of polarization at the electrodes, the results proved to be unsatisfactory. With alternating current and clean electrodes the potential distributions were practically independent of frequency over the range of the oscillator. Generally an electrolyte of high resistivity was found to be preferable in these experiments, because the ill effects of contaminated electrodes become less important as the resistivity becomes higher. Ordinary distilled water proved to be satisfactory.

Just as in the actual full journal bearing the pressure must be a periodic function of period 2π, so in the model the voltage must be the same at θ as at $\theta+2\pi$. In order to meet this condition in the present case the potentials at $\theta=0$ and at $\theta=2\pi$ were forced to have the same value by inserting metal strips at both ends and connecting a metal strip at one end to the corresponding strip at the other end. As the pressure in the bearing of infinite width is independent of z, a continuous metal strip running from one side of the tank to the other at $\theta=0$ was connected to a like strip at $\theta=2\pi$, and both were kept at zero potential. In the bearing of finite width, however, the pressure in the z direction is not constant, but the periodicity requirement in θ must still be maintained. In order to meet this additional requirement the metal strips at each end were insulated from one another. While the condition that the pressure and consequently the voltage must be periodic is thus easily satisfied, the method utilized may in itself introduce a very serious error in the distortion of the field. Some experiments have been carried out which indicate that the best approximation to the ideal case is secured by the use of a large number of very thin strips. Actually 39 fine stainless steel wires were finally used at each end.

Experimental Results

Bearing of infinite width

A simplified diagram of the electrical circuit for the bearing of infinite width is shown in Fig. 4.

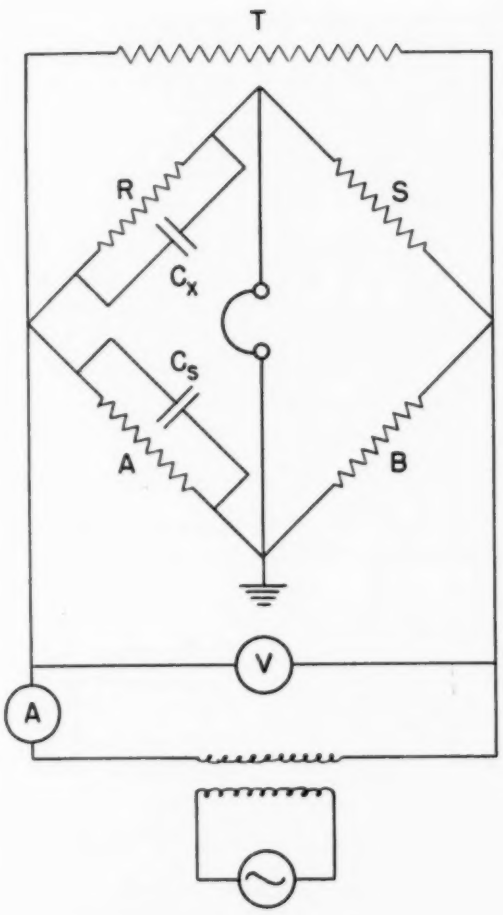

FIG. 4. Simplified diagram of electrical circuit for determining the potential distribution in the model of a journal bearing of infinite width.

In the diagram A and B are the two arms of a potential divider of total resistance 10,000 ohms. Arms R, S, and T represent the conducting strip, which corresponds to the lubricating film in the case of the bearing, with the potential probe between R and S. Some capacitance was always required in order to balance the bridge, but the best position for the condenser depended upon the location of the probe or test electrode with respect to the other electrodes. With electrodes that had not been thoroughly scoured the capacitance necessary for a balance was, in some cases, extremely high; and its magnitude, as well as the ratio A/B, varied greatly with the frequency. With polished electrodes, however, A/B was practically independent of frequency and the capacitance was very low.

If the unknown capacitance in the liquid is such that it may be represented by a condenser of capacitance C_x in parallel with the resistance R, the conditions under which no current will flow through the telephones are that:

$$B/A = S/R, \quad \text{and} \quad B/S = C_x/C_s. \qquad (21)$$

It follows immediately that, if the capacitance can be represented in this manner, the ratio of the resistances as read from the potential divider will be the same as the ratio of voltages in the liquid bath. Hence as the total resistance of the potential divider is 10,000 ohms the voltage across S will be:

$$V_s = BV/10{,}000, \qquad (22)$$

where V is the reading on the voltmeter.

It is probable, however, that the equivalent capacitance of the liquid cannot be strictly represented in such a simple manner, but that one or more series condensers would also be required to complete the analogy. Under such circumstances Eq. (21) may not hold, and the potential drop over S will not be given rigorously by Eq. (22).

Errors may also arise from other sources. Capacitance currents to ground through the telephones may result in a false balance, or skin effects in the liquid itself may lead to errors.

In the actual experiments C_s was always small and the resistance balance was for all practical purposes independent of frequency irrespective of the position of the balancing condenser. This indicates that the phase angle was small enough to be safely neglected. While a slight improvement was observed with a Wagner earth circuit, the effect on the final result was very small.

In Figs. 5 and 6 both the experimental data and the theoretically predicted results are shown for the model corresponding to the bearing of infinite width for two settings of the current electrode. The curves, themselves, which represent the theory, were plotted in accordance with Eq. (16). As the total resistance of the potential divider was maintained constant at 10,000 ohms, comparison with experiment could be made most directly on the basis of resistance rather than of voltage. To do this the theoretical scale was changed in such a way that at the position along the axis of abscissas corresponding to the movable electrode position the ordinate was 10,000,

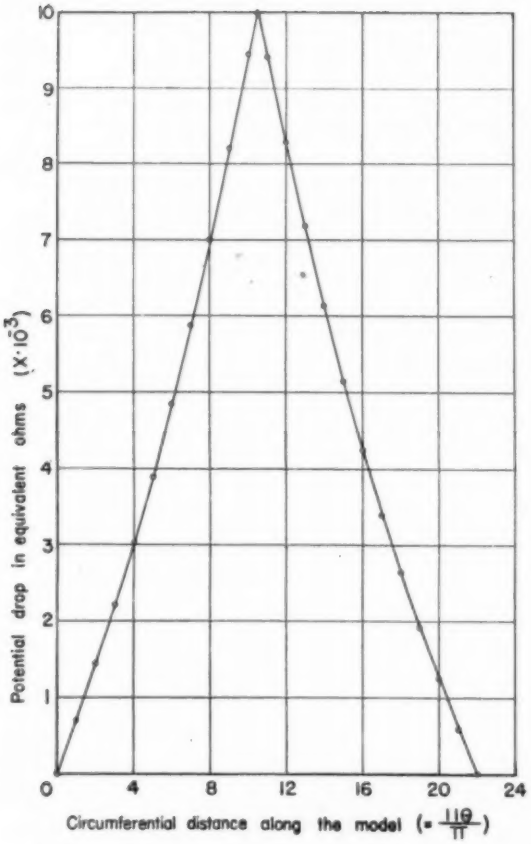

FIG. 5. Potential distribution in model for infinitely wide bearing with a line source 10.5 inches from the maximum conductor thickness. Solid curve: calculated by Eq. (16); o: experimental data.

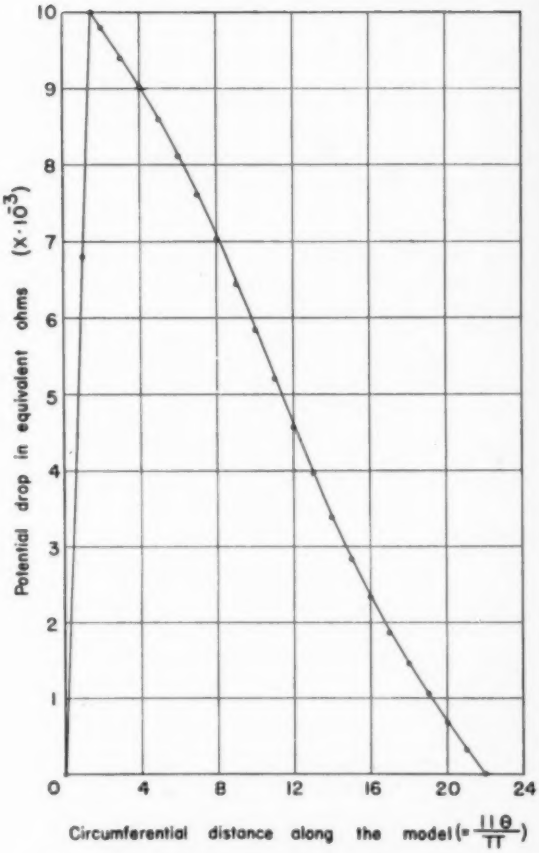

FIG. 6. Potential distribution in model for infinitely wide bearing with a line source 1.5 inches from the maximum conductor thickness. Solid curve: calculated by Eq. (16); o: experimental data.

and the ordinates of all other points to the left of the given point were altered in the same ratio. The points on the curve to the right of the position corresponding to the movable current electrode were obtained by similarly modifying the scale so that the ordinate corresponding to the supplementary abscissa was 10,000.

For the final comparison with the Sommerfeld curve, the various curves such as those of Figs. 5 and 6 were weighted in accordance with Eq. (10) and added algebraically to those obtained for positions of the movable current electrode on the other half of the model. It is obviously not necessary actually to secure data for positions of the electrode for both halves as the corresponding curves for the two halves will simply be the negatives of each other. In the actual experiments, curves were obtained for each of eleven settings of the current electrode spaced at 1-in. intervals beginning with ½-in. from the end ($\theta = 0$).

The method followed in assigning the appropriate weight to the various curves was not exact. The current theoretically should be supplied in a continuous manner according to a sine curve, while, for experimental reasons, it actually was introduced at specific points in equal areas. The smaller the areas the better is the approximation to the true value. Actually, however, if the areas are of considerable size the errors may be at least partially compensated by choosing for $\sin\theta$ the average value for the interval rather than its value at the center of the area, and by introducing the current at the center of gravity of the area in question. In case the areas are small, as they were in this part of the experiments, the errors introduced by taking the values of $\sin\theta$

at the centers of the areas are less than the errors arising from the actual setting of the electrodes.

The points in Fig. 7 were obtained by combining the curves such as those of Figs. 5 and 6 in the above manner. The curve, itself, corresponding to the solution given by Sommerfeld, was drawn in accordance with Eq. (14). While the lack of symmetry is not very great due to the low value (0.1) of the eccentricity, it is nevertheless quite apparent.

Both in Fig. 7 and Figs. 5 and 6 the agreement between the theoretical and experimental results are clearly sufficient to establish the reliability of the model.

Bearing of finite width

After the curve for the infinitely wide bearing has been obtained, the potential distribution for the model of the bearing of finite width may easily be found. To do this it was only necessary to impress potentials equivalent to those of the bearing of infinite width at the boundaries which correspond to the open ends, and to subtract the potentials observed throughout the model, when modified in this way, from the potentials for the infinitely wide case. As in the model of the bearing of infinite width, the theoretically continuous boundary distribution was approximated by a limited number of segments. However, due to symmetry, it was only necessary to extend these segments over half of the boundaries, while the other half was held at ground potential. The first measurements were made with six conducting segments of equal width, but this number was later increased to twelve with only slightly different results. The necessary potentials were sup-

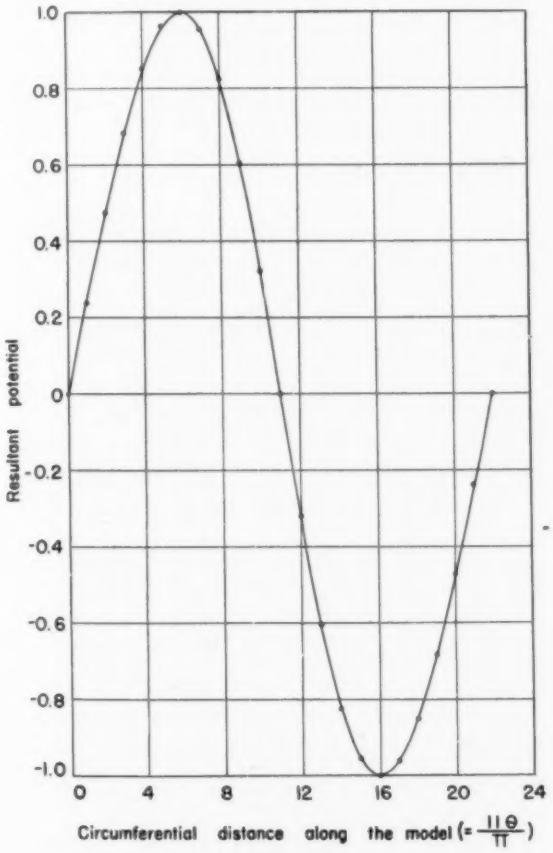

FIG. 7. Resultant potential distribution in an electrical model of a bearing of infinite width. Solid curve: calculated by Sommerfeld theory—Eq. (14); o: experimental determinations; journal eccentricity = 0.1.

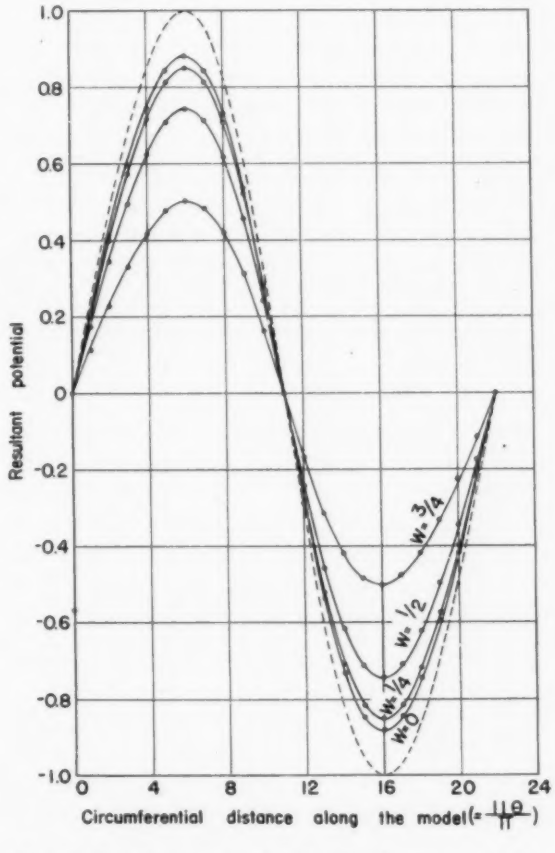

FIG. 8. Resultant potential distribution in an electrical model of a bearing of width = 0.88 perimeter. Solid curve: calculated theoretically; o: experimental determinations; broken curve: distribution for infinitely wide bearing; w = (axial distance from center)/(half-width of bearing); journal eccentricity = 0.1.

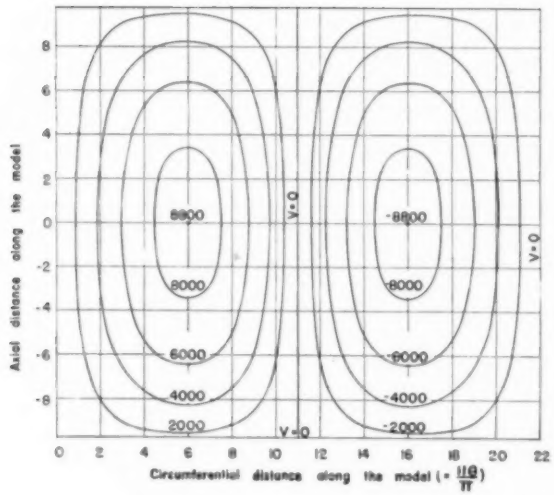

FIG. 9. Equipotential curves for model of a journal bearing of width = 0.88 perimeter.

plied to the segments by means of a potential divider, the final adjustment at each strip being made with the aid of the measuring probe. The potential was made continuous at the sides corresponding to $\theta = 0$ and $\theta = 2\pi$ by the method already described, and holes in the top of the Bakelite container again served to establish the position of the measuring electrode. Potential measurements were made along the center line of the model and along lines $\frac{1}{4}$, $\frac{1}{2}$, and $\frac{3}{4}$ of the distance from the center line to the edge in the z direction.

Figure 8 shows the results obtained. The curves themselves again represent the theoretically predicted[8] results, while the points correspond to experimental data. The agreement is obviously satisfactory. By contouring such data one may obtain the equipotential or equi-pressure curves of the system. While the few traverses of Fig. 8 are hardly sufficient to give very accurate contours, their general features are indicated in Fig. 9.

Bearing with circumferential groove

The experimental arrangement of the model of the bearing with a circumferential groove was quite simple, and the results obtained were even more elementary. As shown theoretically,[8] such a groove simply divides the bearing into two end-fed bearings each having half the original width and with feed pressures which are uniform about the circumference at the groove. The pressure distribution in a bearing equivalent to twice the width of the model may be therefore obtained by measuring the potential distribution in the model when one side (corresponding to an open end of the bearing) is maintained at a uniformly high potential and the other side is grounded.

Figure 10 shows an example of the pressure variation from one end of the model to the other. Within experimental error the pressure gradient was the same along the whole circumferential length of the model, as was to be expected theoretically. Consequently, to find the pressure distribution in one half of a bearing with such a groove, it is only necessary to superpose a pressure which decreases linearly from the groove pressure at one end to atmospheric at the other upon the normal flooded bearing distribution.

Bearing with source of lubricant

Because the number of possibilities in the location of the source of lubricant, whether it be a point source or groove, is so enormous, no attempt was made to exhaust this phase of the

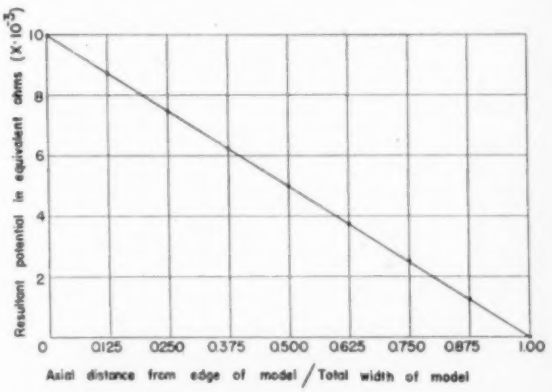

FIG. 10. Axial potential distribution in the electrical model for a bearing with a circumferential groove. Solid curve: theoretical distribution; o: experimental data.

subject. Only two positions and two diameters of the source were given consideration. The calculations involved in even this limited program were quite tedious when carried out to the full extent to which the theory has been developed.

Figure 11 is a schematic diagram of the apparatus and electrical connections used for these experiments. Obviously the same circuit may be used for the study of any type of grooving.

The points in Fig. 12 represent the measured

potential distribution for the source on the center line of the model, 270 degrees from the position of maximum film thickness. The curves represent the calculated values. As before, the setting of the voltage divider, which is actually proportional to the potential itself, has been plotted. The four curves refer again to the four circumferential lines parallel to the ends of the model along which potential readings were taken. The uppermost curve corresponds to the line through the center of the bearing, while the other lines are at distances 0.25, 0.50, and 0.75 of the half-width of the bearing from the center line. The equi-pressure contours are pictured in Fig. 13.

The effective radius of the source of lubricant was obtained by plotting the observed potential drop in resistance units against the logarithm of the distance from the center of the electrode which acts as the source of current. This is illustrated by Fig. 14. The effective radius so obtained was 0.030 in. while the measured value was 0.031 in. This agreement is quite satisfactory in view of the approximations involved.

Summary

The analogy between the flow of electricity in a conducting sheet and the motion of a viscous liquid has been successfully applied to the problem of lubrication of full journal bearings of infinite width, flooded bearings, bearings with circumferential grooves, and bearings with point sources of lubricant. The ratio of journal displacement to radial clearance was 0.1.

While the model of the journal bearing of infinite width is of no practical importance, the results obtained, nevertheless, served their purpose by proving conclusively that the model itself may be relied upon to give consistent and useful information on lubrication. The models of the flooded bearing, the bearing with a circumferential groove, and the bearing with a point source of lubricant—as distinguished from a groove—gave results of interest for two reasons. In the first place, the various analytical solutions have been confirmed. Secondly, the excellent

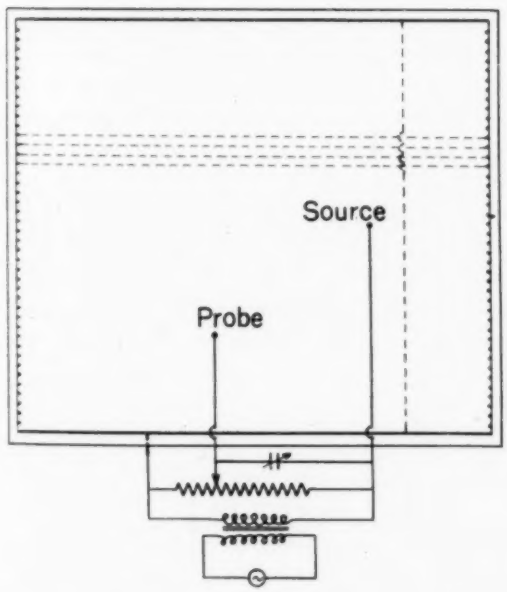

Fig. 11. Diagram of model of a bearing with a lubricant source together with the corresponding electrical circuit. All opposite electrodes connected as illustrated.

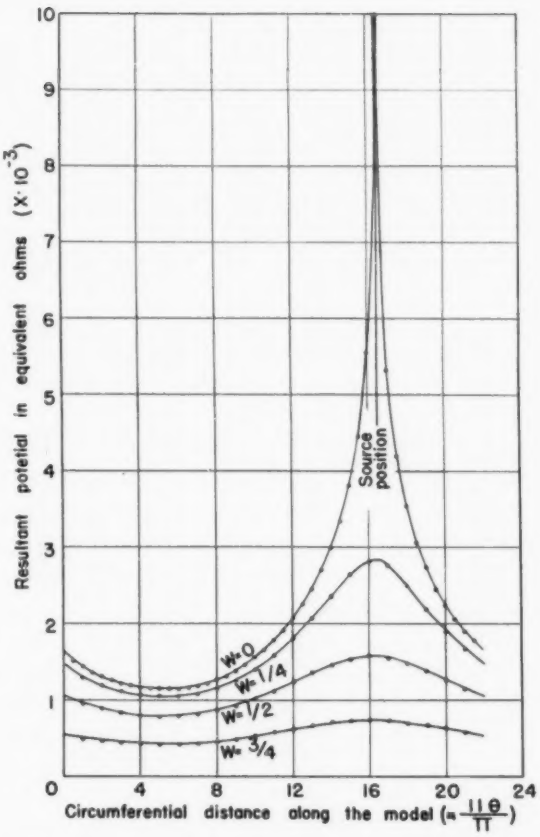

Fig. 12. Potential distribution due to a current source set 270° from position of maximum film thickness in an electrical model of a bearing of width = 0.88 perimeter. Solid curves: calculated theoretically; o: experimental determinations; w = (axial distance from center)/(half-width of bearing); journal eccentricity = 0.1.

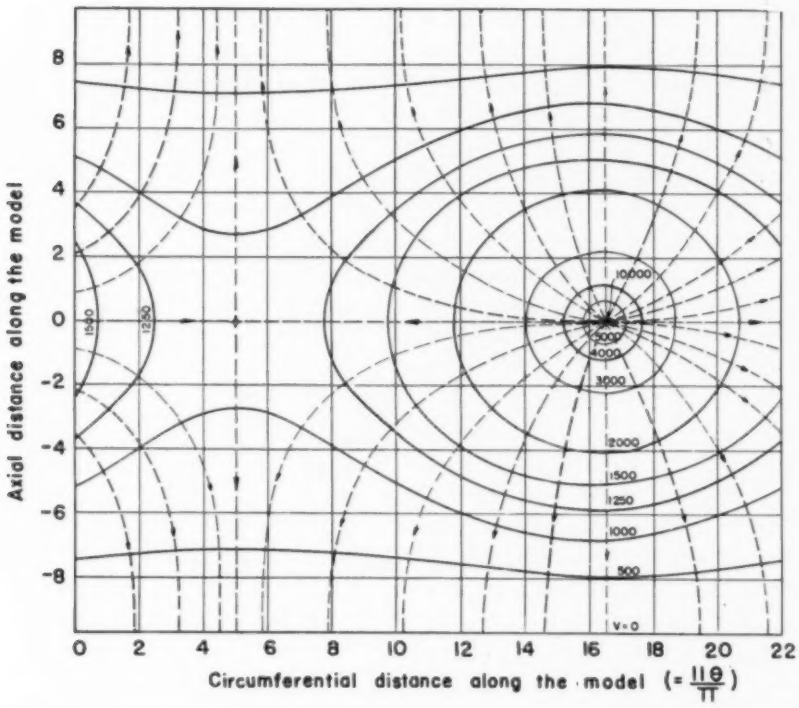

FIG. 13. Equipotential curves due to a current (lubricant) source set 270° from position of maximum film thickness. Same geometry as in Fig. 12. Dotted curves roughly represent stream lines.

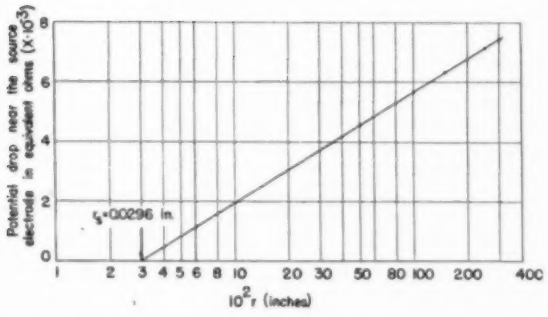

FIG. 14. Potential distribution in the vicinity of the source electrode. r=distance from the source electrode along the circumference; source electrode set 270° from position of maximum film thickness. r_0=effective radius of source electrode.

agreement that has been obtained has led to greater confidence in the reliability of the model as long as the eccentricity is not too great.

A practical application of the present model will be made in a study of various types of bearing grooving. An attempt is also being made to construct a model that can be utilized for the study of journal bearings of much greater eccentricity.

The authors are indebted to Dr. W. N. Arnquist for valuable discussions and to Dr. Paul D. Foote, Executive Vice President of the Gulf Research & Development Company, for permission to publish the paper.

The Behavior of Willemite Under Electron Bombardment

E. R. Piore* and G. A. Morton
RCA Manufacturing Company, Camden, New Jersey
(Received June 27, 1939)

Under scanning conditions in a specially designed tube, it was found that a willemite screen not only deviates from the potential of the accelerating electrode, but also shows potential variations on the surface. These potential variations are functions of scanning frequency and current density and may become of the order of several thousand volts. Light measurements were also taken. The dependence of the light intensity on voltage can be represented by a power law.

Introduction

IN the study of phosphor under electron bombardment the quantity of immediate interest is the light output as a function of current density in, and the energy of, the electron beam. The energy with which electrons strike the phosphor is determined by the surface potential of the phosphor. The surface potential, V_s, is in turn determined by the voltage, V_A, applied to the accelerating electrode, and by the secondary electron emission characteristics of the phosphor. The phosphor potential will adjust itself to such a value as to make the average rate of arrival of incident electrons equal to the rate of departure of electrons from the phosphor to the accelerating electrode. If the voltage applied to the accelerating electrode is such as to produce one or more secondary electrons for every incident electron (a gain of unity or more), then V_s will be to a first approximation the same as V_A. If V_A is such as to produce less than one secondary electron, then V_s will adjust itself to such a value as to give a gain of unity. The phosphor potential will then be less than the accelerating potential. The potential at which V_s begins to deviate from V_A will be referred to as the break point potential V_c.

Thus far all observations on willemite have given the static potential of the phosphor. Although the screens were bombarded with both a stationary and a moving electron beam, the methods[1–6] used permitted the measurement of only an average or static potential of the phosphor.

In a tube specially designed to measure directly surface potentials of phosphors, it was found that when willemite is bombarded with a moving beam a potential variation is produced along the surface of the phosphor. This variation occurs whenever V_s becomes less than V_A. The two willemite screens with different values of V_c were studied. One was very thick and the other of intermediate thickness. Both exhibited this potential variation. Light measurements made on this tube were in accord with the voltage measurement.

Experimental Tube and Procedure

The tube designed to measure the potential difference between the phosphor surface and the accelerating electrode is shown in cross section in Fig. 1. In the evacuated envelope there are two electron guns, whose beams are normal to each other. Beam G_1 bombards the phosphor surface S_1, the surface under investigation. Beam G_2 travels parallel to the surface S_1 and strikes a willemite screen S_2. When a potential difference is established between the phosphor and the accelerating electrode A, beam G_2 is deflected from its equilibrium position. The deflection is observed on screen S_2 and the magnitude of the deflection is proportional to the potential difference. Fig. 2 is a photograph of a tube similar to the one used in these experiments but with twice the deflection sensitivity.

The deflection of beam G_2 was calibrated by applying known voltages between the electrode A (a platinized glass surface indicated by a heavy

[1] W. B. Nottingham, J. App. Phys., **8**, 762 (1937); **10**, 73 (1939).
[2] T. B. Brown, J. Opt. Soc. Am. **27**, 186 (1937).
[3] I. Maloff, Electronic Conference, M. I. T., March, 1937.
[4] H. Nelson, Electronic Conference, M. I. T., March, 1937.
[5] C. Hagan and H. Bey, Zeits. f. D. **104**, 681 (1937).
[6] S. T. Martin and L. D. Hedrick, J. App. Phys. **10**, 116 (1939).

* At present with the Television Laboratory, Columbia Broadcasting System.

line in the figure) and a tantalum plate that replaced screen S_1. In this calibration the length, l, of the plate, the length, L, of the electron path after leaving the deflecting field, the magnitude, x, of the deflection, the deflecting voltage, E, and the accelerating potential, V, of the beam, were

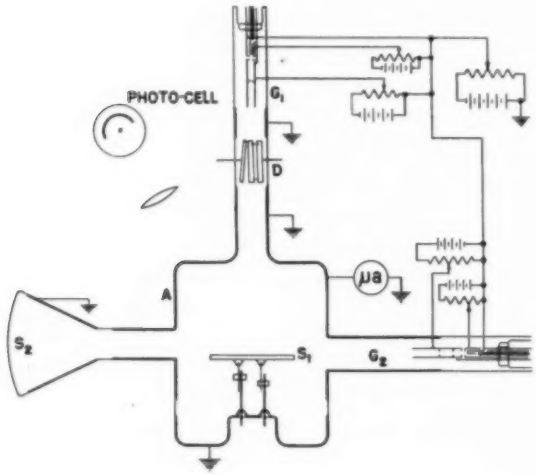

FIG. 1. A cross section of the experimental tube.

known. Substituting these quantities in the formula $x=(lEL)/(2dV)$ (which gives the deflection suffered by a beam traveling between two parallel plates), it was found that d, the separation for equivalent parallel plates, determined for a given E and V, was the same for all E and V.

The values for L and l were 227 and 44.5 mm. The distance between the screen S_1 and beam G_2 was 9 mm while d was 22.5 mm.

Under scanning bombardment when the accelerating voltage applied to A was greater than V_c, beam G_2 was no longer deflected to a stationary position, but instead produced a pattern on screen S_2.

Figure 5(c) reproduces a typical pattern. To interpret these patterns, the screen S_1 was replaced with nine metal strips, to which individual potentials could be applied. By applying various potentials to the metallic strips and observing both the horizontal and vertical deflection of beam S_2, it was possible to determine the voltage V_b, corresponding to the bottom of the pattern and V_T corresponding to the top of the pattern. V_b could be determined within 3 percent while V_T could be determined within 8 percent.

Willemite screen I was settled on a Pyrex plate. It was composed of particles two microns in diameter and its thickness was 5.37 mg/cm². Screen II was sprayed on Nonex with particle size of 1–2 microns and 0.77 mg/cm² in thickness. The glass plates were supported with tungsten rods. Between the W rods and the willemite there was at least 2 mm of glass. The leakage current to the rods was less than 0.01 μa with 3000 v between A and S_1.

The screens were bombarded with current densities in the spot ranging from 10^{-3} to 10^{-1} amp./cm² with a scanning beam and from 2×10^{-6} to 10^{-3} amp./cm² with a static beam. The current was measured with a meter inserted in the lead to electrode A. Guns G_1 and G_2 were operated at the same voltage. The current in G_2 was kept to 0.5 μa or less. From measurements with a metal plate it can be said that under operating conditions the current from G_2 striking screen S_1 was negligible. With 10 μa in G_2 less than 0.01 μa arrived at S_1. Under scanning bombardment the wave form applied to the deflection plates, D Fig. 1, was always a sine wave. The scanning frequency normal to the axis of G_2 ranged from 20 to 300 cycles. At right angles to this, the frequency used was much higher, ranging from 3000 to 15,000 cycles.

FIG. 2. A photograph of an experimental tube.

The light output was measured by projecting the image of the willemite surface, through an opening in electrode A, by means of a lens, onto a cesiated silver oxide photosurface. This is shown diagrammatically in Fig. 1. L was measured from the side of the willemite on which the beam was incident.

The tube used in this study was baked for at least three hours at 450°C, the metallic parts degassed, and the guns activated. Before sealing off, barium getters were exploded.

The vacuum, before the tube was removed from the pumps, was better than 5×10^{-6} mm.

Results

The relation between V_S and V_A under dynamic conditions

When V_A is in the neighborhood of or greater than V_c, under scanning bombardment, beam G_2 produces a pattern on screen S_2. A typical pattern is shown in Fig. 5(c). The presence of the pattern indicates that the surface potential is not uniform but varies along the screen. No longer can a unique value be assigned to V_S.

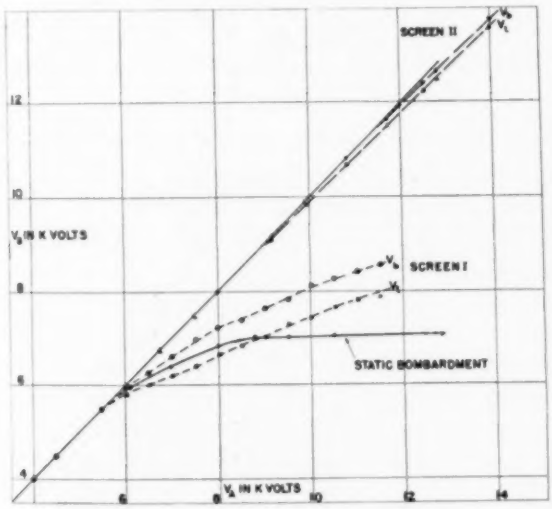

FIG. 3. Surface potential plotted against accelerating voltage.

However, the maximum voltage, V_T, corresponding to the top of the pattern and the minimum voltage, V_b, corresponding to the bottom, can be determined. Fig. 3 gives typical curves for the screen potential *versus* V_A for

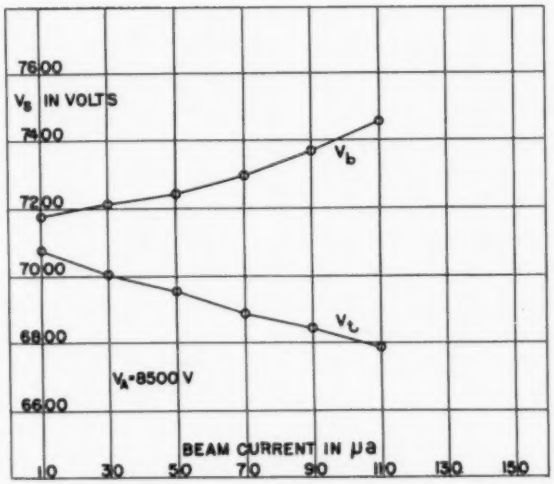

FIG. 4. Variation of surface potential with beam current at constant accelerating potential.

both screens, showing the presence of two branches above a certain bombardment voltage.

The patterns are also functions of both the current density in the incident beam and the scanning frequency. As the current density is increased, V_T becomes more negative and V_b less negative, approaching V_A. This is shown in Fig. 4 for $V_A=8500$ v. The variation of the pattern with frequency is rather interesting. As the deflection frequency normal to the direction of beam G_2 is increased, the size of the pattern decreases and finally degenerates into a point. In this process V_T, the maximum negative voltage, approaches V_b, while the latter changes very little. With sine scanning, the degeneration into a point takes place in the neighborhood of 3000 cycles. The actual value depends on V_A and the current density.

Examination of Fig. 5(c) reveals that the pattern is composed of two loops that meet at the bottom. The presence of the two loops indicates that the potential distribution on the surface of the willemite is not symmetrical around the beam; i.e., the potential distribution in front of the beam is not the same as behind the beam. This can be attributed to the fact that the area directly in front of the beam had a longer time to discharge than the area behind the beam.

As far as the actual shape of the potential distribution is concerned, it can be said that the area directly under the beam is most negative.

This was ascertained by applying an impulse synchronized with the scanning to the grid of gun G_1, and changing the phase between the impulse and scanning. It was then noted that when beam G_1 was on the left side of S_1, beam G_2 was on the right of S_2: when beam G_1 was in the center of S_1, G_2 was in the center of S_2 and deflected to its maximum vertical position. Some estimate can be made of the width of the potential distribution. This information can be ascertained by comparing the ratio of the width to the height of the observed pattern with that obtained in the calibration of the patterns with the nine metallic strips. The observed pattern was best approximated with a voltage variation confined to two of the nine strips. With a scanning line $\frac{1}{2}$ mm wide, the potential distribution was approximately 8 mm wide on a willemite screen 44.5 mm wide.

The potential distribution cannot be interpreted simply by ohmic conduction along the screen, as shown in Fig. 5(a) because the resistance of the screen is too great to permit changes of potential at the rate required to produce the observed patterns. This indicates that besides the ohmic conduction on the willemite screen, secondary emission and a redistribution of electrons on the surface play a role. The redistribution electrons are those secondary electrons produced by the incident beam which return to the phosphor rather than to the accelerating electrode. These secondary electrons may strike the screen on either side of the beam. Because of the potential gradient established by ohmic conduction, these electrons may produce a new group of secondary electrons. In some regions, the secondary emission ratio for the redistributed electrons will be greater than unity, in others less. The region with gain less than one will be in the immediate neighborhood of the beam. Farther from the beam, the redistribution current density being less, ohmic leakage causes a potential difference which makes the gain of the returning electrons greater than unity. Once a ratio greater than unity has been established, the screen tends to become more positive in that region. A possible potential distribution is drawn in Fig. 5(b).

In the case of screen II, the thinner screen, the surface potential begins to deviate from V_A around 9000 v. This deviation remains small even at 15,000 v as compared to the deviation above 6000 v for screen I, the thick screen. It cannot be assumed that V_c for screen II is 9000 v and that the small deviation is due to leakage resistance, because the leakage resistance for both screens are of the same order. However, the difference can be attributed to the requirement of a field to produce the full secondary emission yield from the screen.[1] Except for the magnitude of the potential variations involved, the patterns formed by screen II were the same as those described above.

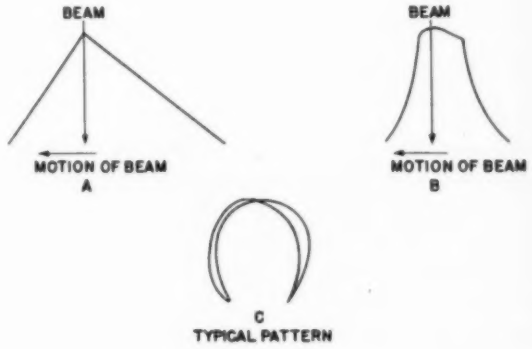

FIG. 5. Typical patterns.

The relation between V_S and V_A under static bombardment

Under a stationary beam, the state of affairs is relatively simple. G_2 is deflected a given vertical distance and V_S is read off on the calibrated curves. In Fig. 3 a typical curve showing the relation between V_S and V_A is given for screen I. For screen II the relation between V_S and V_A is linear up to 10,000 v. At 12,000 v the difference between V_A and V_S is 150 v. V_c for screen I is in the neighborhood of 7000 v and for screen II V_c is above 10,000 v. Both these values are in agreement with those reported in the literature.[1, 3, 6]

The point of interest in Fig. 3 is that the transition between $V_S = V_A$ and $V_S =$ a constant, is not sharp but gradual. This may be another indication that a field is required to obtain a full secondary emission yield from the willemite screen in the neighborhood of V_c.[1] The leakage resistance, estimated to be about 10^{14} ohms, is too small to account for the gradual transition of V_c under static conditions.

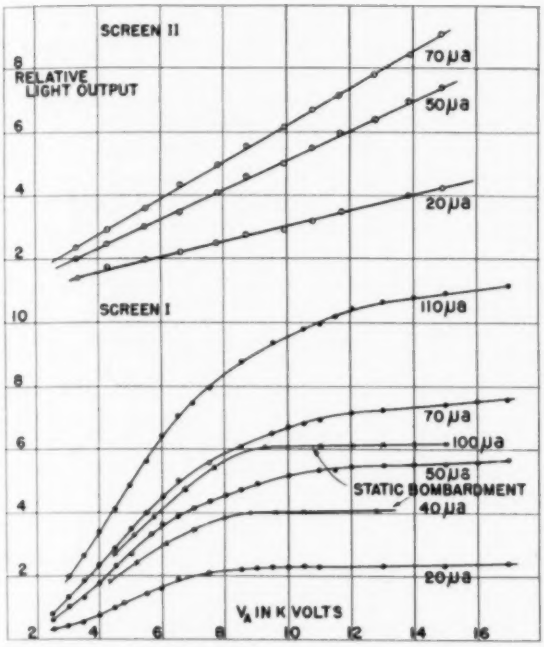

FIG. 6. Relative light intensity as a function of accelerating voltage.

The relation between L and V_A

Figure 6 gives a plot of L against V_A for screens I and II. For the former both the static and dynamic curves are shown. The behavior of L with respect to V_A is similar to the behavior of V_s. The light output begins to saturate with V_A at approximately the same voltage as the screen potential. The contrast between dynamic and static bombardment appears here too. With stationary beam L becomes constant above V_c, while with the dynamic beam L increases with V_A, but less rapidly above V_c than below. Screen II shows no saturation of L up to 15,000 v; while the thicker screen shows saturation in the neighborhood of 7000 v.

If L is plotted against V on a double logarithmic scale, it was found that the data below V_c can be represented by $L \propto V_A^n$. For screen I, $n=1.96$ for static bombardment and 1.84 for dynamic, and for the thinner screen, II, $n=1.23$ for both cases. Similar values have been reported elsewhere.[1-3, 6]

In conclusion we would like to express our gratitude to Dr. V. K. Zworykin for his encouragement and interest in this problem, to Dr. L. B. Headrich and Mr. H. W. Leverenz for supplying the screens, and to Mr. R. R. Goodrich for his aid in the construction of the tubes.

Letters to the Editor

Concerning "Physics of Flames and Explosions of Gases"

Doctors B. Lewis and G. von Elbe[1] in Section 4 of their paper on "Physics of Flames and Explosions of Gases" state that calculated explosion pressures using spectroscopy data generally agree with experimental explosion pressures determined in spherical vessels with central ignition, and, indeed, that under certain conditions experimental pressures exceeding the theoretical are found. They go on to state that in such cases there exists in the burned gas a momentary excess of translational energy and a corresponding deficiency of molecular internal energy. It is probable that something of this kind occurs in detonation, but not, it is thought, in normal closed vessel explosions. Since the art of pressure indicating has been perfected the only experiments which show experimental pressures equal to or even greater than the calculated are those of Lewis and von Elbe. The recent experiments of Fenning and Whiffen at the National Physical Laboratory[2] confirm those of David and Leah[3] and show that the measured pressures are always considerably below the calculated pressures. The inference is that there is an excess of molecular internal energy and a deficiency of translational energy. I have called this excess of internal energy "latent energy," and suggested that it probably resides in metastable molecules formed in the flame front.

Lewis and von Elbe go on to point out that temperatures of open flames determined by the sodium line reversal method are in a number of cases higher than the theoretical temperatures and these, they claim, lend support to their theory of momentary excess of translational energy. But it does not seem that they have placed in proper perspective the large numbers of measurements of flame temperatures by the sodium method. For example the measurements of temperatures of flames resulting from combining proportions of carbon monoxide and air mixtures determined by Griffiths and Awbrey, Loomis and Perrott, Jones, Lewis and Seaman, and Ellis and Morgan are between 200 and 300 degrees centigrade below the theoretical temperatures, corresponding (after allowing for heat losses) to a latent energy of something like 20 percent of the heat of combustion.

The latent energy in flames burning at constant atmospheric pressure is very much greater than in exploded

gases and an attempt to give the reason for this has been made in various publications.[4] It may be that many industrial processes involving flame gases owe their effectiveness in large measure to latent energy.

W. T. DAVID

Engineering Department,
The University,
Leeds, England,
October 11, 1939.

[1] Lewis and von Elbe, J. App. Phys. **10**, 344 (1939).
[2] Fenning and Whiffen, Phil. Trans. Roy. Soc. (**A**), p. 149 (1939).
[3] David and Leah, Phil. Mag. **22**, 513 (1936).
[4] E.g., Phil. Mag. **23**, 352 (1937) and Nature **139**, 67 (1937).

Answer to Communication by W. T. David*

Compilations of experimental and calculated explosion pressures in mixtures of hydrogen and oxygen and carbon monoxide and oxygen with diluent gases may be found on pages 301–4 and 308, respectively, of the book *Combustion, Flames and Explosions of Gases*.[1]

In the former group the agreement between experimental and calculated pressures in *five* independent investigations precludes the existence of the large amounts of latent energy claimed by Professor David and his students. For example, experiments with diluent argon and small excess of hydrogen show an average deviation of 0.07 percent; with large percentages of diluent oxygen or nitrogen the experimental pressures are systematically above the calculated, of the order of 1 percent.

In the $CO-O_2$ group experiments by Pier, and David and Leah are included. In David and Leah's experiments the agreement between experimental and calculated pressures is very close, differences of the order of 1 percent occurring in either direction. Pier's experiments show somewhat larger deviations, also in either direction. Taking into account the much longer duration of $CO-O_2$ explosions as compared with H_2-O_2 explosions, appreciable heat losses by radiation are to be expected in the former, and were indeed found by David and his students to be of the order of several percent. This would bring at least all of David and Leah's experimental pressures above the calculated. Considering the various mixture compositions the results generally are consistent with the assumption of momentary excess of translational energy (excitation lag) as discussed in the above-mentioned book.

The recent results of Fenning and Whiffen are similar to the above, and as these authors state (page 182) ". . . it is desired to point out that these particular experiments (CO explosions) give no support to the theory advanced in some quarters, David and Davies, 1930, that the freshly formed gas has a higher energy content than the ordinary carbon dioxide."

For further and independent criticism of David's latent energy theory see also W. Jost.[2]

The question of flame temperatures has been brought up by Professor David on a previous occasion when it was discussed at some length.[3] It should be pointed out that temperatures of totally colored (with Na) flames determined by the line-reversal method will always be found to be considerably below the theoretical due to cool layers of gas at the boundary of the flame. If only the central portion of a Méker flame is colored heat losses occur mainly to the grid and by radiation, and for suitably rapid gas flow it is possible to find temperatures in agreement with or even in excess of theoretical flame temperatures (see above-mentioned book, pp. 337–45).

BERNARD LEWIS†

Bureau of Mines,
Pittsburgh, Pennsylvania

GUENTHER VON ELBE

Coal Research Laboratory,
Carnegie Institute of Technology,
Pittsburgh, Pennsylvania

* Published by permission of the Director, Bureau of Mines, U. S. Department of the Interior, and the Director, Coal Research Laboratory, Carnegie Institute of Technology (not subject to copyright).
† Physical chemist, Explosives Division, Central Experiment Station.

[1] B. Lewis and G. von Elbe, *Combustion, Flames and Explosions of Gases* (Cambridge Press, 1938).
[2] W. Jost, *Explosions- und Verbrennungs-vorgänge in Gasen* (Springer, Berlin, 1939), p. 222.
[3] W. T. David, Eng. **138**, 475 (1938); **139**, 195 (1935); **140**, 232 (1935); The Engineer **157**, 558 (1934); **159**, 230 (1935); Phil. Mag. **20**, 65 (1935). B. Lewis and G. von Elbe, Eng. **139**, 168 (1935); **140**, 203 (1935); The Engineer **159**, 230 (1935); Phil. Mag. **20**, 44 (1935). See also Laure and Gaudry, Chal. et Ind. **19**, 52 (1938).

EPPLEY THERMOPILES *for* RADIANT ENERGY MEASUREMENTS

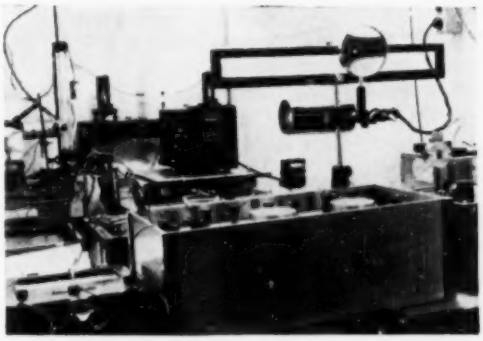

A view of some of the apparatus used for calibrating thermopiles at the Eppley Laboratory, Inc.

Adequate manufacturing, testing and calibrating equipment in the hands of our skilled and experienced technicians insures satisfaction to the users of Eppley Thermopiles.

We are prepared to furnish thermopiles of either bismuth-silver or copper-constantan, mounted in vacuum or air type cases. We also furnish thermopiles and mountings especially designed to meet individual needs. A card will bring you our Bulletin R–3 which contains illustrations, sample curves, complete descriptive matter, prices, references, etc., with regard to Eppley Thermopiles.

EPLAB

THE EPPLEY LABORATORY, INC.
SCIENTIFIC INSTRUMENTS
NEWPORT, R.I.
U. S. A.

KODASLIDES

. . . Mounted Kodachrome, Ready to Project, at Film Cost Only

Actual-size black-and-white reproduction of a Kodaslide.

THE Eastman Kodaslide program is a development of revolutionary significance in the field of visual presentation—both scientific and general. It is made possible by the availability of Kodachrome Film in 35 mm. and Bantam sizes, and return of the processed film in the form of individual transparencies in 2″ x 2″ cardboard mounts. Thus, anyone with a camera that will accommodate Kodachrome in either of these sizes can now obtain full-color, ready-for-projection slides at the cost of the film only . . . less than 15 cents per slide.

Save Space . . . No Breakage

Kodaslides are much lighter in weight than glass slides and require only a fraction of the filing space . . . they are not susceptible to breakage . . . and, with the new Kodaslide Projectors, they provide both simplicity and effectiveness in showing. Black-and-white transparencies may be similarly mounted in low-cost Kodak Ready-Mounts.

Detailed information about any phase of the Eastman 2″ x 2″ projection-slide program will be furnished on request.

Eastman Kodak Company, Rochester, N. Y.

Innovations in Instruments

Portable A.C. Ultraviolet Meter

A new portable alternating-current-operated ultraviolet measuring device, employing one of three ultraviolet photo-tubes, and useful for measuring the output of various types of ultraviolet sources has been announced by the Westinghouse Lamp Division, Westinghouse Electric and Manufacturing Company, Bloomfield, New Jersey.

Used with a tantalum photo-tube, the meter is particularly useful in measuring the output of such ultraviolet lamps as the Westinghouse Sterilamp; with a titanium photo-tube the meter may be used for measuring ultraviolet radiation of the sun, or employed to determine the proper time of exposure for sun baths or sun lamp treatments; with a platinum photo-tube the device measures radiations in the ozone-producing region.

Amount of radiation is determined in the new meter by the integrating method and indicated by a mechanical counter. The number of counts registered in given time indicates the intensity of ultraviolet radiations impinging upon the photo-tube, placed at a given distance from the source at a rate proportional to the exposure time.

The complete meter and its carrying case weigh about 30 pounds. Photo-tube, grid-glow tube, and control condenser are mounted in a separate removable housing (shown at the left of the accompanying figure) and attached to the counter mechanism by an extension cord. On a chromium plate inside the case are the control switch and counter. A full wave rectifier is built into the case. An extension cord is provided for connection with 115-volt outlets.

Additional information may be obtained from the Special Products Department, Westinghouse Lamp Division, Bloomfield, New Jersey.

1,400,000-Volt X-Ray Tube

General Electric is building for the National Bureau of Standards one of the highest voltage x-ray tubes ever made, a multisection giant 28 feet, 6 inches long, to operate at 1,400,000 volts. At the same time, one of the most powerful constant-voltage, direct-current generators ever made is being built to operate the tube. The complete equipment will be used for research work in the high voltage field.

The new device will serve several important purposes at the Bureau. The first of these relates to the measurement of x-ray dosage. This will be of value to the medical profession, which has for several years been employing 200,000-volt x-rays in the treatment of cancer and other diseases, and has recently been extending its work in this field to higher and higher voltages.

The same high voltage generator with another multisection tube, duplicating in many respects the x-ray tube, can later be used for the production of neutrons and artificial radioactivity.

The high voltage generator can also be used for another important function, namely, to extend the high voltage measurement work of the Bureau to higher levels.

The tube is rated at 1,400,000 volts and 10 milliamperes and is composed of ten sections of 140,000 volts each. The construction of the tube permits a unique method of applying energy to the electron beam after leaving the cathode. Starting at zero velocity the beam is accelerated through the first section of the tube to 140,000 electron volts velocity. As it enters the second section, it receives an additional voltage kick of 140,000 which still further increases its velocity. The process is repeated through each section of the tube so that when the electron beam finally reaches the target it has the velocity and the energy which it would have, had it been given a single 1,400,000 kick. Its speed is about 180,000 miles a second or very nearly the velocity of light.

The tube may be operated at will at any lower voltage down to 300,000. This flexibility is important for the research work to be undertaken.

General Electric announced in a recent news bulletin that the transformer equipment, built in the Pittsfield works of the Company, and the x-ray tube, constructed in the Research Laboratory in Schenectady, would be delivered soon after January 1.

A NEW ANEROID-Wall Type BAROMETER

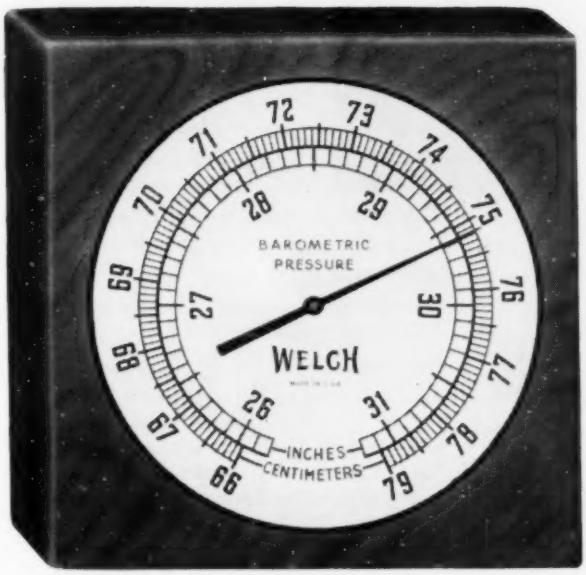

NO. 1233

12 Inch Dial

Five to ten times as sensitive as the usual type

Small Temperature Error

No Back Lash—Read like a wall clock
Operating Torque 40 Times that of ordinary Aneroid.

Length of Pointer—7¾ inches
High Order of Accuracy

Large Size makes for extremely rugged construction.

Write for complete circular

WELCH

Catalog lists over 10,000 items for Science Laboratories

WRITE FOR IT

W. M. Welch Scientific Company

Established 1880

1515 Sedgwick Street Chicago, Illinois, U.S.A.

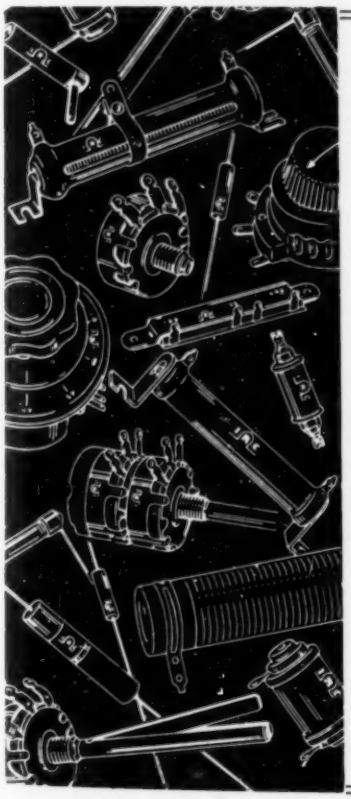

RESISTANCE ENGINEERING DATA BULLETINS

These IRC Resistance Engineering Data Bulletins contain the results of many years of specialized experience in the production of more resistance types for more applications than any other manufacturer in the world. They have been classified and prepared to bring exact needed engineering information to assure selection of the *right* resistor for *any* job. Please ask for them by number.

1. Metallized and Wire Wound Volume Controls and Potentiometers up to 2 watts and 20 meg. resistance.

2. Metallized Type Resistors: Insulated 1/2, 1 and 2 watts; high frequency; high range; high frequency power resistors; high voltage power resistors.

3. Insulated Wire Wound Resistors: Type BW from 1/2 to 1 and 2 watts; Type MW 5 to 20 watts.

4. Power and Precision Wire Wound Resistors: Power types from 10 to 200 watts, fixed and adjustable types, in wide variety of shapes, mountings, etc. Inductive and non-inductive. 14 Precision types to as close as 1/10 of 1% accuracy.

5. Attenuators: Unique new IRC molded motor commutator type 20-step attenuator; also, conventional type 30-step units. Ladder, Potentiometer or Bridge T.

6. Power Rheostats: Quick heat-dissipating all-metal (aluminum) 25 and 50 watt types.

IRC

INTERNATIONAL RESISTANCE CO.

419 N. BROAD ST., PHILADELPHIA, PA.

WRITE FOR 44 PAGE ENGINEER'S DATA BOOK

Metallic Bellows

Shaft seals and automatic pressure controls for oil-burner-pump equipment

HYDRON Metallic Bellows are used as control elements in temperature-and-pressure-control devices, and for liquid or gas seals of compressors and pumps. We are specialists in the design and production of complete thermostatic and pressure units for temperature and pressure controls. We are, therefore, prepared to extend the fullest co-operation to engineering departments of control manufacturers in the solution of design and engineering problems.

CLIFFORD MANUFACTURING CO.
564 E. FIRST STREET, BOSTON
BOSTON CHICAGO DETROIT LOS ANGELES
PRODUCERS OF BELLOWS EXCLUSIVELY
SERVING AUTOMATIC CONTROL MANUFACTURERS

Use
POLAROID* FILM
for Economy

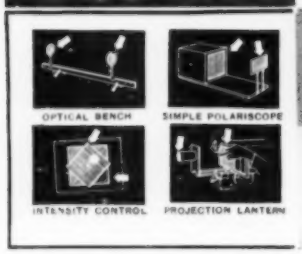

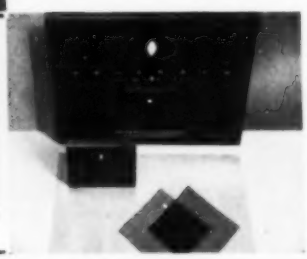

In classroom and laboratory experiments

Polaroid Type II Film is in the form of durable, flexible sheets, easily cut with scissors to fit improvised apparatus for working with polarized light in projectors, microscopes, polariscopes, polarimeters, refractometers, pocket mineralogy polariscopes, densitometers, light intensity controllers, 3-dimensional picture demonstrations, photometers, and devices for scientific exhibits.

It is economical. Nine pairs of microscope attachments may be cut from one standard 4" square of film—at a cost of less than 50c each. Two sheets, 4" square, price: $7.50.

Write Division 4 . . . for catalog.

POLAROID CORPORATION
719 Main Street, Cambridge, Mass.

*T. M. REG. U. S. PAT. OFF.

Recent Booklets

A 66-page, condensed catalog, recently issued, lists the entire Leeds & Northrup line of instruments for research teaching and testing—standards, galvanometers and dynamometers, bridges, potentiometers, photometric apparatus, miscellaneous apparatus, primary elements, accessories, supplies, instrument parts. Every standard L & N item is briefly described, and most of the principal ones are illustrated. For more complete descriptions and much supplementary information, the reader is referred to more detailed L & N publications. However, in choosing instruments and accessories for specific work in laboratory, plant or field, many instrument users will find this condensed catalog a useful guide. A copy will be sent promptly to anyone who asks Leeds & Northrup Company, 4934 Stenton Avenue, Philadelphia, for Catalog E—"Electrical Measuring Instruments For Research, Teaching and Testing."

The General Radio Experimenter, publication of the General Radio Company, 30 State Street, Cambridge A, Massachusetts, includes in the November, 1939 issue, a special article on "A Signal Generator for the Ultra-High Frequencies." The December table of contents lists the following articles: "Network Testing with Square Waves" and "High Quality Audio Transformers."

"Tinning Plant of Latest Design Installed at Ebbw Vale," "The Supposed Brittleness of Tin at High Temperatures," and "Hydrogen Swells in Canned Fruits," are representative titles of articles printed in the magazine, *Tin and its Uses*, Numbers 1, 2, and 3 of which appeared in April, July, and October, respectively. This magazine is a publication of the International Tin Research and Development Council, whose purpose is "to acquire and disseminate scientific and technical knowledge relating to tin, its alloys and chemical compounds, and their production and uses." The American headquarters for the Council are located at the Battelle Memorial Institute, 505 King Avenue, Columbus, Ohio.

The October-November issue of the *Du Mont Oscillographer* contains Section 1 of a two-part article entitled "Study of Phase Displacement in Electrical Circuits from Linearly Expanded Lissajous Figures." This paper is written by H. D. Brailsford of the Underwriters' Laboratories, Inc. The *Du Mont Oscillographer* is published by the Allen B. Du Mont Laboratories, Inc., 2 Main Avenue, Passaic, New Jersey.

The December issue of *Cenco News Chats*, publication of the Central Scientific Company, Chicago, devotes the Cencographs page to a group of photographs taken at the laboratories of the Procter and Gamble Company, Cincinnati, Ohio. The major portion of the publication introduces new Central Scientific products with accompanying illustrations.

Linde

RARE GASES
AND MIXTURES

NEON
ARGON
HELIUM
KRYPTON
XENON
MIXTURES

. . . highest purity
. . . for scientific purposes

Linde rare gases are of consistently high purity. They are used in the study of electrical discharges, in rectifying and stroboscopic devices, and in inert atmospheres where heat conduction must be reduced.

Linde rare gases are shipped in spherical glass bulbs, designed to facilitate removal without contamination. Special mixtures for experimental purposes can be supplied upon request.

The Linde Air Products Company
Unit of Union Carbide and Carbon Corporation
30 East 42nd Street UCC New York, N. Y.
Offices in Principal Cities

The word "Linde" is a trade-mark.

OPTICAL
LITHIUM FLUORIDE
POTASSIUM BROMIDE
SODIUM CHLORIDE
SODIUM NITRATE

For infrared and ultraviolet spectroscopy and for polarizing optics. . . . Lithium fluoride crystals are grown up to eight pounds in weight—Potassium bromide, sodium chloride and sodium nitrate, up to twenty-five pounds in weight. . . . Write for information.

THE HARSHAW CHEMICAL CO.
SPECIAL PRODUCTS DIVISION . . . . CLEVELAND, OHIO

A complete explanation of the new meter-kilogram-second system of units to go into effect this year.

MKS UNITS AND DIMENSIONS
and
A PROPOSED MKOS SYSTEM

By *G. E. M. Jauncey* and *A. S. Langsdorf*

This manual explains the properties of the MKS system of basic units adopted by the I.E.C. in 1935, to be put into effect in 1940; describes the methods for changing from the c.g.s. system; gives reasons for the adoption of the ohm as the 4th basic unit; describes a proposed MKOS system, and discusses the difference between magnetic flux density and magnetic field strength.
$1.00

MACMILLAN NEW YORK

"JAGABI"
HAND TACHOSCOPE

This combined speed-counter and stop-watch gives the exact number of revolutions in the exact time in which they were made. Measures speed with "split-second accuracy" up to 20,000 r.p.m.

Write for Bulletin 1505-R describing these and other speed-measuring instruments.

JAMES G. BIDDLE CO.
ELECTRICAL AND SCIENTIFIC INSTRUMENTS
1211-13 ARCH STREET PHILADELPHIA, PA.

TYPE S POTENTIOMETER

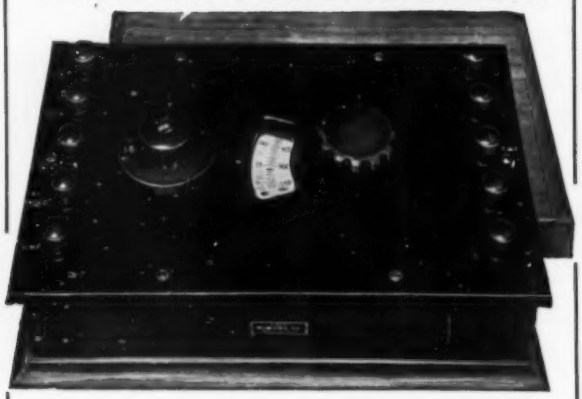

An accurate and inexpensive laboratory potentiometer suitable for all measurements of potential difference and for student instruction in the potentiometer method. Two ranges—1.6 volts and 16 M.V. Coils are accurate to within 1/20 per cent. Price seventy-five dollars.

ASK FOR BULLETIN 270.

RUBICON COMPANY

Electrical Instrument Makers

29 N. SIXTH STREET PHILADELPHIA, PA.

FINE WIRES

TAYLOR PROCESS

THE TAYLOR PROCESS is a method for making wires from substances which lack ductility. The elements or alloys, because the drawing is done in glass or quartz, are in a very pure state. Lengths of more than a few feet cannot be obtained. The wires may be had with or without the glass insulation. We make Taylor Process wire of Pt, Rh, Au, Ag, Cu, Fe, Zn, Cd, Pb, Sb, Bi, Sn, Se, Te, Tl, Ga, and In, Constantan, Bi-Sn, Cd-Sb (used where large E.M.F. is desired) and many other alloys. Our wires are packed in containers holding one foot and, with few exceptions, the sizes are from one *mm* to one micron. We manufacture, too, fine wire by the Wollaston Method, by extrusion and by bare drawing.

WE ARE SPECIALISTS IN PLATINUM AND CAN SUPPLY IT IN WHATEVER FORM YOU REQUIRE

BAKER & CO., INC.

113 Astor Street, Newark, New Jersey

INDEX TO ADVERTISERS

Name	*Page*
BAKER & COMPANY, INC. — Platinum crucibles, dishes, triangles, filter cones, anodes, cathodes, electrodes, platinum tipped crucible tongs, fine wires and bismuth foil.	viii
JAMES G. BIDDLE COMPANY — "Jagabi" Rheostats; Adam Hilger and Kipp & Zonen Optical Instruments; "Pointolite" Lamps; Electrical Testing and Speed-measuring Instruments.	vii
CAMBRIDGE UNIVERSITY PRESS	vii
CENTRAL SCIENTIFIC COMPANY — Manufacturers of Cenco Physical Apparatus and Instruments to meet all requirements of University, College and High School Physics Laboratories. Specializing in high vacuum pumps and development of instruments and apparatus for various sciences.	Cover 4
CLIFFORD MANUFACTURING COMPANY — Hydron metallic bellows for temperature and pressure control devices. Data for engineers.	vi
EASTMAN KODAK COMPANY — Purified Organic Chemicals for research purposes; Plates for Photography, Photomicrography, Spectroscopy, Photometry, Astronomy; Wratten Light Filters; Cameras and Films.	iii
THE EPPLEY LABORATORY, INC. — Standard Cells, thermopiles, pyrheliometers and temperature bridges.	iii
GAERTNER SCIENTIFIC CORPORATION — Spectroscopes, Spectrometers, Spectrographs, Spectrophotometers, Heliostats, Measuring Microscopes, Comparators, Cathetometers, Reading Telescopes, Interferometers, Chronographs, Dividing Machines, etc.	ii
GENERAL RADIO COMPANY — Manufacturers of electronic measuring instruments; vacuum-tube voltmeters, amplifiers and oscillators; wave analyzers, noise meters and analyzers, stroboscopes; laboratory standards of capacitance, inductance and frequency; impedance bridges, decade resistors and condensers; air condensers and variable inductors; rheostats, Variacs, transformers; other laboratory accessories.	Cover 3
HARSHAW CHEMICAL COMPANY — Optical Lithium Fluoride grown in single crystal to predetermined size. Industrial Chemicals.	vii
INTERNATIONAL RESISTANCE COMPANY — Manufacturers of metallized and wirewound fixed and variable Resistors including high voltage and high frequency types.	v
LEEDS & NORTHRUP COMPANY — Manufacturers of Galvanometers, Resistors, Bridges, Condensers, Inductances, Potentiometers, Testing Sets; Temperature Measuring, Recording and Controlling Apparatus; Instruments for Measuring and Controlling Conductivity of Electrolytes and Hydrogen Ion Concentrations.	i
THE LINDE AIR PRODUCTS COMPANY — Oxygen, Argon, Helium, Krypton, Neon, Xenon, Rare Gas Mixtures, Nitrogen, Hydrogen, Calcium Carbide, Acetylene, equipment for Oxy-Acetylene welding and cutting.	vii
MACMILLAN COMPANY	vii
MCGRAW-HILL BOOK COMPANY, INC.	ii
POLAROID CORPORATION — Polaroid experimental kit for demonstration. Polarized light. Handbook. Sheet Polaroid.	vi
RUBICON COMPANY — Galvanometers, electrometers, potentiometers, Wheatstone and Kelvin bridges, resistance boxes, hydrogen ion and conductivity apparatus.	viii
W. M. WELCH SCIENTIFIC COMPANY — Scientific instruments—laboratory apparatus. Catalog lists 10,000 items.	v

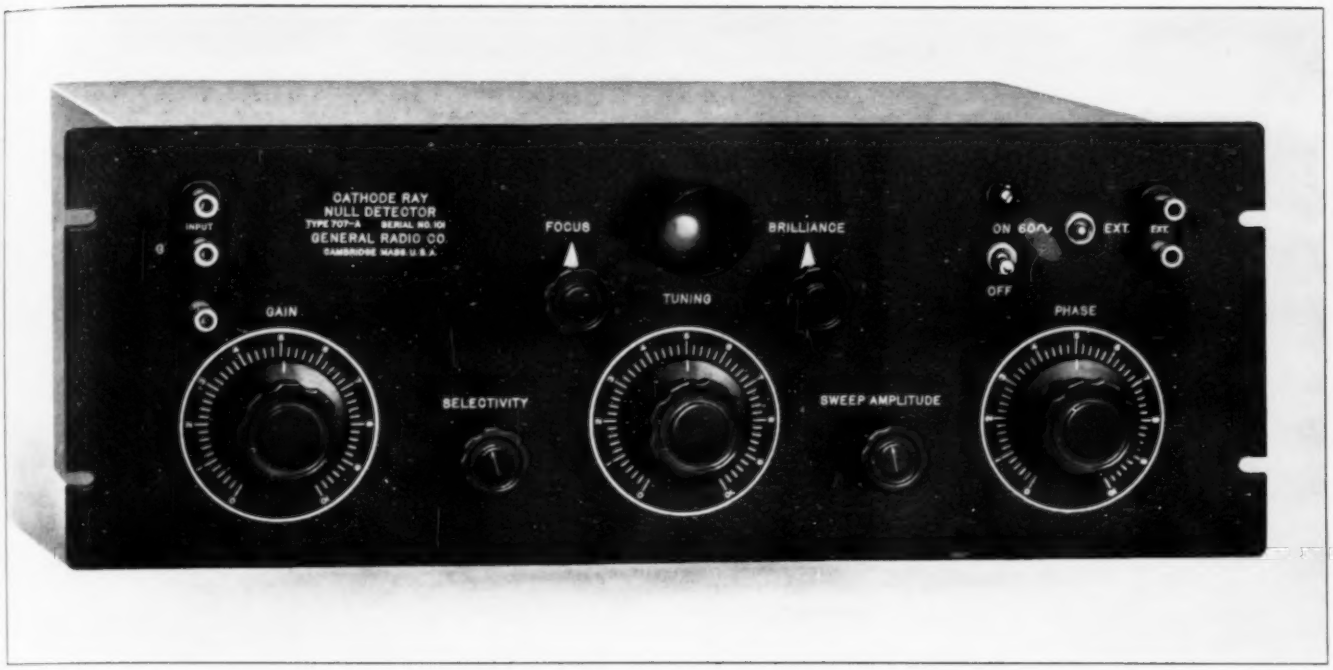

IMPROVED NULL DETECTOR

for a-c Impedance Bridges

SENSITIVE • RUGGED • CONVENIENT TO OPERATE

THE G-R TYPE 707-A NULL DETECTOR uses a one-inch cathode-ray tube in a new non-inductive degenerative amplifier circuit, with tuning and phasing networks and sweep and sensitivity controls. This new detector offers many advantages which include:

- Operation in noisy locations
- Not affected by strong fields
- May be used at all frequencies up to 20 kilocycles
- Separately indicates balance of the resistive and the reactive components
- Makes possible precise balancing of either component with only moderately close balance of the other
- Precise measurement of the steady component can be made while the other varies erratically
- Shows immediately any drift of either or both components
- Provides positive indication of the direction of off-balance for either component as selected
- Can be calibrated to show the degree of unbalance
- Can be used at all times at maximum sensitivity, even with the bridge far off balance
- Supplies instantaneous response
- Will withstand any overload caused by marked off-balance, and is instantaneous in recovery

The input impedance of the null detector is 1 megohm. Its sensitivity is 100 μv at 60 cycles and 200 to 300 μv at 1000 cycles. Its selectivity is 40 db against the second harmonic. Plug-in units tune the amplifier to any operating frequency desired between 20 and 2,000 cycles, with a continuous tuning range of $\pm 5\%$ for each unit.

TYPE 707-A CATHODE-RAY NULL INDICATOR $195.00

WRITE FOR BULLETIN 547 FOR COMPLETE INFORMATION

GENERAL RADIO COMPANY

Cambridge, Massachusetts

Branches in New York and Los Angeles

Simple—Practical

PHOTOELECTRIC DEMONSTRATION UNIT

With Infrared Control Lamp

80937

FOR demonstrating photocell principles and photoelectric equipment used in such practical applications as open or closed circuit burglar alarms, fire alarms, illumination control, liquid level control, turbidity control, smoke indication, etc. Through the use of additional equipment, such as magnetic counters, power relays, etc., the demonstrations may be extended to an unlimited number. The set is so simple that an extensive knowledge of electronics is not required for performing the demonstrations.

The set consists of an amplifier-relay control unit, a demonstration panel, a light source with invisible infrared beam filter, and instructions for performing a number of demonstrations. An emissive type photocell of high sensitivity and long life and a type 7E6 amplifying tube with loctal base are provided. The base plate of control unit case is detachable to permit examination of the transformer, relay, condenser, resistors, photocell and amplifier sockets, and potentiometer. An adapter plug with lead wires is furnished for use in place of the photocell on the amplifier-relay control unit for demonstrations of other means of electrical control than that of the photocell. Two single-pole, double-throw knife switches, a buzzer, and a miniature screw base lamp socket with 1½ candlepower lamp are mounted on the demonstration panel. By proper manipulation of the switches, either audible or visual signals can be given in either open or closed circuit demonstrations. The light source will control the amplifier-relay control unit from a distance of approximately 20 feet.

80937 **PHOTOELECTRIC DEMONSTRATION SET, Cenco,** complete with amplifier-relay control unit, demonstration panel, and infrared light source, for operation from 115 volts, 60 cycles A.C. only, but *without* magnetic counter, etc. *Each* $17.50

Ask for Circular 1103

CENTRAL SCIENTIFIC COMPANY

SCIENTIFIC INSTRUMENTS & LABORATORY APPARATUS

CHICAGO
1700 Irving Park Blvd.,
Lakeview Station

TRADE MARK CENCO REG. U.S. PAT. OFF.

BOSTON
79 Amherst St.,
Cambridge A Station

LANCASTER PRESS, INC., LANCASTER, PA.